MISSISQUOI BAY FIELD STUDY AND HYDRODYNAMIC MODEL VERIFICATION

Submitted to:

Vermont Geological Survey
Vermont Agency of Natural Resources
103 South Main St., Center Building
Waterbury, VT 05671

Submitted by:

Daniel Mendelsohn
Henry Rines
Tatsusaburo Isaji
Applied Science Associates, Inc.
70 Dean Knauss Drive
Narragansett, RI 02882

ASA Project 96-73

October 1997

TABLE OF CONTENTS

LIST OF FIGURES

LIST OF TABLES

Executive Summary

Missisquoi Bay is a small embayment that makes up the northeast corner of Lake Champlain. The Swanton-Alburg Route 78 bridge is located at the mouth of the bay at its southern end and includes two causeway sections extending 640 m (2100 ft) from the Swanton shore and 490 m (1600 ft) from the Alburg shore with a 170 m (560 ft) bridge section. Changes have been observed in the bay since the bridge was built, including apparent transformation of areas of sandy and cobble bottom to silt and organic material as well as infilling with vegetation. It has been speculated that the observed deterioration of habitat values in the bay have resulted from the presence of the bridge causeways constricting flow to the bay and reducing flushing.

There exist very little data about the condition of Missisquoi Bay before the construction of the bridge, and thus it is difficult to establish a causal relationship between the presence of the causeways and the changes in the bay. It is possible, however, to simulate conditions with and without the causeways with a computer model. Initial modeling work carried out by Applied Science Associates (ASA) for the Vermont Agency of Natural Resources investigated circulation patterns and effects, including suspended sediment and phosphorus, with and without the causeway.

This study, however, lacked an adequate data set to calibrate and verify its predictions. To address this gap, ASA carried out a field progam to provide a data set with which to run the model and compare model predictions to field findings. The resulting calibrated model could then be used in long-term model simulations of phosphorus concentration and suspended solids concentration and sedimentation in the bay with and without the causeway.

The field study consisted of (1) one month deployments of current meters, water level sensors and a weather station in and near Missisquoi Bay; (2) Drogue studies on the open bay on two days of the equipment deployments; and (3) acquisition of lake level, river flow and weather data from various agencies after the study.

The water level sensor data demonstrated that the water level in the bay rises in response to southerly winds and falls in response to northerly winds and that this difference is generally greater at the north end of the bay than at the south end. The north-south difference rarely reached a magnitude greater than 5 cm (2 inches).

Currents at the center of the bridge were uniform over the measured water column, with little detectable difference in speed or direction with depth. Measurements at the ends of the bridge were unsatisfactory, but calculations of water flux through the bridge opening suggest that flow through the bridge was uniform through the entire cross section.

Additional data, such as the wind data from the weather station and river flow, provided inputs used in forcing the model.

The calibrated model predicts an overall smoother current record than was measured by the current meters at the bridge. This naturally results from the smoothing process inherent in modeling a complex system. The model did a good job of simulating the volume flux through the bridge opening, though, again, yielded a smoother record than was calculated from the current meter data. The model appears to simulate what happens on a larger scale without the tiny variations that are seen at shorter time scales.

The original questions to be addressed in modeling Missisquoi Bay were as follows:

> Will removal of the causeway, either all or in part, have any predicted effects on currents, sediment distribution, and phosphorous in Missisquoi Bay and the Northeast Arm of the Lake?
>
> If predicted effects can be shown, how significant are they? How far will the effects extend into the Bay and the Northeast Arm?

The model predicts that removal of the causeway will reduce phosphorus concentrations and sedimentation (of the finest fractions, only) in Missisquoi Bay by about 1%. The exported phosphorus and suspended sediment will be transported to the Northeast Area of the lake and beyond. Changes in currents are only noticeable in the area of the bridge, where the constriction caused by the causeway results in large currents. Removal of the causeway will result in considerably smaller currents in this area. There will also be an increased gross transport (exchange flow) of water back and forth. This increase in exchange flow produces much smaller flushing benefits because the flows are generally of short duration, with little mixing between water masses.

1. INTRODUCTION

Background

Missisquoi Bay is a small embayment that makes up the northeast corner of Lake Champlain. It covers an area of approximately 77.5 km^2 and has a maximum depth of approximately 4 m (14 ft) (Myer and Gruendling, 1970). Major tributaries to the bay are the Missisquoi, Pike and Rock Rivers. The Swanton-Alburg Route 78 bridge is located at the southern end (mouth) of the bay and consists of causeway sections extending 640 m (2100 ft) from the Swanton shore and 490 m (1600 ft) from the Alburg shore with a bridge section 170 m (560 ft) long (Figure 1.1).

Citizens have observed changes in the bay since the bridge causeway structure was built in 1937. The bay bottom is thought to have consisted primarily of sand, with vegetation clumps, with a series of sandy beaches throughout the bay. There were also areas with clean cobble bottom in shallow water, which provided fish (walleye) spawning habitat. Today the bottom sediments tend to be silt and organic material, and many areas have filled in with vegetation. This has adversely affected fish habitat as well as recreational uses of the bay.

Residents have noted that the bay has deteriorated over time and believe that the causeways at the Route 78 bridge have restricted flushing sufficiently to cause the observed changes. Another potential cause is increased nutrient and sediment loading from the rivers and runoff. With the present observed levels of phosphorus in the bay it is entirely possible that eutrophic conditions are causing the increase in organic materials on the bottom. Changes in land use can increase sediment loads in the tributaries to the bay.

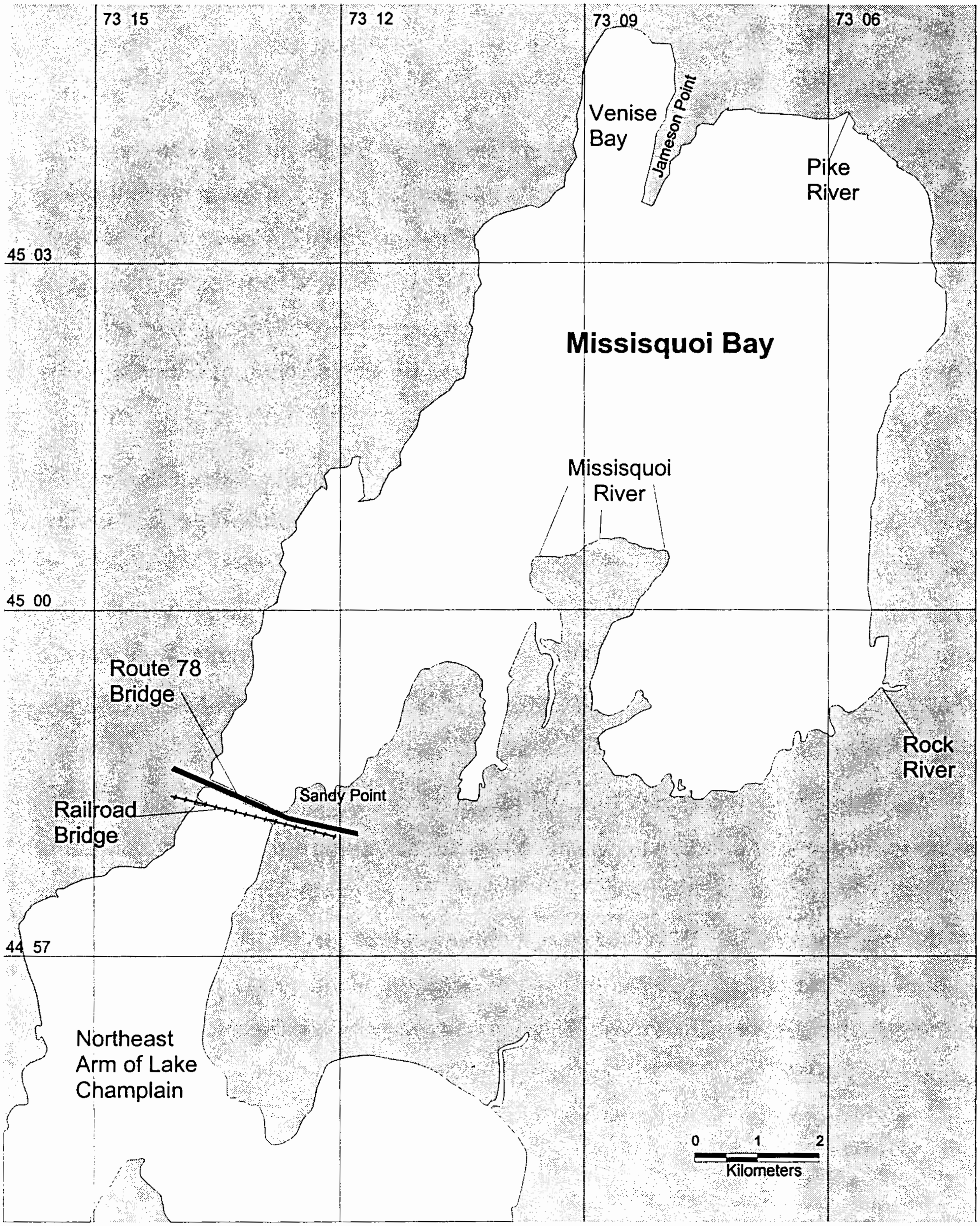

Figure 1.1 Missisquoi Bay study area.

Unfortunately there is a dearth of data relative to the condition of Missisquoi Bay before the construction of the bridge. Thus there is no conclusive way to prove or disprove the potential adverse effects of the causeway on the bay. It is possible, however, to evaluate possible impacts by simulating the conditions with and without the bridge through the use of a computer model.

The Vermont Agency of Natural Resources (ANR) contracted with Applied Science Associates, Inc. (ASA) for a modeling study of Missisquoi Bay which was carried out and completed in March 1997 (Mendelsohn et al., 1997). This modeling study was intended to simulate the hydrodynamic conditions (currents) in the bay and to investigate circulation patterns and effects predicted by model simulations with and without the causeway. Sediment transport and phosphorus model components were also included in the study.

The ASA study ran a matrix of 35 cases to predict the effects of the causeway on the circulation, phosphorus concentrations and suspended solids sedimentation in the bay, and to test the sensitivity of the model's predictions to changes in values of input variables. Findings included:

> Surface currents in the bay generally follow the wind direction, with some return flow evident at depth in some of the deeper areas. The area north of the causeway shows strong variable currents, with circulation cells under some conditions. For all the steady wind cases, net flow through the bridge opening is equal to the inputs from the rivers.
>
> The large differences between cases with differing wind and river flow forcing was not accompanied by corresponding differences between conditions with and without the causeway. The differences observed due to changes in the causeway were limited to a narrow region north and south of the causeway, implying that the causeway does not hydraulically restrict the water flow between the bay and the Northeast Arm.
>
> The direction from which the wind is blowing is very important in determining the flushing characteristics of the bay, due to flow patterns that develop within the bay. Flushing is expected to be least effective with winds origination from the south. The model predicts that there is a slight decrease in flushing time (increase in flushing rate) with the removal of the causeway under most of the conditions tested. The difference, with and without the causeway, increases with increasing wind speed, and with decreasing river flow.

Suspended solids from the rivers are expected to settle mostly within the bay, and sedimentation patterns agree generally with flushing model concentration patterns.

Only small differences in phosphorus distribution are predicted for cases with and without the causeway and these differences are similar to those predicted for flushing and sedimentation.

The resulting model application lacked an adequate data set with which to calibrate and verify its predictions. The missing data most important to such an effort are currents in the bay specific to known wind velocities. To address this gap, a field program was designed and carried out by ASA in October 1996. In addition to measuring winds and currents at the bridge, data on lake height were also collected to evaluate local changes that accompany the observed wind and current changes. During two days of this period, drogue studies were carried out at various areas around the bay to evaluate currents at these locations.

The purpose of this field program was to provide a data set with which to run the model and compare model predictions to field findings. Results could then be used to adjust model parameters to improve the correlation of predictions to data. The resulting calibrated model could then be used in a long-term model simulation of phosphorus concentration and suspended solids concentration and sedimentation in the bay with and without the causeway.

Study Objectives

This study was designed to meet three objectives:

(1) Carry out a one-month field study to provide a real data set of winds, currents under the bridge and lake heights in the region of the bay to be used in the calibration of the existing hydrodynamic model of Missisquoi Bay.

(2) Compare data from the field study to the existing hydrodynamic model and use the data to calibrate and verify the model.

(3) Use the calibrated model to carry out long term simulations of phosphorus concentrations and sediment accumulation in the bay for the present condition with the causeway and for the complete removal of the causeway.

In the following report, the field study and data collection efforts are described in Section 2. Results of the field study are discussed in Section 3. Section 4 describes the models used in the analysis, and the technical approach. Section 5 describes the actual application of the model. The results of the modeling are described in Section 6, and Section 7 presents some conclusions from this work.

2. FIELD STUDY METHODS

The field study consisted of several components: (1) current meters, water level sensors and a weather station were deployed for about one month in or near Missisquoi Bay, internally recording data for later retrieval; (2) Drogue studies were carried out on the open bay on two days during the equipment deployments and water sampling for bay concentrations of phosphorus and total suspended solids were carried out by ANR personnel on two days during this period; (3) Data on lake level, river flows and a remote weather station for the period of the field study were acquired from various agencies following the study.

Long Term Deployments

A total of seven instruments were deployed for the month of October 1996 as part of this study. These included three water level sensors, three current meters (of two types) and a weather station. The distribution of these instruments is shown in Figure 2.1. Water level sensors (WLS) were deployed at three locations, intended to measure water level differences that might occur across the bridge opening and across the width of the bay. The first WLS ("south bridge") was deployed just south of the bridge on a dock piling located between the railroad bridge and the Route 78 bridge on the east shore, at the property of Dennis Ryan. The second WLS ("north bridge") was installed just north of the bridge, on sandy point, at the property of Stephen Boucher. The third WLS ("north bay") was installed on the north side of the bay, near the end of Jameson Point, at the property of Micheline Allard. The south bridge WLS was a Coastal Leasing MicroTide instrument which records absolute pressure over the sensor. Like all the WLSs, it was programmed to record a one minute average value every 10 minutes. Because absolute pressure at the sensor also changes with atmospheric pressure, it is necessary to correct the output from the MicroTide for barometric changes.

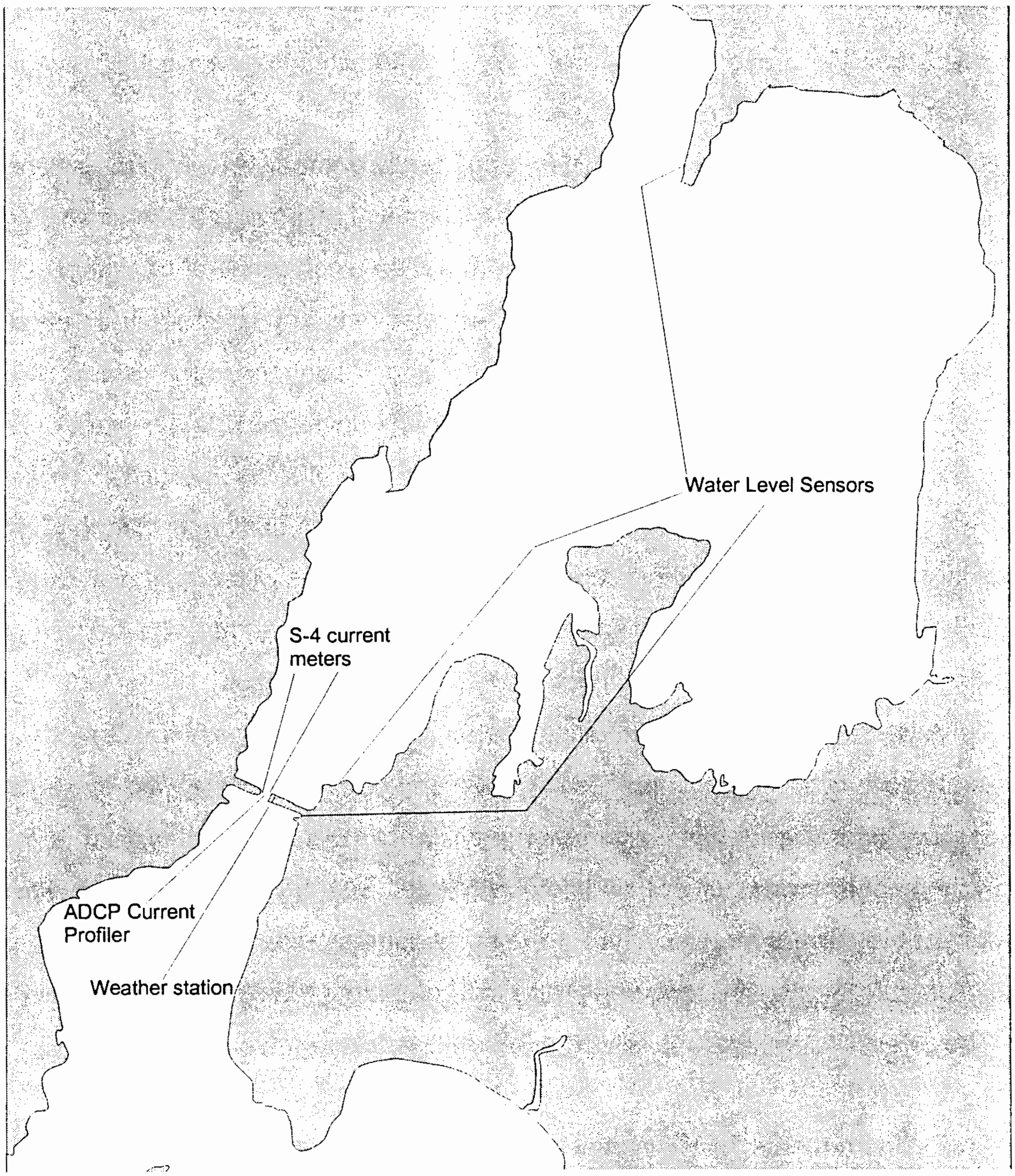

Figure 2.1 Locations of long term installations of instruments deployed as part of the Missisquoi Bay field study.

Data for this correction were provided by the weather station, described below. The North Bridge and North Bay WLS, were both Endeco Model 1029 water level recorders. These instruments record differential pressure, compensating for atmospheric pressure changes, and thus required no corrections.

Because each WLS was installed independently of the others, and they were not surveyed in, it is difficult to verify the absolute water level recorded by each instrument relative to the others. They were intended to record the occurrence of transitory changes of lake level in different parts of the bay relative to one another, and they did this well. In order to set each of the three records at as nearly the same reference point as possible, a period of relative quiescence in the water level, wind and current data was chosen. The average value from about noon October 8 to noon October 10 was set to zero in each of the three records. Differences between stations before and after this period are interpreted as differences in lake level between those stations. Later calm periods in the wind record generally coincide with periods of near-zero differences in heights between gauges, which is taken to verify this assumption.

Three current meters were installed in openings of the bridge. In order to evaluate possible horizontal differences in flow in and out of the bay across the width of the bridge opening, InterOcean S4 current meters were installed at about 1.2 meters depth at the east and west full openings of the bridge. See Figure 2.2 for the relative placement of the current meters. The S4 meter measures currents electromagnetically in the region surrounding the instrument and thus each records currents at a single point. They were programmed to record a one minute average value every five minutes.

An RD Instruments 1200 Khz acoustic Doppler current profiler (ADCP) was installed at the bottom in the center span (Figure 2.2). The ADCP measures currents acoustically throughout the water column and was chosen to evaluate possible vertical differences in flow in and out of the bay. It was programmed to average 130 instantaneous readings every five minutes, recording currents for each 0.25 meter bin from near the bottom to near the surface. Inherent properties of the ADCP function make data within about one meter of the surface or the bottom unreliable.

The weather station used for this study was a Davis Instruments Weather Monitor II with a Weather Link data logger attached. This system was installed in the bridge tender's building on the north side of the east shore of the bridge opening. The anemometer was installed on a 10 foot mast attached to the building. Wind speed and direction, outside temperature and barometric pressure were averaged and recorded every half-hour.

All but two of the above instruments were installed on October 2, 1996. The weather station and south bridge WLS were installed on October 3. All of the instruments were downloaded and reinitialized on October 8, in order to verify their function. They were finally downloaded and removed on October 30.

Drogue Studies

It was beyond the scope of this study to mount current meters in additional locations around the bay. In order to provide calibration data for the model, however, it is desirable to have information on currents at various locations in the bay itself. In order to get as much information as possible in a practical time frame, a drogue study was planned.

A drogue is a device which is suspended in the water column at a fixed depth and with a large enough cross section to be carried along by the water currents while pulling its surface buoy along with it. The design used in this study is shown in Figure 2.3. Large (18 by 36 inch) sheets of PVC are attached together in a cross shape (the drogue) and suspended from a surface buoy by a string which may be adjusted to control the depth at which the drogue hangs. A weight attached to the drogue stabilizes the system.

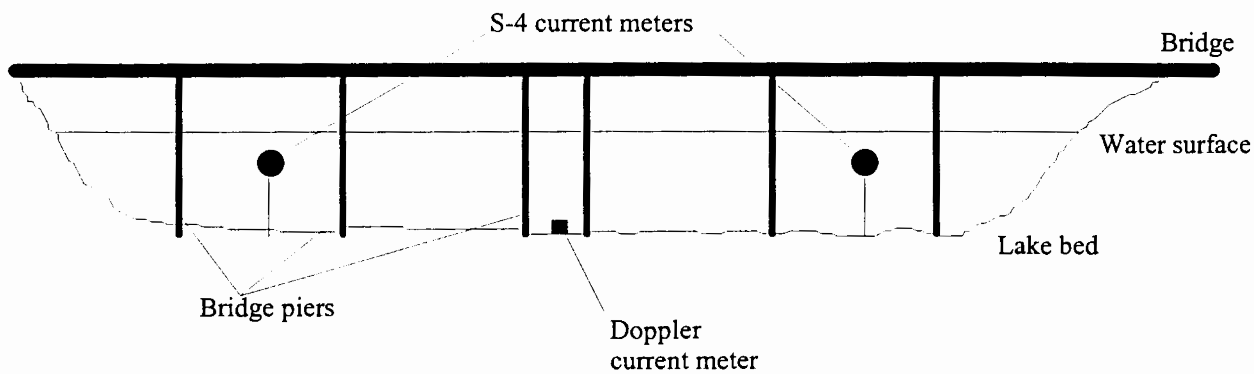

Figure 2.2 Arrangement of current meters deployed at the Route 78 bridge.

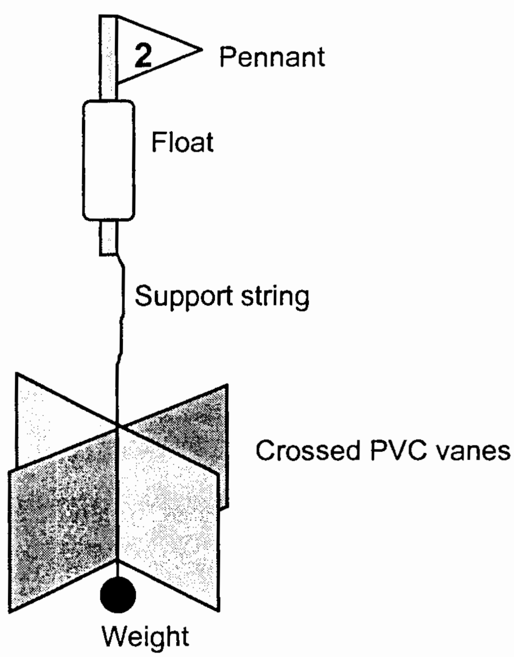

Figure 2.3 Drogue design. Vanes are made up of 18" by 36" sheets of 1/8" PVC

The large cross section of the drogue relative to the surface buoy means that currents at the drogue depth will overwhelm currents and wind effects at the surface so that motion of the surface buoy reflects currents at whatever depth the drogue is suspended.

Drogue study surveys were carried out on the morning and afternoon of October 10 and 29, for a total of four surveys. Each involved the use of eight (October 10) or nine (October 29) drogues. The drogue release sites are illustrated in Figure 2.4. October 10 sites are marked by stars, October 29 sites are marked by circles. At all of the October 10 sites and at the four October 29 sites in the center of the bay, two drogues were released at each site, one suspended at about one meter depth, the other at three meters (two meters for some in shallow areas).

As each drogue was released, a position fix was taken with a global positioning system (GPS) receiver. The GPS unit was provided by the Vermont Agency of Transportation and operated by personnel from the Northwest Regional Planning Commission At approximately one hour intervals, for the following three hours, a new GPS position fix was taken on each drogue. Thus, for most of the studies, there are four position fixes, giving three current velocity measurements (distance and direction of the drogue displacement over the time between fixes). Positions recorded by the GPS were post-processed with base station data recorded by Vermont Agency of Transportation to differentially correct the readings. This increases position accuracy by up to a factor of ten (reducing average error from tens of meters to a few meters).

Additional Data Sets

The field study alone did not provide all the data required for this model calibration. Following the field work, several data sets were acquired by Eric Smeltzer of ANR. These included:

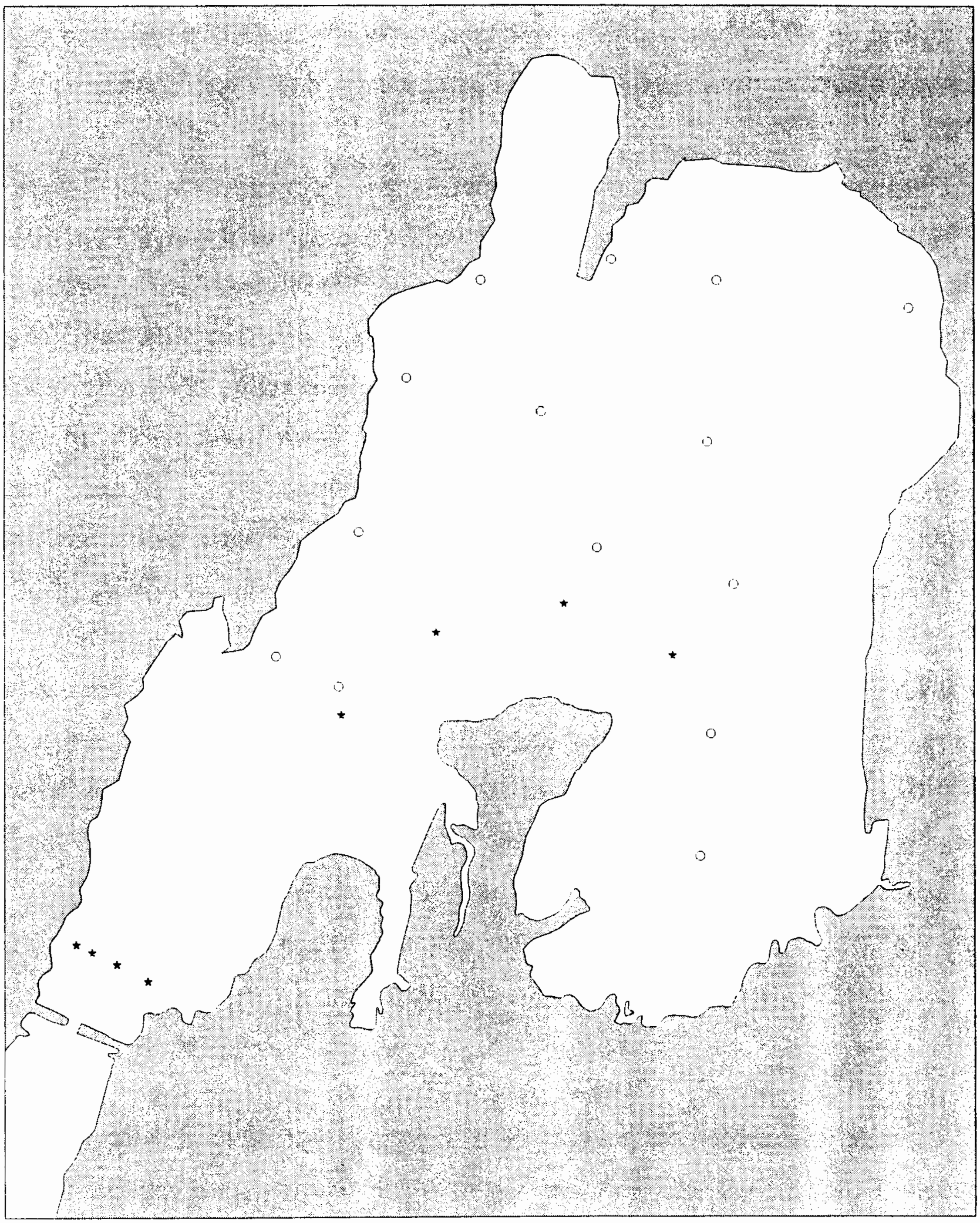

Figure 2.4 Release sites for drogues. Stars are release sites for the October 10 surveys; circles are release sites for the October 29 surveys. Drogues were released at two depths for each site on October 10 and at each of the four sites in the center of the bay on October 29.

(1) Daily time series flows and loads of chloride, total phosphorus and total suspended solids for 1991 and for September and October of 1996. The flow data were provided by the U.S. Geological Survey. Load time series were calculated by VTDEC using tributary monitoring data from 1990-1996.

(2) Monthly mean effluent flow and chloride and total phosphorus concentrations for the Swanton Wastewater Treatment Facility for 1991. These data were taken from the Lake Champlain Diagnostic-Feasibility Study database.

(3) Daily lake levels at Burlington Harbor and Rouses Point for the period October 1995 through October 1996, provided by the U.S. Geological Survey.

(4) Hourly wind data for 9/22/96 to 12/9/96 from the Sandbar Bridge area, provided by Vermont Electric Power Company. This data was requested to verify proper functioning of the weather station set up for the present study.

(5) Lake sampling data for chloride, total phosphorus and total suspended solids from stations in Missisquoi Bay and the Northeast Arm. Data for 1991 were obtained from the Lake Champlain Diagnostic-Feasibility Study database. Data for October 23 and October 28, 1996 were collected by the Vermont DEC for this study.

3. FIELD STUDY RESULTS

Lake Level

The three water level sensors were deployed to measure lake height differences across the bridge opening and across the bay's width. The middle sensor, just north of the bridge, failed to properly compensate for changes in barometric pressure and gave a poor quality record. While discussions with the manufacturer continue on how to best extract a good data record, it happens that this record is inconsequential to the conclusions: the differences between the south bridge and north bay sensors are so small that any sensor located between them, which would reflect some intermediate value, would contribute little to the analysis.

The lake height records from the south bridge and north bay sensors are shown in Figure 3.1. As noted in Section 2, these records are each referenced to a zero value for the mean of each record over the relatively flat period of October 8 to 10. There are small differences between the north and south side of the bay, but they are generally much smaller than the overall bay level changes in the signal. These bay-wide changes result from wind-forcing causing filling and emptying of the bay as well as from larger-scale changes in the overall level of Lake Champlain. The lake height as recorded at Burlington by the USGS is shown in Figure 3.2. Note that the range of the vertical scale is the same as in Figure 3.1, simplifying comparison. Some of the major trends on the Missisquoi Bay level records are accounted for by changes seen at Burlington, such as the generally falling trend from October 2 to October 18 and the sharper rise in level from October 20 to 26. However, there remain some fairly significant lake level changes in the bay at much shorter time scales that are not seen in the Burlington record. These correspond very closely to changes in direction and magnitude of the wind.

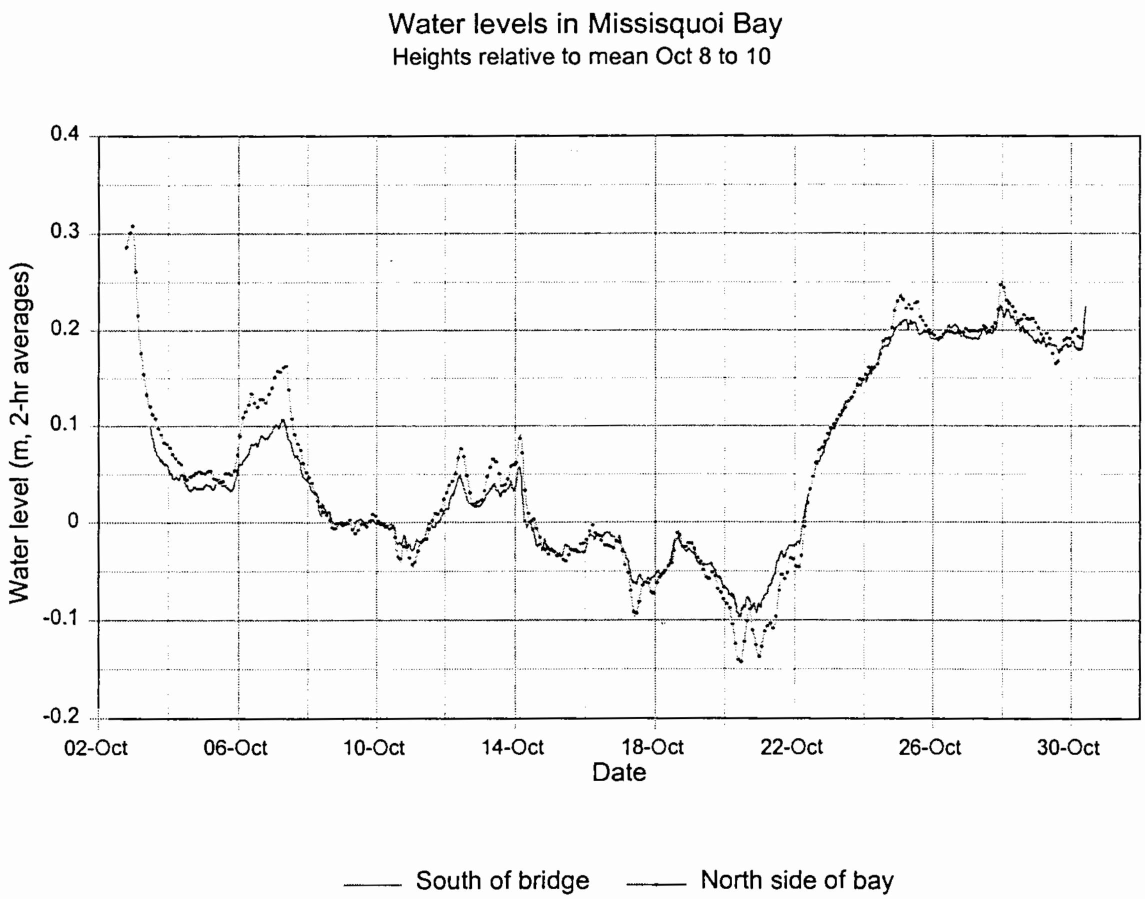

Figure 3.1 Relative water levels recorded for the month of October 1996 at stations south of the Route 78 bridge and on the north side of Missisquoi Bay. The two records have been set to a common level by setting each record to zero during the relatively quiescent period of October 8-10.

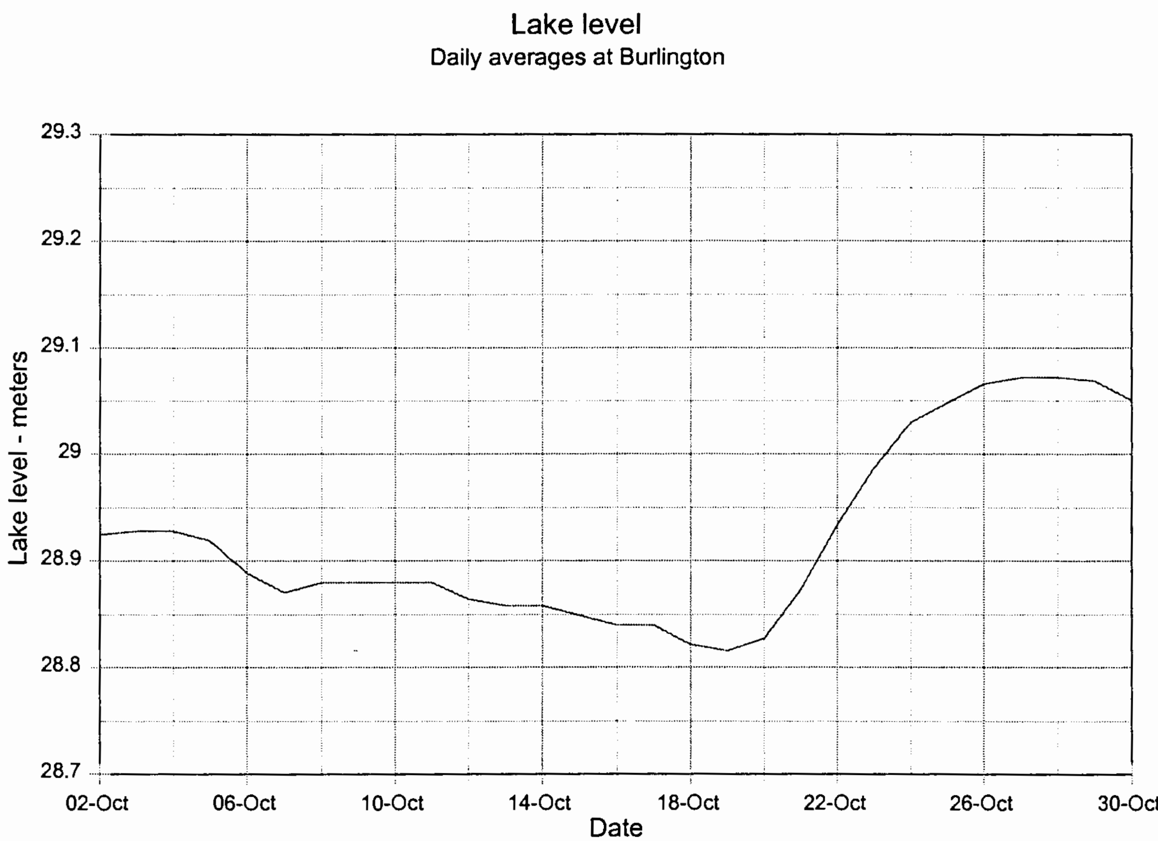

Figure 3.2 Daily average lake level in meters at Burlington VT, as reported by the U.S. Geological Survey.

A stick-plot of the wind data is shown in Figure 3.3. Each line on this plot represents the wind averaged over one half-hour period. The line originates at the time of the record on the horizontal axis and points in the direction towards which the wind is blowing. The length of the line reflects wind speed corresponding to the scale on the vertical axis (so only for north and South winds can you read the speed directly; for others you must compare line length to the vertical scale). The high frequency of parallel vectors in this plot is caused by the fact that the weather station only reports wind directions corresponding to 16 points of the compass. Note that the water level in the bay at both stations rises in response to southerly (northward) winds and falls in response to northerly (southward) winds. Note, too, that this difference is generally greater at the north end of the bay than at the south. Figure 3.4 is a plot of the difference between the two stations. The vertical scale is increased nearly five-fold here compared with Figure 3.1. Most of the differences in water height across the width of the lake are accounted for by the speed and direction of the wind shown in Figure 3.3. The expanded scale makes some of these differences look large. Note, however, that the largest of these differences, occurring only during a couple of events over the month, correspond to about five centimeters or two inches of difference. The correspondence between water height differences and wind can be seen most clearly in Figure 3.5. In this Figure, each lake height difference is plotted against the wind recorded for that time period. The wind value is given as the value of the vector component of the wind traveling straight through the bridge opening. Thus, northward-blowing winds will be generally positive and southward-blowing winds will be generally negative.

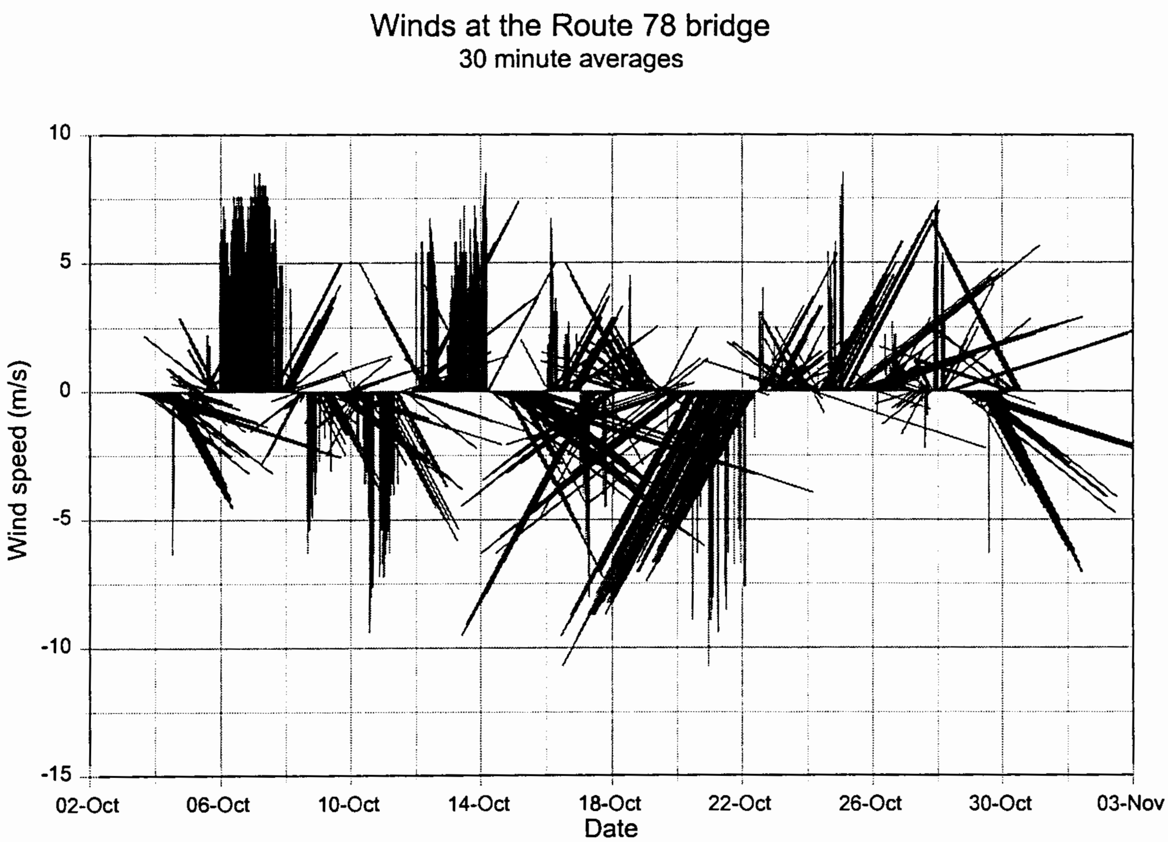

Figure 3.3 Stick plot of half-hourly average wind data from the Route 78 bridge. See the text for an explanation of this plot.

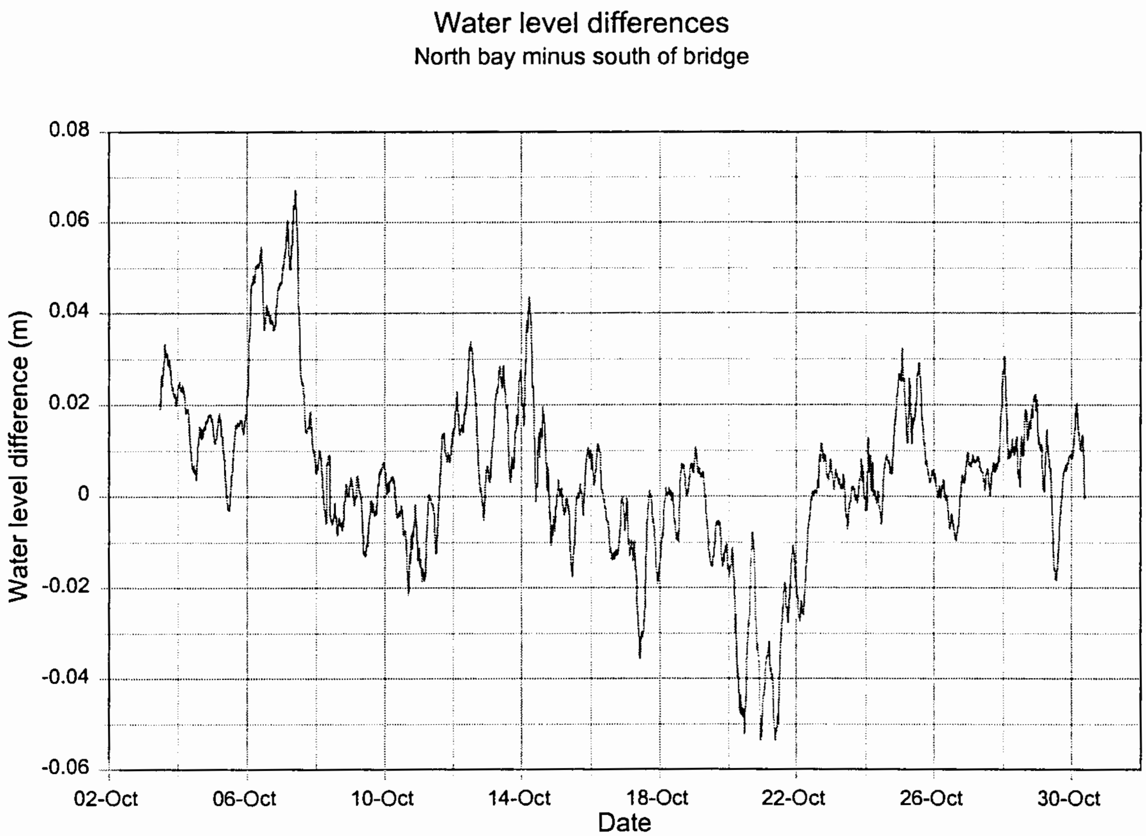

Figure 3.4 Water level differences between the north and south sides of Missisquoi Bay vs the vector component of the wind blowing directly through the Route 78 bridge opening.

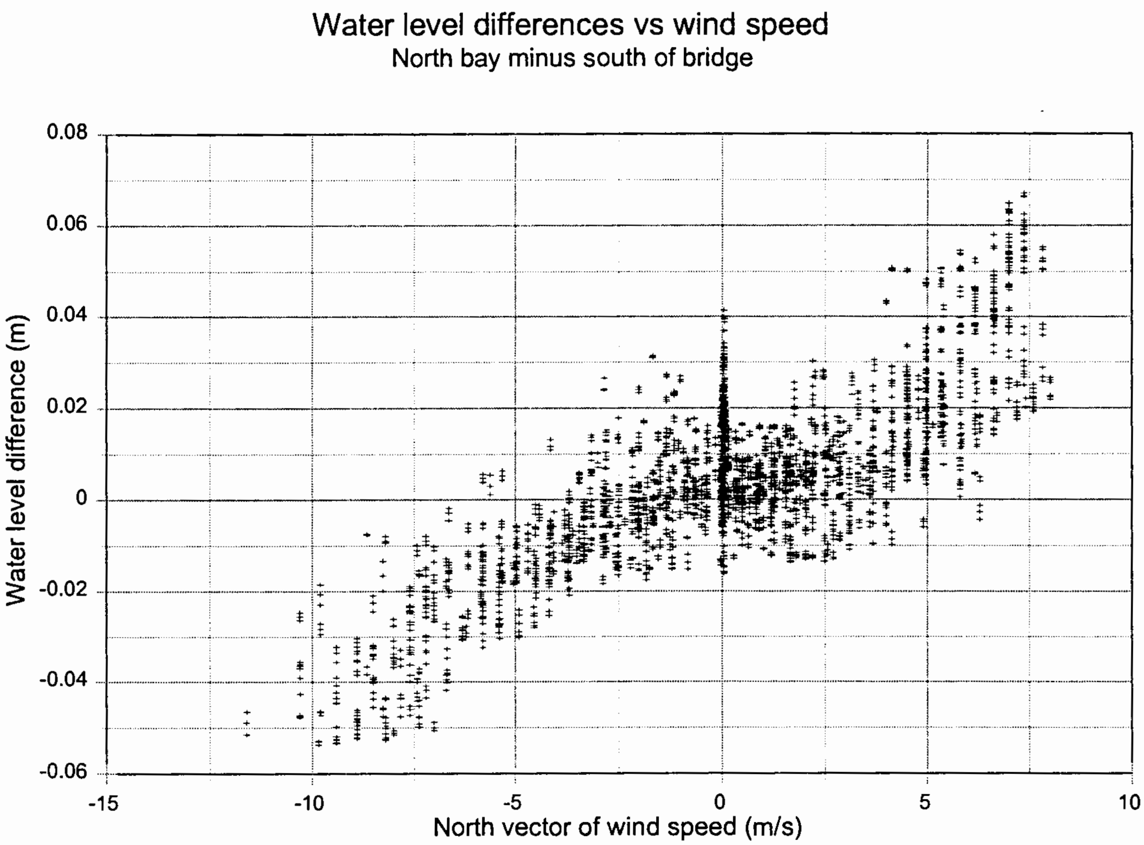

Figure 3.5 Water level differences between the north and south sides of Missisquoi Bay vs the vector component of the wind blowing directly through the Route 78 bridge opening.

Currents

Current measurements included the ADCP, mounted on the bottom at the center of the bridge opening, monitoring most of the overlying water column, and the two S4 meters, suspended near the ends of the bridge opening, monitoring currents across the width of the bridge.

Profiles of currents measured by the ADCP were routinely quite uniform surface to bottom, with little indication of differential surface and bottom flow. The ADCP cannot measure currents in the half-meter closest to the bottom so that alterations of the currents due to bottom friction are not obvious. The ADCP creates a very large data record which is difficult to summarize and communicate concisely. Data from the one, two three and four meter bins were extracted and are presented in Figure 3.6 as a progressive vector diagram. Note that the depths given are measurements up from the top of the ADCP (which is about one foot off the bottom), in a water column of about five and a half meters, and that each bin represents the average currents measured in one quarter meter of water centered about the nominal distance.

The progressive vector diagram can best be understood if one imagines a particle in the current flow at the time of each measurement. For each time period, we calculate the distance that particle would travel over the time between measurements, as well as the direction of travel. This movement (distance and direction) is a vector. The vectors for each time period, for the whole period of ADCP deployment, are added together, end to end, to produce the progressive vector diagram.

Several features of Figure 3.6 should be noted. First, it is evident that over the course of this study, the currents from near the surface to near the bottom were quite uniform. The lines representing the four depths are mostly parallel, with a small divergence. At the end of the deployment, the vector sums vary between depths by at most a few percent of the total distance, with a divergence angle of less than 10 degrees. Much of the divergence between depths appears to occur during periods of reversal in flows in or out of the bay, when there is a side-stepping of the line directions.

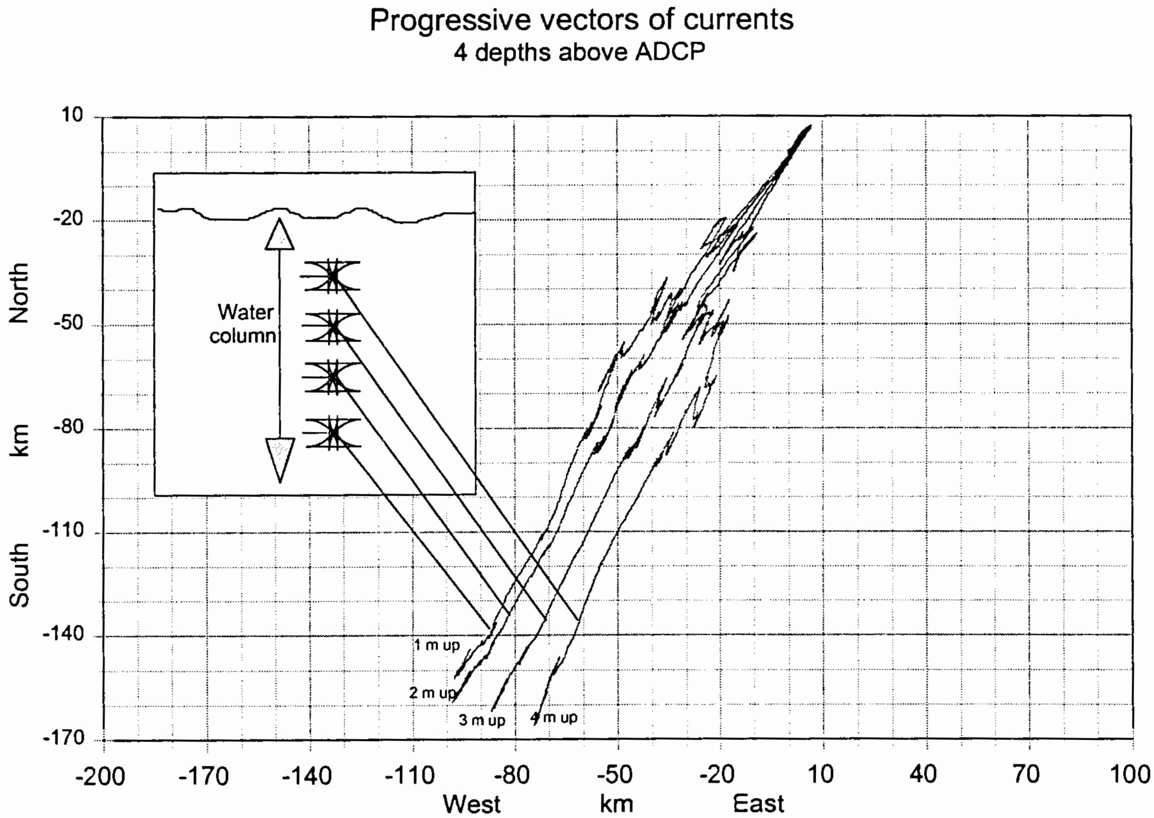

Figure 3.6 Progressive vector diagram of currents measured at the center span of the Route 78 bridge at four depths above the ADCP. See the text for an explanation.

This lateral motion appears to be more towards the west near the bottom and more toward the east near the surface.

The overall angles of these lines correspond very closely to the angle of the long axis of the bay and normal to the bridge opening. That is, the water passes straight through the bridge opening. If should come as no surprise that almost all the transport is negative, to the south and west, reflecting the net river flow inputs to the bay passing through the bridge and out of the bay. The occasional, usually short-lived, reversals in flow are the result of strong southerly winds reversing this mean flow, forcing water back into the bay.

An alternate view of ADCP currents is presented in Figure 3.7. The five-minute records recorded by the ADCP were averaged into half-hour records for this plot. Each line on this plot originates at the time of the record as shown on the horizontal axis and points in the direction towards which the currents were flowing at 2.5 meters above the ADCP. The length of each line (not its end point) represents the current speed as shown on the vertical scale. To get actual current speed, the line length would have to be compared with the scale.

Figure 3.7 makes it clear just how variable the currents are at the bridge opening with alternating periods of northeast (filling the bay) and southwest (draining the bay) currents. Currents of up to and exceeding one knot (about 50 cm/second) were not uncommon during this period, occurring for some period of time about every couple of days. Overall, currents are dominated by the river flow-generated southwest net transport much as would be expected from the progressive vector analysis. Compare the currents shown in Figure 3.7 with the stick plot of winds in Figure 3.3. The effect of the wind is clearly evident in the current record, but the currents are more complex. While a strong southerly wind will cause currents to flow into the bay, these reversed currents can only last a short time before the build-up of water level in the bay and the continuous addition of water from the rivers overwhelms the wind effect. Thus, more frequent and rapid changes in direction are seen in the current record than are apparent in the wind record.

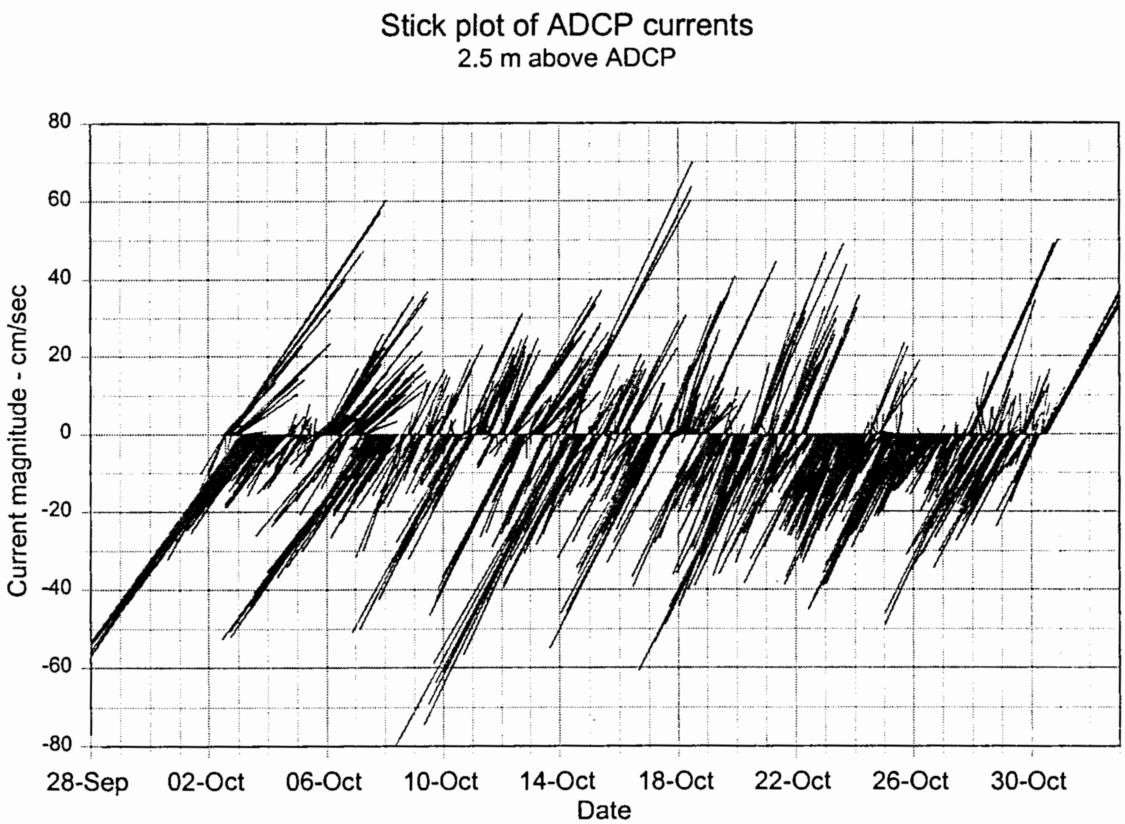

Figure 3.7 Stick plot of currents measured at 2.5 meters above the ADCP at the center span of the Route 78 bridge. Each line represents a half-hour average. See the text for an explanation.

A sudden change in wind direction can be accompanied by a greatly amplified change in currents such as the morning of October 14 when currents flowing into the bay at over 50 cm/sec (one knot) reversed to flow out of the bay at over 50 cm/sec in one hour as the winds changed from southerly to north westerly.

The InterOcean S-4 current meters at the ends of the bridge opening were intended to detect horizontal shear in current flows in and out of the bay near the surface. Initial data analysis of the S-4 records suggested that while currents were similar in magnitude, directional data were quite erratic. It appears that the compasses on the S-4 meters were not functioning properly. The reason for this is not clear, but InterOcean has suggested that if there were enough iron in the bridge structure (such as the deck substrate and the rebar in the piers) that they could have been shrouded by the bridge, negating the compass function.

It was finally decided to dispense with the S-4 data records when they were shown to be inadequate to account for flow under the bridge, while the ADCP data alone worked quite well. The bay water levels and river flows to the bay were tabulated over the time course of the current meter deployments and used to calculate water flux under the bridge. This flux was calculated as the sum of the flows from the Missisquoi, Pike and Rock Rivers, with a small correction for ungaged flows, plus the net bay volume change over the study period. Current meter data - all three together, each for its own segment of the bridge, as well as the ADCP alone for the entire bridge cross section - were likewise used to calculate water fluxes. The few soundings taken to set up the current meter deployments were used together with drawings of the bridge to evaluate the cross section area of the bridge opening. (Drawings alone were inadequate, as the bottom proved to be several feet deeper in some areas than shown in the drawings.) Current meter fluxes were calculated as the product of the current through the bridge and the cross sectional area of the bridge opening below the water surface, summing these values for each current record over the period of deployment. The resulting calculations showed that about 95 million cubic meters of water should have passed under the bridge out of the bay during this period to account for river flows and lake level changes. Calculating flux with the S-4 and ADCP data included could account for only about half of this amount, while using only ADCP data for the whole bridge opening yielded a flux of 96 million cubic meters of water flowing out of the bay, which agrees with the river/lake level data to a precision better than our knowledge of the bridge opening area.

Weather

The weather station was installed primarily to provide data on wind speed and direction at Missisquoi Bay and incidentally provided barometric pressure data, useful in providing corrections for one of the water level sensors.

A stick plot of wind data has already been shown, Figure 3.3. Wind data are also given here as wind speed (Figure 3.8) and wind direction (Figure 3.9) over time. The stepped appearance in the direction plot results from the fact that the direction data are only recorded as 16 points of the compass. Where there are prolonged periods of no apparent wind change (e.g., October 6, October 13) it was decided to verify that the station was providing good direction data. Comparisons were made to a record from Sandbar Bridge which corroborated the data here to within the precision of the instrument. There were enough differences between the records, especially in wind magnitude, that it is clearly justified to use the local wind station data for forcing the model instead of relying on a more remote data source.

Drogue Study

A total of four drogue studies were carried out on the mornings and afternoons of October 10 and 29. On both days there were northerly to northwesterly winds which were about five to ten knots in the morning and became brisk, 15 knot half-hour means, in the afternoon. The rate and direction of drogue movement during these studies are summarized in Table 3.1, which gives the mean values for each drogue over the whole study. More detailed data are provided in the Appendix, Table A-1, which gives the speed and direction of transport for each reading interval. Two figures illustrate the movements of the drogues. Figure 3.10 shows each position recorded for all of the

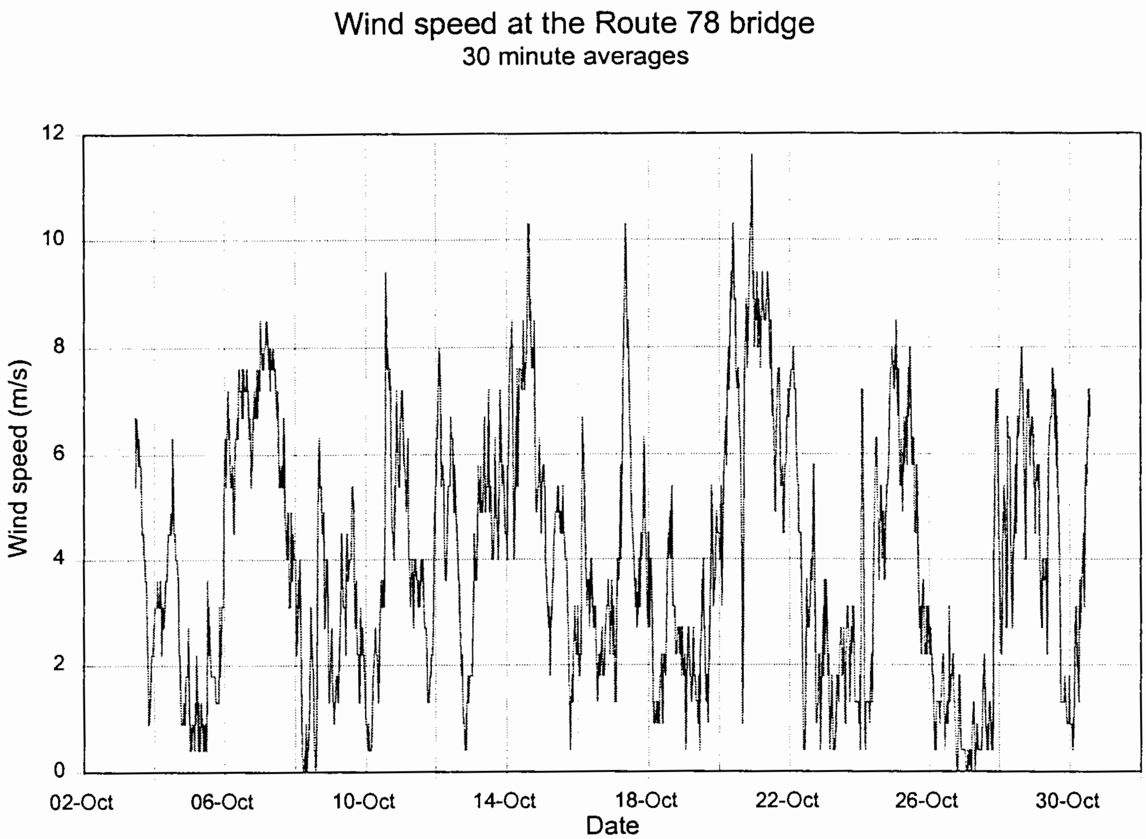

Figure 3.8 Wind speed at the Route 78 Bridge. Values are half-hour averages.

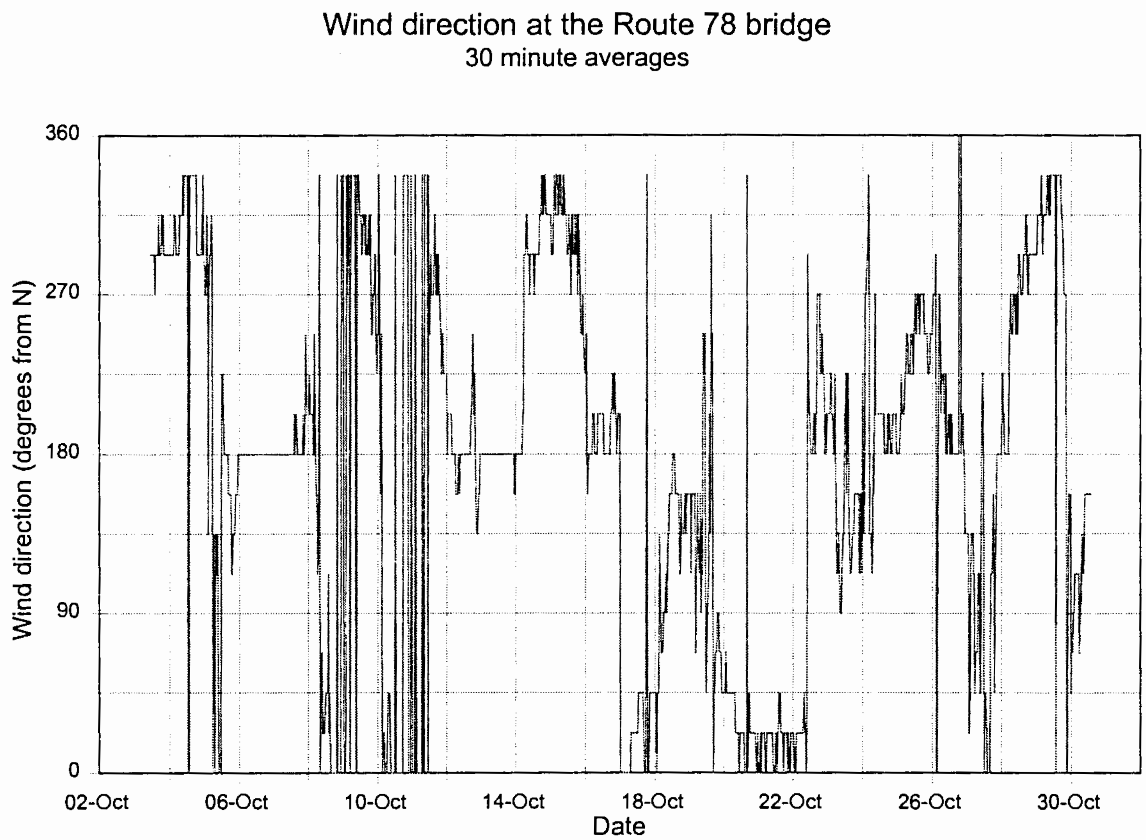

Figure 3.9 Wind direction at the Route 78 Bridge. Values are half-hour averages. The stepped appearance of the record results form the fact that only 16 points of the compass are recorded by the weather station data logger.

Table 3.1 Summary drogue study data for the Missisquoi Bay field study, October 10 and 29, 1996.

Drogue number	Depth (m)	Comments	Speed (cm/s)	Direction (deg, true)	Longitude (final)	Latitude (final)
Morning survey, October 10						
1	1		1.23	188	-73.2203	44.9811
2	2		1.45	209	-73.2209	44.9811
3	1		1.98	198	-73.2183	44.9797
4	3		1.89	213	-73.2187	44.9800
5	1		2.27	197	-73.2143	44.9782
6	3		2.25	206	-73.2146	44.9783
7	1		3.25	217	-73.2106	44.9760
8	2		3.28	214	-73.2106	44.9759
Afternoon survey, October 10						
1	1		4.95	181	-73.1773	45.0031
2	3		4.24	184	-73.1776	45.0039
3	1		5.59	233	-73.1691	45.0140
4	3	Grounded	3.89	238	-73.1671	45.0155
5	1		4.68	195	-73.1424	45.0163
6	3	Grounded ?	3.97	199	-73.1425	45.0172
7	1		6.59	182	-73.1235	45.0081
8	3	Grounded ?	2.98	184	-73.1232	45.0120
Morning survey, October 29						
1	1		2.55	109	-73.1627	45.0463
2	1		1.60	148	-73.1528	45.0570
3	1		3.35	162	-73.1429	45.0401
4	3		2.93	168	-73.1434	45.0404
5	1		2.87	159	-73.1160	45.0375
6	3		2.02	170	-73.1168	45.0381
7	1		2.75	127	-73.1302	45.0593
8	1		1.51	102	-73.1140	45.0580
9	1		9.42	153	-73.0798	45.0484
Afternoon survey, October 29						
1	1		1.75	158	-73.1175	44.9906
2	1		4.56	80	-73.1105	45.0068
3	1		0.47	-77	-73.1135	45.0234
4	3		0.16	257	-73.1131	45.0233
5	1		3.60	163	-73.1337	45.0244
6	3		3.02	165	-73.1341	45.0248
7	1		1.71	126	-73.1723	45.0285
8	1		2.95	138	-73.1850	45.0131
9	1		5.04	115	-73.1714	45.0096

drogues in the four studies, with increasing symbol size representing later readings. In Figure 3.11, symbols are placed at the release site of each drogue, and arrows show the direction and relative speed of each drogue. Each arrow is drawn to the length of the actual distance traveled by that drogue over the whole study. Only the surface drogue is indicated where deeper drogues were also deployed (all October 10 drogues and the four release sites in the middle of the bay on October 29). The deeper drogue usually traveled in the same direction and slightly less distance than the surface drogue. Close examination of Figure 3.10 in which individual positions are shown, will reveal the separate terminal positions of the surface and bottom drogues. Four position fixes were taken for each drogue except during the October 29 afternoon study, when only three position fixes were taken on each drogue.

All of the drogues deployed on the morning of October 10, just north of the causeway, traveled uniformly toward the causeway, with a gradient of increasing transport rate toward the east side. Mean transport rates ranged from 1.23 to 3.28 cm/sec, with very little difference between one meter and the deeper (two or three meters) drogues. That afternoon, drogues were released at one and three meters around the Missisquoi River delta. Transport was generally downwind, and rates picked up, consistent with the increase in wind speed. North of the west point of the delta there was a strong westward displacement of the drogues relative to the others. Mean surface speeds varied from 4.68 to 6.59 cm/sec. Several of the deep drogues probably hit bottom late in the survey, but comparisons earlier in the study suggest that deeper drogues were traveling somewhat slower than at the surface.

On the morning of October 29, nine drogues were deployed at seven locations in the north half of the bay. In the center of the bay, transport was directly downwind at two to three cm/sec, surface or deep. Drogues along the west shore and off Jameson Point were transported directly offshore. In the center of La Grande Baie, there was slow transport directly to the east, while along the east shore of La Grand Baie the drogue moved along the shore at up to 10 cm/sec.

The final deployment, on the afternoon of October 29, took place along the southern part of the bay. Transport along the western shore was once again directly

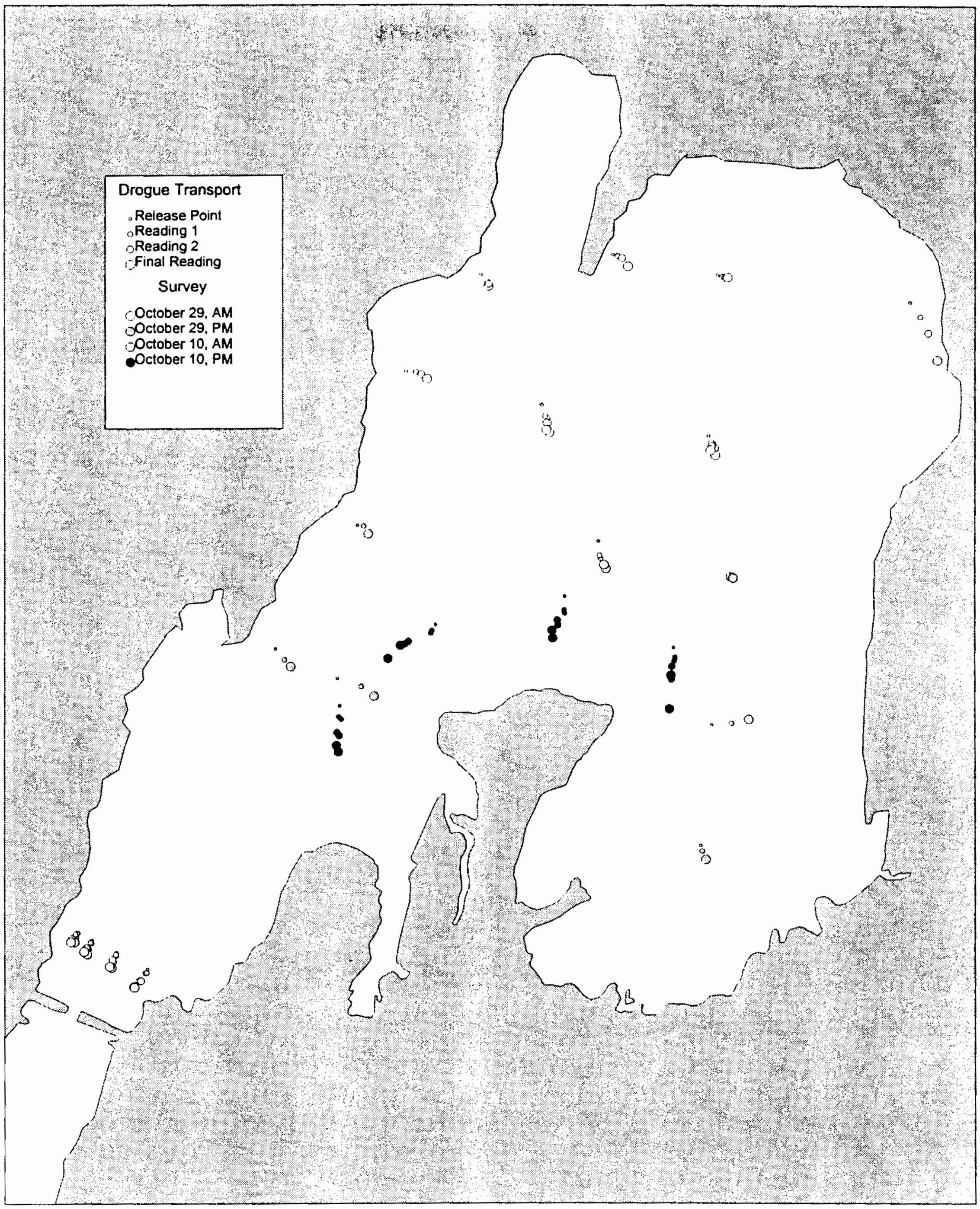

Figure 3.10 Positions of drogues for each reading during the four drogue studies. Note that two drogues, shallow and deep, were deployed at some of the release locations. Each individual drogue is represented by four symbols for each of the studies except for the October 29 afternoon study, when only three readings were taken for each drogue. Winds were predominantly from the north on October 10 and from the north-northwest on October 29.

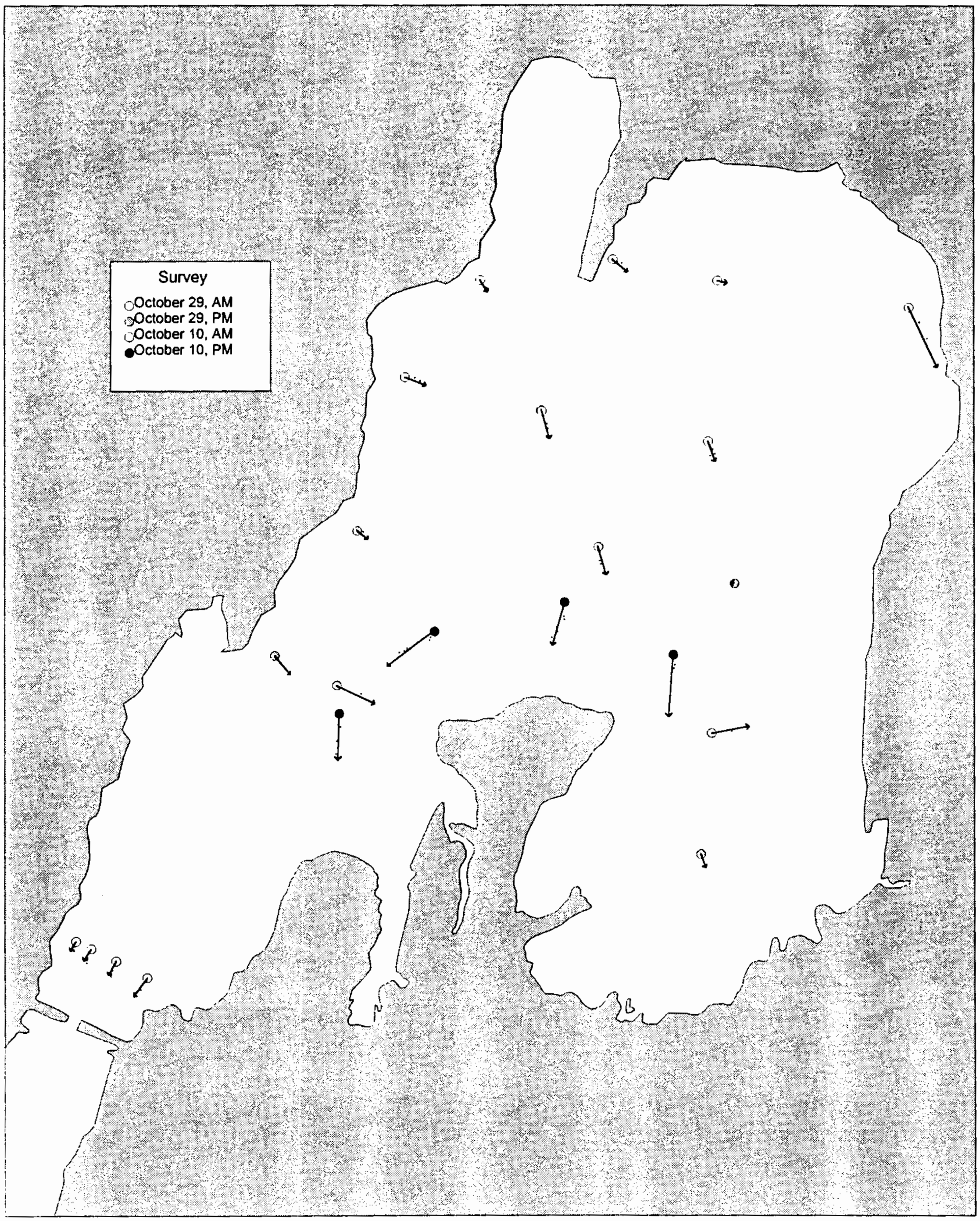

Figure 3.11 Transport of each drogue during the four drogue studies. Symbols are placed at the release site of each drogue. The arrows, which represent transport speed and direction, are drawn the length of the actual distance traveled by the surface drogue during the full study. Winds are predominantly from the north on October 10 and from the north-northwest on October 29. See the text for further explanation.

offshore. Drogues deployed east and west of the Missisquoi River delta moved strongly eastward at about 5 cm/sec. In the middle of the embayment east of the delta transport was directly downwind, as it was in mid-bay, but a drogue placed east of the mid-bay drogue hardly moved at all. These mid-bay drogues were deployed in surface/deep pairs that showed very similar movements at both depths.

Other Data

River flow and load data as provided by ANR for the period of the field study are shown in several figures. Figure 3.12 shows daily river flows for the Missisquoi and Pike Rivers for October 1996. Data for the Rock River were not available for this period, but it has been shown in the past to have less than one third the flow of the Pike River and thus provides only a small contribution of water volume. Daily phosphorus loads from these two rivers are shown in Figure 3.13. These are not measured loads, but rather are values calculated from river flows and regressions of water concentration on river flow from historical data. This same approach was used to calculate total suspended solids loads, shown in Figure 3.14. Water quality samples, including total phosphorus and total suspended solids concentrations, were collected from numerous stations in and near Missisquoi Bay by ANR personnel on October 23 and October 28, 1996. Some of the results of these surveys are shown in the following Figures. Figures 3.15 and 3.16 show the distribution of total phosphorus and total suspended solids, respectively, found in the bay from the October 23 survey. The same data from the October 28 survey are shown in Figures 3.17 and 3.18. October 23 was a period when peak loads of phosphorus and suspended solids were being delivered to the bay (Figures 3.13 and 3.14) and this peak was just past on October 28. There is enough natural site to site variation in these constituents that it is not clear that any pattern emerges from these distributions. The patterns seen here may have resulted from the patchy distribution of blue-green algae, which were in a sustained bloom at the time of the study. In addition, the variations probably reflect transitory sources such as resuspension, resulting from more immediate weather events, as well as local circulation patters accompanying this weather, as much as they do the riverine sources that may ultimately control long term mean values that would be found in the bay. Many more points in time would be required to evaluate typical concentration distributions caused by loads from the rivers.

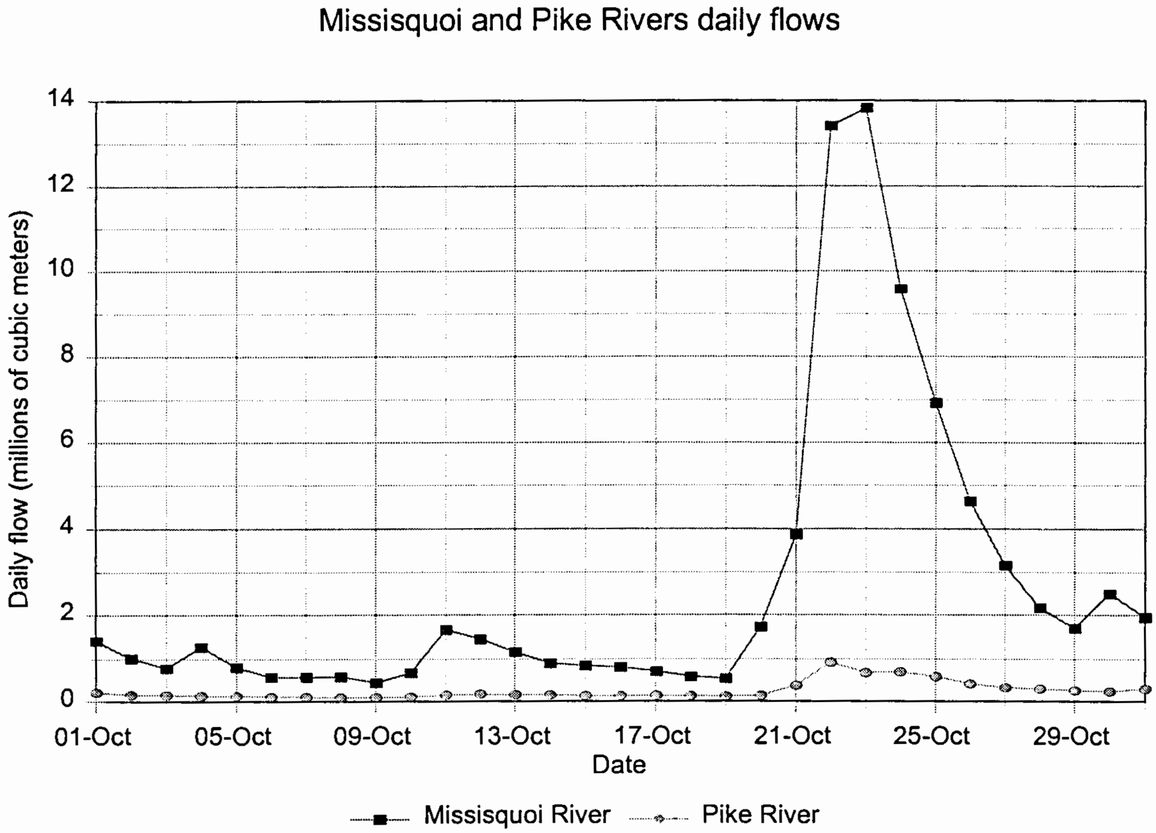

Figure 3.12 Daily flows of the Missisquoi and Pike Rivers. USGS and Quebec Ministry of Environment and Wildlife data provided by ANR. Values are adjusted to reflect ungauged areas as well as gauged flows.

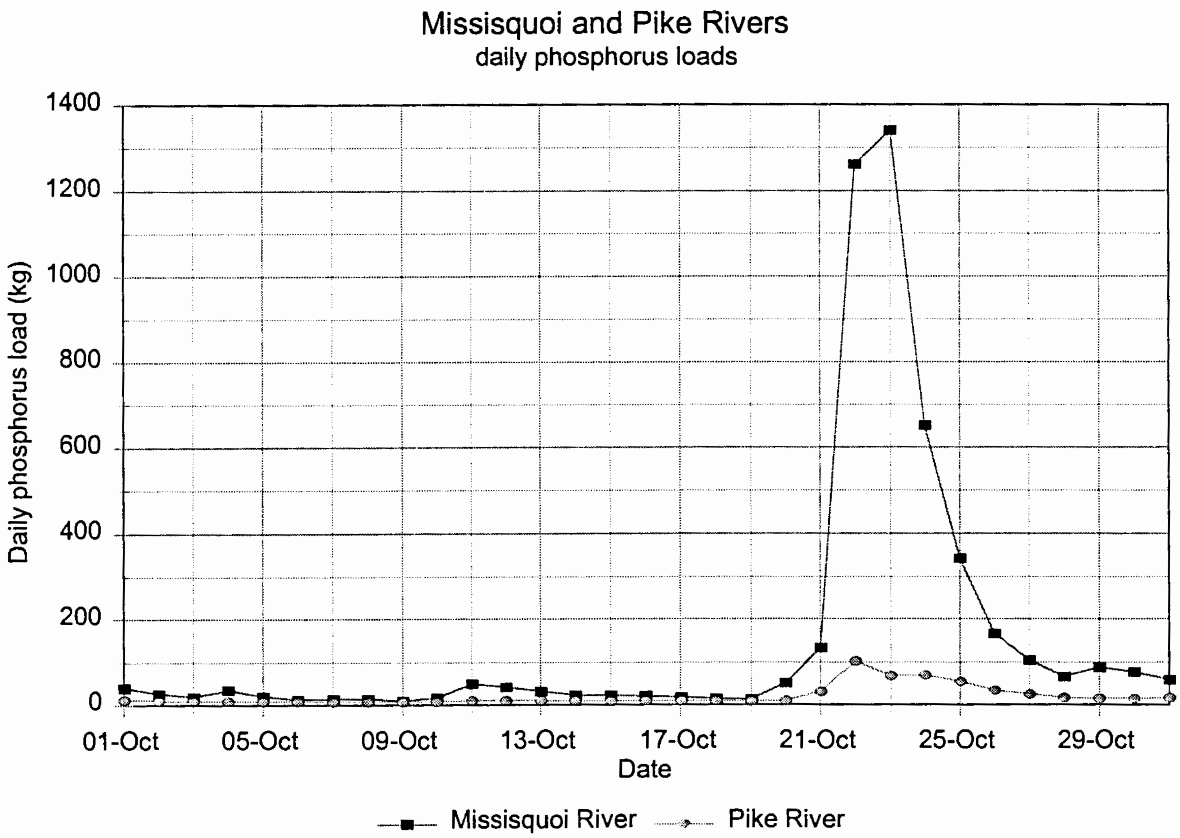

Figure 3.13 Daily total phosphorous loads from the Missisquoi and Pike Rivers. Values provided by ANR, are calculated from a regression of concentration vs. flow.

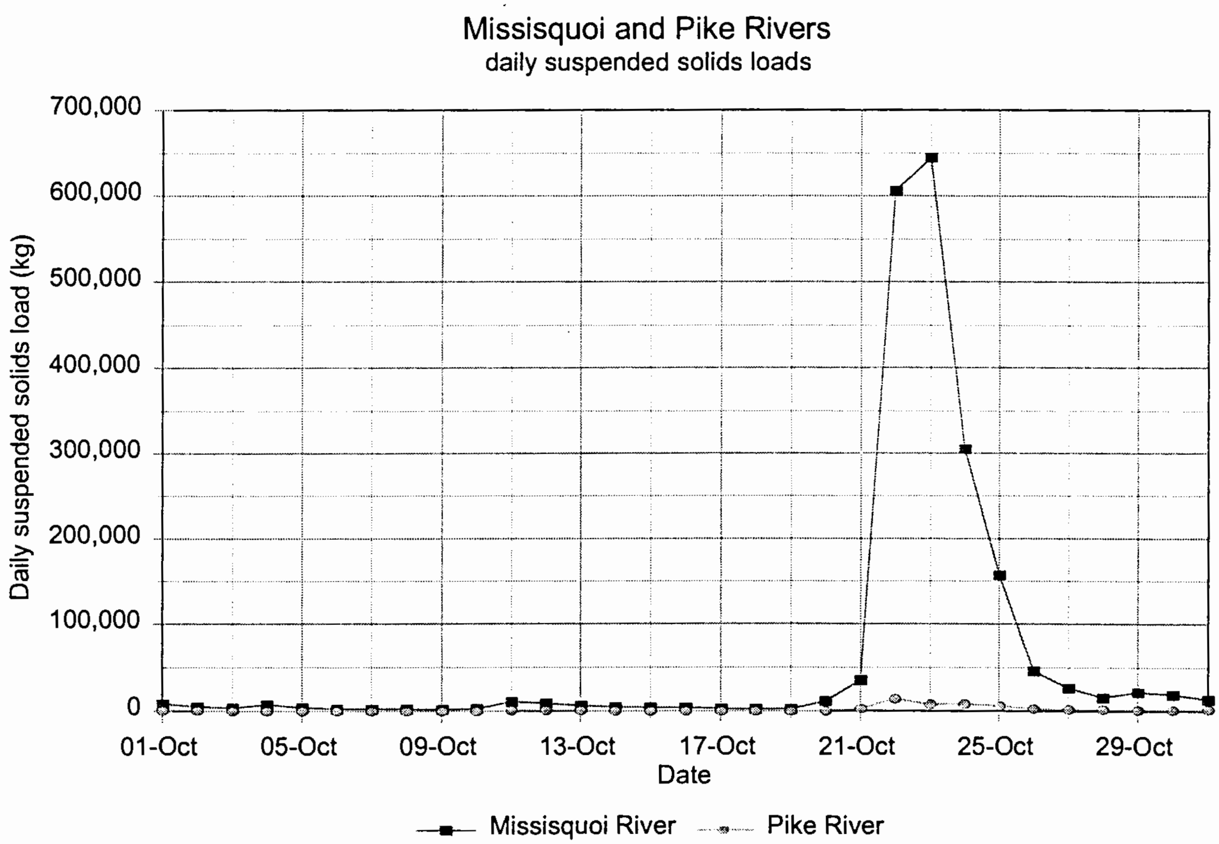

Figure 3.14 Daily suspended solids loads from the Missisquoi and Pike Rivers, provided by ANR. Values are calculated from a regression of concentration vs. flow.

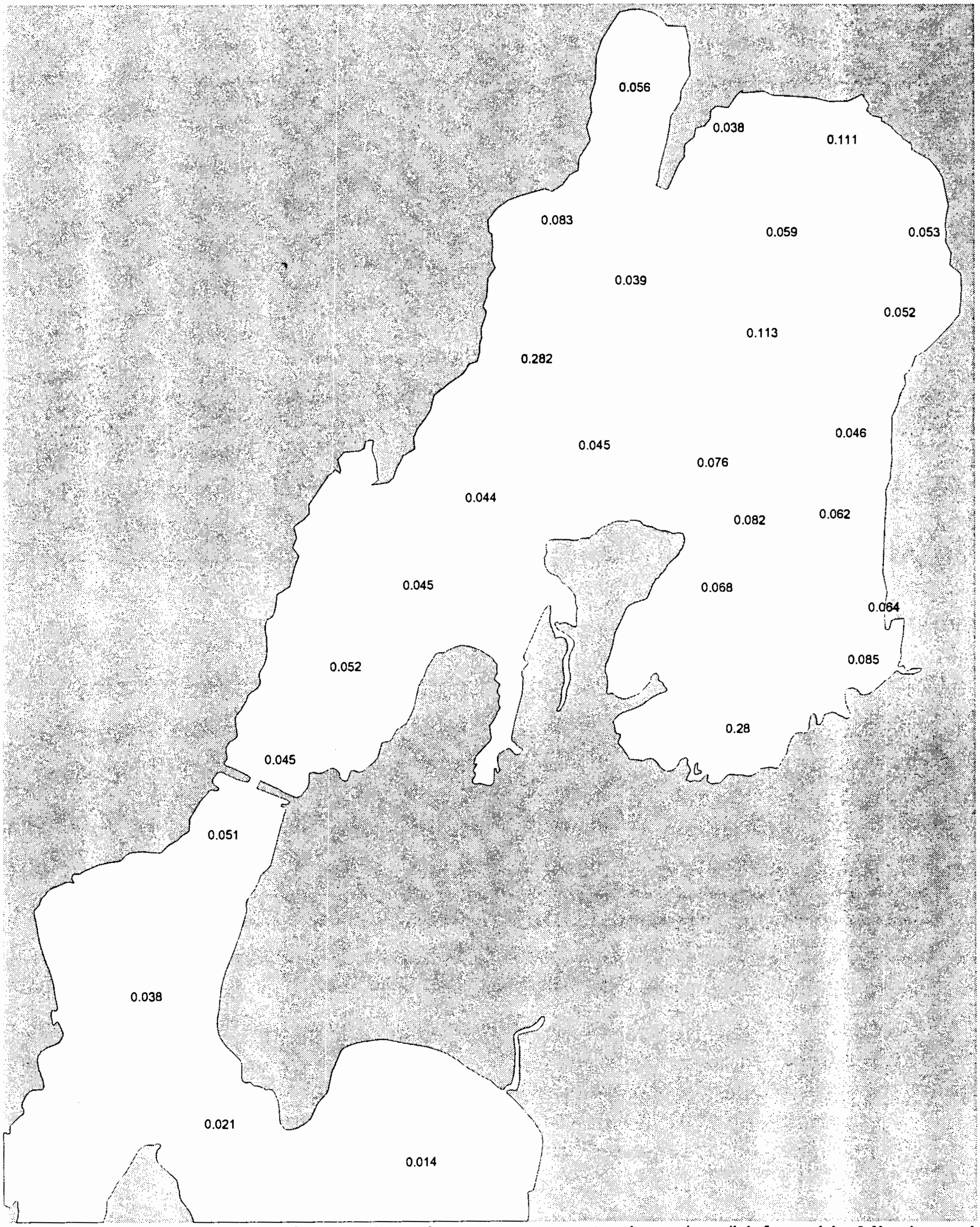

Figure 3.15 Distribution of total phosphorous concentrations (mg/L) found in Missisquoi Bay on October 23, 1996.

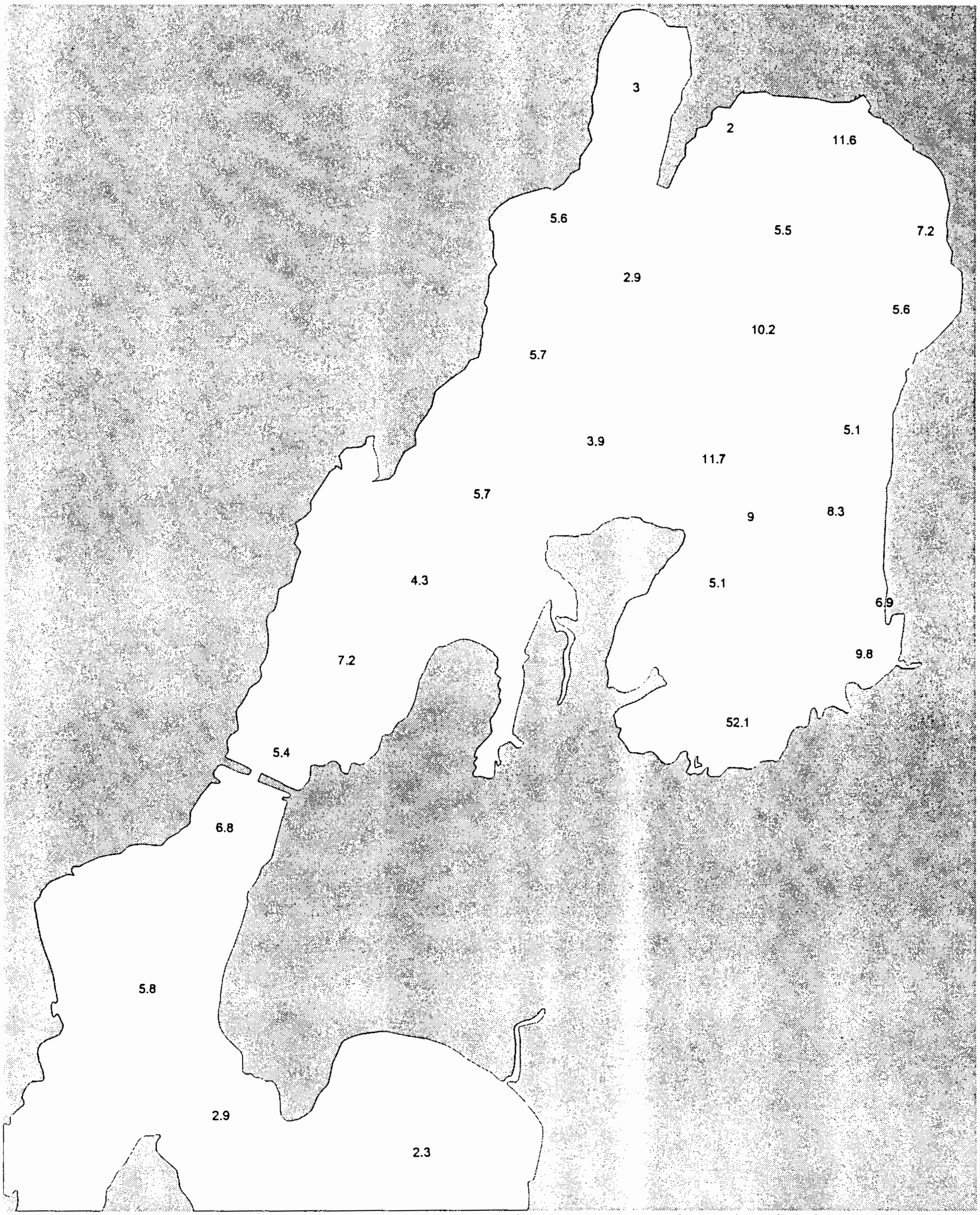

Figure 3.16 Distribution of total suspended solids concentrations (mg/L) found in Missisquoi Bay on October 23, 1996.

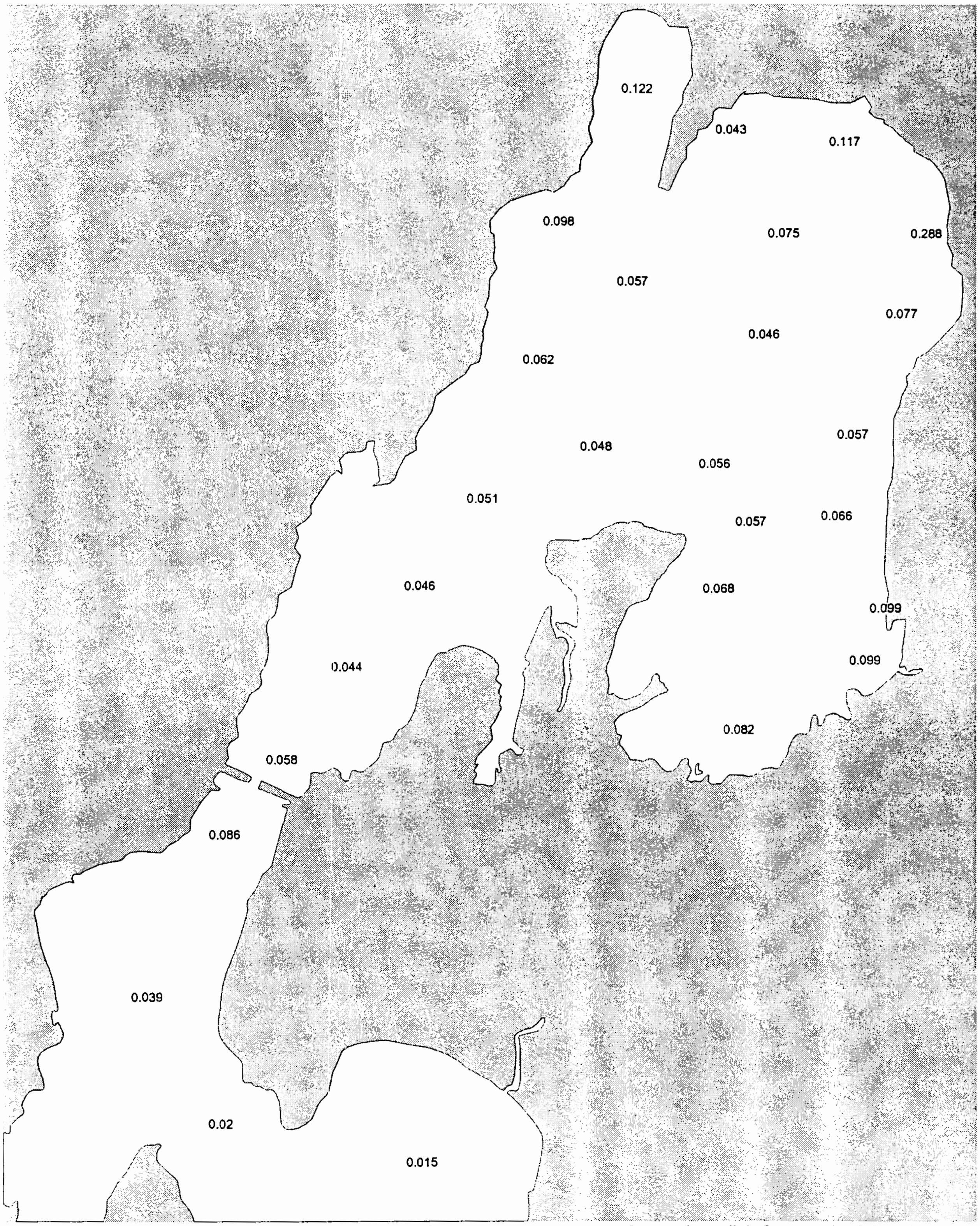

Figure 3.17 Distribution of total phosphorous concentrations (mg/L) found in Missisquoi Bay on October 28, 1996.

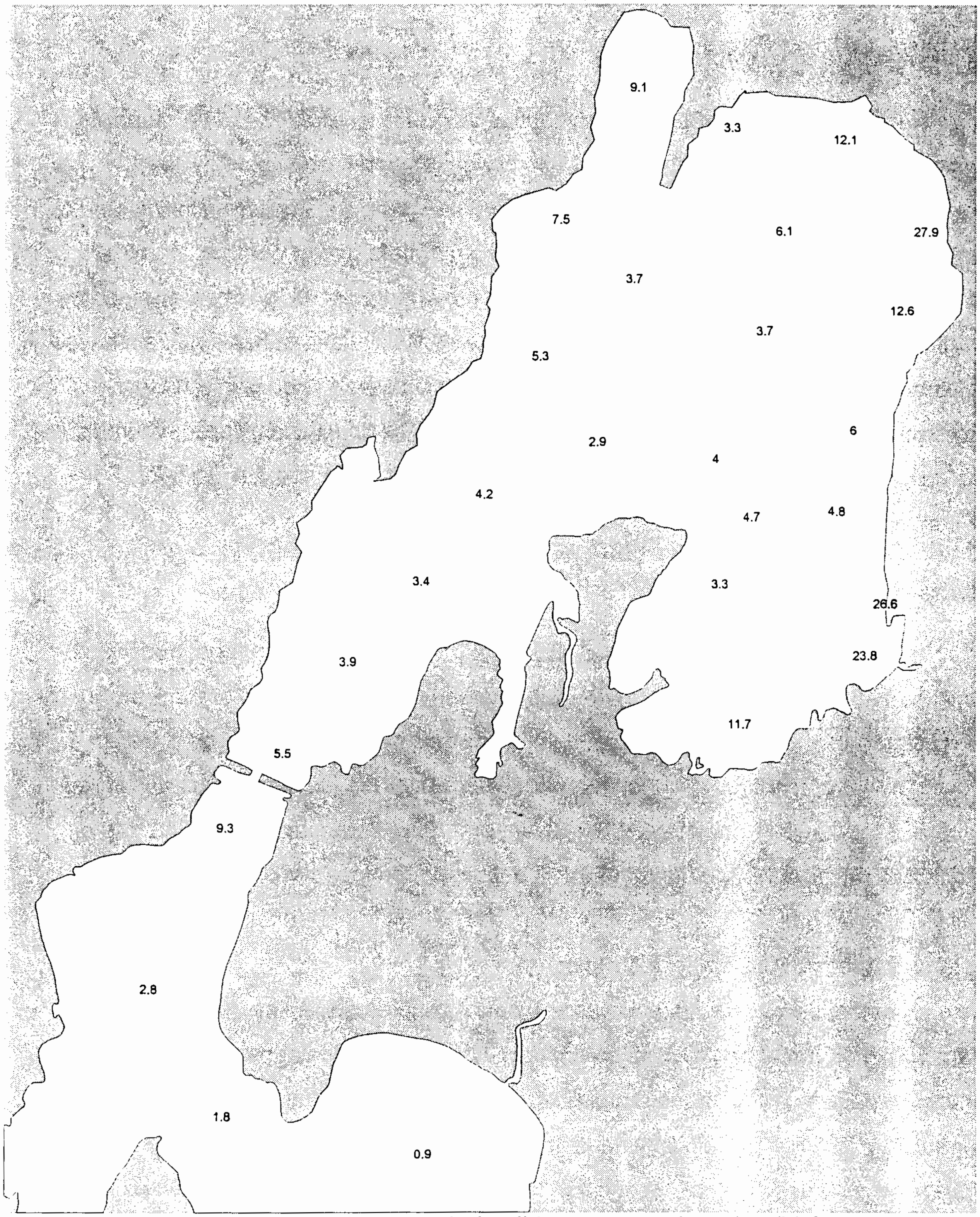

Figure 3.18 Distribution of total suspended solids concentrations (mg/L) found in Missisquoi Bay on October 28, 1996.

4. MODEL DESCRIPTION

For the Missisquoi Bay hydrodynamics study we used a PC-based modeling system, WQMAP (Mendelsohn et al, 1995; Swanson and Mendelsohn, 1994; Mendelsohn and Swanson, 1992), which integrates geographic information (land use, watershed attributes, point sources), environmental data (water quality parameters, stream flows, bathymetry) and process models (hydrodynamics, pollutant transport, sediment transport, waves). The component of WQMAP used in this application was the three-dimensional boundary fitted hydrodynamic model linked with the three-dimensional single constituent mass transport model variously configured to simulate the flushing of a conservative substance, sediment transport and a simplified phosphorus reaction.

Hydrodynamic Model

The numerical model selected for use in this study is a boundary fitted model which matches the model coordinates with the shoreline boundaries of the water body. This approach is consistent with the highly variable geometry of Missisquoi Bay. Development of this model, which has proceeded over the last decade, is described in several documents (Spaulding, 1984; Swanson, 1986; Swanson et al., 1989; Muin, 1993; and Muin and Spaulding, 1996). A detailed description of the model was included as an appendix to the initial ASA modeling study (Mendelsohn et al., 1996). A brief description of the model follows.

The boundary fitted method uses a set of coupled quasi-linear elliptic transformation equations to map an arbitrary horizontal multi-connected region from physical space to a rectangular mesh structure in the transformed horizontal plane (Spaulding, 1984). The three dimensional conservation of mass and momentum equations, with approximations suitable for lakes, rivers, and estuaries (Swanson, 1986; Muin, 1993) that form the basis of the model, are then solved in this transformed space. In addition, an algebraic transformation is used in the vertical to map the free surface and bottom onto coordinate surfaces (Gordon, 1982). The resulting equations are solved using an efficient semi-implicit finite difference algorithm for the exterior mode (two dimensional vertically averaged) and by an explicit finite difference leveled algorithm for the vertical structure of the interior mode (three dimensional) (Madala and Piascek, 1977; Swanson, 1986).

The basic equations are written in spherical coordinates to allow for accurate representation of large model areas. The conservation equations for water mass, momentum (in three dimensions) and constituent mass (e.g. chloride) form the basis of the model. It is assumed that the flow is incompressible, that the fluid is in hydrostatic balance, the horizontal friction is not significant and the Boussinesq approximation applies.

The boundary conditions are as follows. At land, the normal component of velocity is zero. At open boundaries the free surface elevation must be specified. A wind stress is applied at the surface. A bottom stress or a no slip condition can be applied at the bottom.

To allow the same relative resolution of the vertical structure throughout the model domain, a vertical coordinate transformation is employed. This technique maps the free surface and bottom topography onto coordinate surfaces analogous to the boundary fitted approach in the horizontal.

There are a number of options for specification of vertical eddy viscosity, A_v, (for momentum) and vertical eddy diffusivity, D_v, (for constituent mass). The simplest formulation is that both are constant, A_{vo} and D_{vo}, throughout the water column. They can also be functions of the local Richardson number which, in turn, is a function of the vertical density gradient and vertical gradient of horizontal velocity. A more complex formulation adds the dependence on mixing length and turbulent energy. Details can be found in Muin (1993).

The set of governing equations with dependent and independent variables transformed from spherical to curvilinear coordinates, in concert with the boundary conditions, is solved by a semi-implicit, split mode finite difference procedure (Madala and Piascek, 1977; Swanson, 1986). The equations of motion are vertically integrated and, through simple algebraic manipulation, are recast in terms of a single Helmholtz equation in surface elevation. This equation is solved using a sparse matrix solution technique to predict the spatial distribution of surface elevation for each grid.

The vertically averaged velocity is then determined explicitly using the momentum equation. This step constitutes the external or vertically averaged mode. Deviations of the velocity field from this vertically averaged value are then calculated, using a tridiagonal matrix technique. The deviations are added to the vertically averaged values to obtain the vertical profile of velocity at each grid cell thereby generating the complete current patterns. This constitutes the internal mode. The methodology allows time steps based on the advective, rather than the gravity, wave speed as in conventional explicit finite difference methods, and therefore results in a computationally efficient solution procedure (Swanson, 1986; Swanson et al., 1989; Muin, 1993).

Constituent Transport Model

The constituent transport model solves the conservation of mass equation on the same boundary fitted grid used for the hydrodynamic model (Muin, 1993; Mendelsohn and Swanson, 1992). The constituent transport model uses the current data calculated by the hydrodynamic model to simulate the transport of the material being modeled (e.g. chloride, sediments, phosphorus) and predict where it will go and its concentration in the water. This precludes the necessity for aggregation or interpolation of currents thereby avoiding unnecessary diffusive or numerical smoothing effects often associated with such postprocessing.

The model includes various configurations of loss terms to allow the simulation of wide variety of different materials. The loss rate terms include linear and non-linear decay, settling and bulk loss. Single and multiple, constant and time varying loads can be applied.

5. MODEL APPLICATION TO MISSISSQUOI BAY

The WQMAP system was applied to Missisquoi Bay and adjacent waters in the Northeast Arm. The same grids used in the previous study (Mendelsohn et al., 1996) were used in this application. The base map for the grids was digitized from NOAA chart #14781, (Riviere Richlieu to South Hero Island). Then a grid of quadrilaterals was created using gridding tools in WQMAP overlaying Missisquoi Bay and the Northwest Arm. The resulting grid is shown in Figure 5.1, and Missisquoi bay is shown enlarged in Figure 5.2. The grid dimensions are 34x84 total cells in the east and north directions respectively. A total of 1415 computational (water) cells were used to model the area. Five levels were used in the vertical direction to simulate the vertical current velocity structure.

At the southern extreme, the grid has an open boundary condition to simulate the small opening to Mallets Bay from the Northeast Arm. In addition, there are two openings, one at Carry Bay to the La Motte Passage and the other at The Gut, between North and South Hero Islands, to the main lake. In Missisquoi Bay the model grid has river boundary cells to represent the three rivers entering the bay: the Missisquoi which has three separate branches, the Rock and the Pike.

Bathymetry data was also taken from NOAA Chart 14781. The data were digitized and input to WQMAP which was used to generate depths for each grid cell by an automatic interpolation routine based on distance weighting.

Two different grids were used in the model simulations in this study to simulate the cases with the present causeway configuration and with the causeway completely removed. The depths were assumed to be at the mean stage.

Two sets of simulations were set up and run as part of this study. (1) Wind and river data collected as part of the field study in October 1996 were used as inputs for running model simulations of that period. Other data collected during that period were then used to compare model predictions with actual measurements, and then to modify

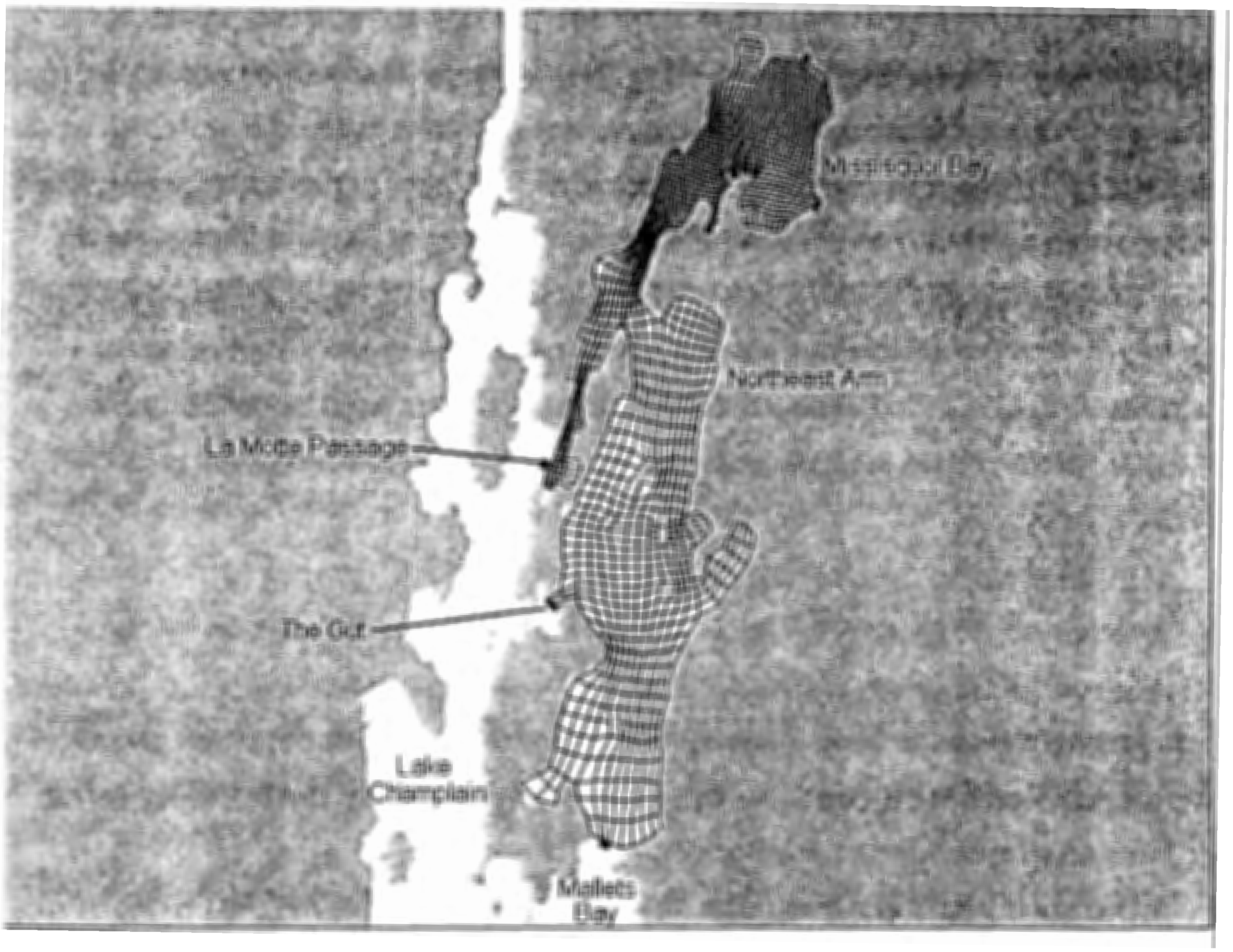

Figure 5.1. Model grid for Missisquoi Bay and the Northeast Arm.

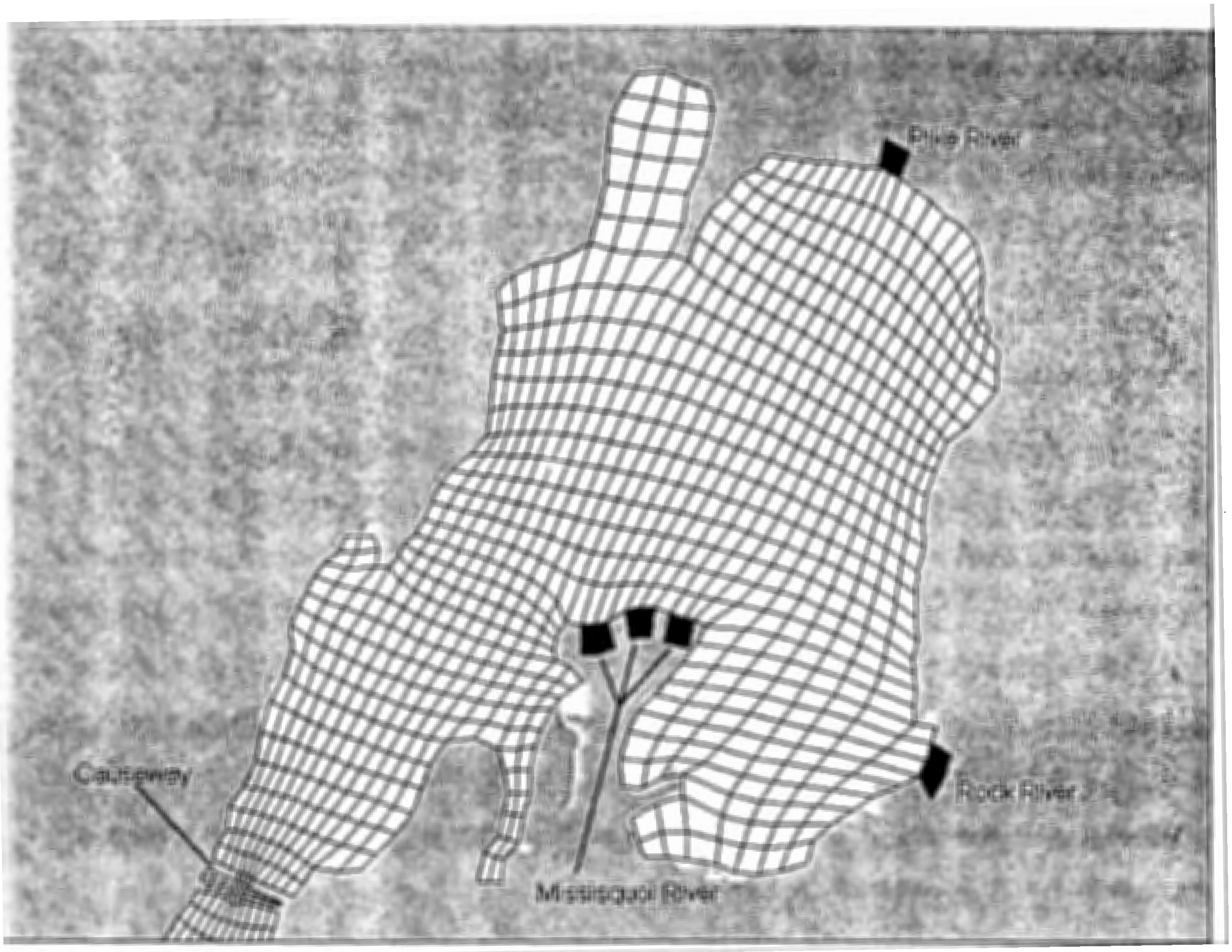

Figure 5.2. Model grid enlarged to show the Missisquoi Bay area.

the model to improve the fit of the predictions to the measurements. This process of calibration then prepared the hydrodynamic model for use in the second part of the study. (2) The calibrated model was used in conjuction with the mass transport model to run long term simulations of phosphorus concentrations and suspended solids sedimentation. These simulations were for six months each from May through October, based on data for this period from 1991. The purpose of these long term simulations was to integrate the many variations of environmental parameters that influence circulation and ultimately phosphorus concentrations and sediment deposition in the bay and to campare these results with and without the causeway.

Hydrodynamic Model

The wind input to the model is applied as a spatially invariant wind field for which the speed and direction are allowed to change with time to correspond to the wind record used for the simulation. This means that at each point in time, the water surface at each location on the model grid experiences an identical wind stress (i.e. no cyclones or "puffs" are modeled). The wind record obtained during the field study, sampled at one hour intervals, was used for the model calibration. Burlington wind data were used for the long term simulation. River flow inputs to the bay were taken from records for the Missisquoi, Pike and Rock Rivers which were interpolated from the daily values provided to the 30 minute model time step.

As the wind and river flow forces are applied to the bay (including the Northeast Arm) the model calculates the change in the current patterns and the surface elevation over time. Five layers were used in the vertical direction to represent the vertical structure of the currents, (e.g. the currents at the surface may be going one way while the bottom currents go in the opposite direction). For the long term simulations, the currents on all five layers and the surface elevation were then stored on an hourly basis for use in the flushing, sediment and phosphorus models.

Sediment Transport Model

For the long term sediment transport simulations the constituent transport model was configured with a settling term, set at various rates to simulate the settling and deposition of various sized particles. The distribution of sediments on the lake bottom suggest that suspended sediments in the tributaries that make it into the lake range from fine sand and silt to clay. It is apparent that even the very fine sand (particle diameter on the order of 62.5µm to 100µm) settles out very quickly near the mouth of the river. To study the sedimentation of river borne suspended material, we chose therefore to concentrate on particles of the size of very fine silt or clay. These particles have diameters in the range of 1µm to 10µm. The various particle sizes are simulated in the model by adjusting the bulk constituent settling velocity. One particle size is modeled at a time. Typical settling rates for a range of particle sizes were taken from Davis (1993). A median value for the material settling rate of 0.2 m/day was chosen, corresponding to very fine silt, with a range determined by halving and doubling that rate. An additional simulation was run with a settling rate of 0.01 m/day, corresponding to the clay fraction.

For each layer in a water grid cell, a certain mass of material is determined to settle (fall) into the layer below at a rate proportional to the settling velocity and material concentration. For the bottom layer the calculated mass settles out to the sediments. Total suspended solids (TSS) loads were based on daily loads for each of the three rivers for the period of the simulation, calculated by ANR from USGS data.

Resuspension of sediments was not considered in the simulations. The resuspension of sediments occur primarily due to local wave action and is more event related. It is not a function of the steadier wind driven currents modeled in this study. The focus of the sediment transport study was to predict the transport and fate of material originating from the rivers and whether or not the causeway in its present configuration has an effect on long term distributions. The fate of resuspended material, and the possible effects of the causeway, may be inferred from the potential flushing calculations reported in the model results section.

Phosphorus Model

The phosphorus simulations used the single constituent transport model configured with a second order loss term (sedimentation rate) as described in the Lake Champlain Diagnostic. Feasibility study (VT DEC and NYJ DEC, 1997) using the sedimentation coefficient of 400 m^3/g-yr as specified in that study. No inital value was assumed for the bay, so that there will be a delay before the model simulates the actual conditions in the bay. River loads were determined as for TSS.

6. MODEL RESULTS

The hydrodynamic model was calibrated based on the October 1996 data described in Sections 2 and 3. Long term hydrodynamics simulations were then run with and without the causeway to evaluate the differences in currents expected in the bay when the causeway is removed. The transport model was then used in the long term simulations of sedimentation and phosphorus with and without the causeway. The results of the simulations and the analysis of those results follows.

Calibration of the Hydrodynamic Model

Initially, the model system was set up the same as it had been in the previous modeling study (Mendelsohn et al., 1996) except that real wind and river flow data were input to force the model. The model as it existed was very nearly complete, and in a sense, calibrated. Had it not worked well with the new data inputs, it would have been necessary to use another model, since its functions are based on first principles about how the world works. With real data to drive the model, it remained to 'tune' it to get a best fit of the data. Only a few parameters remained to be adjusted to obtain this fit. This is an iterative calibration/verification process that completes the model preparation for use.

The parameters considered for adjustment included bottom friction, vertical viscosity, and surface friction. The simulated water volume flux and velocity at the bridge were then compared to the observed record to evaluate the improvements resulting from parameter changes.

Parameter	**Range**	**Value Used**
Surface (wind) friction	0.001-0.002	0.0012
Bottom friction	0.003-0.005	0.003
Vertical viscosity	5-50 cm^2/sec	50 cm^2/sec

Surface and bottom friction control overall velocity amplitude with increasing values of surface friction resulting in larger velocities for a given wind, and increasing values of bottom friction resulting in reduced velocities. Vertical viscosity controls vertical velocity profiles, which are not well characterized, and the model becomes unstable with small values for this parameter. Velocity development at the bridge is due more to water surface setup than to direct wind stress. The overall effect of modifying the model parameters within the tested range was quite small compared , for instance, to the effect of changing the river or wind forcing values.

Most of the results of the model calibration are summarized in Figure 6.1. There is a great deal of data presented in this series of plots, and we need to explain some of the details of what is being shown here. Six data streams for the month of October 1996 are presented. The top two plots are wind and river flow data used to force the model. The wind data is the same data presented in Figure 3.3. At the bottom of the figure are two plots representing, in stick plot form, the currents under the Route 78 bridge as predicted by the model (bottom) and as measured by the ADCP (above the model predictions). The middle two plots represent fluxes of water under the bridge as calculated from the ADCP data (above) and as predicted by the model (below).

It is evident, from the results for both the current predictions and the volume flow predictions, that the model predicts a much smoother world than was measured. This is only to be expected from the nature of the model and modeling process and from the data sources. Half hour average wind velocities at the bridge, which represent an excellent data set, are only a generalization of the complex and constantly varying conditions that actually occur over the surface of the lake system. The real current data, which are five minute averages, reflect all the subtleties of these processes, and thus the stick plot appears quite variable compared to the smoother flow in and out of the bay predicted by the model, for which we show only hourly values. Nevertheless, we see clear similarities of overall pattern between the two records.

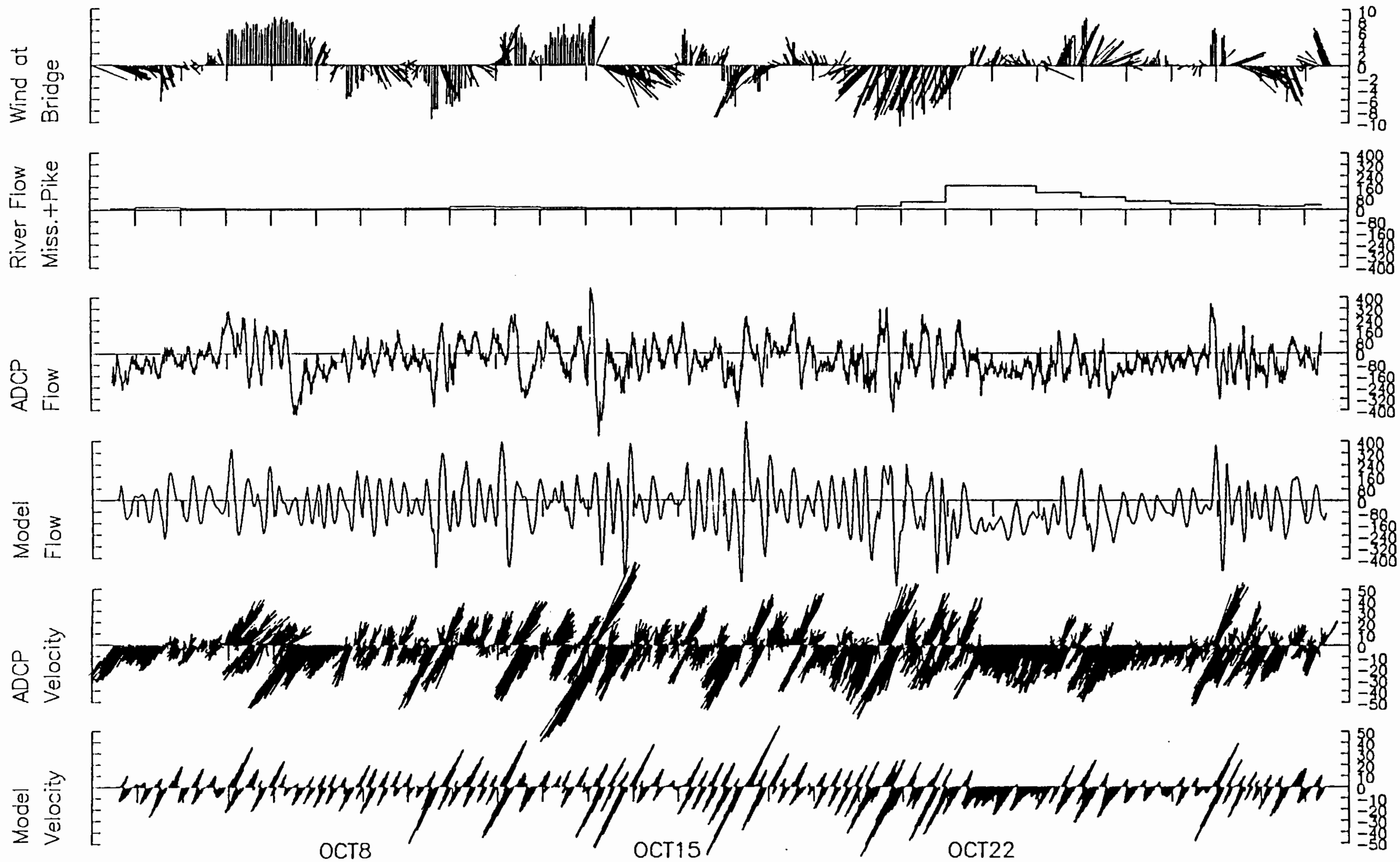

Figure 6.1 Results of the model calibration runs. See the text for an explanation.

The plots of volume flow to some degree integrate the effects of the currents and are easier to examine and compare. The close similarity of the predicted flow to the calculated values is quite evident, with the high variability in the ADCP data appearing largely as high frequency small scale variations on the overall pattern of flows in and out of the bay. The model appears to be simulating quite well what happens on a larger scale without the tiny variations that are seen at shorter time scales.

The scales of the plots in Figure 6.1 were then expanded to a single day to show in clearer detail what happens over the course of two sample days. Figure 6.2 shows the same data types as in Figure 6.1 for October 10 only, and Figure 6.3 shows this data for October 29. It is now much easier to see in detail how predictions vary from measurements. On October 10, even at this level of detail, there is an excellent fit of the predictions to the data. On October 29, there seems to be a mismatch of the current predictions to the data during the early part of the day, though the latter half fits well. This is reflected in the volume flow curves as well. To some degree, the differences look like the model was a little slower in predicting shifts in the currents, but that the overall water exchange was much the same over the course of the day. It is quite striking how sensitive the system, both in the model and in the data, is to relatively small changes in wind speed and direction.

The best fit of the model to the data actually appears to occur with about a one-hour lag in the model. This lag can occur for any number of reasons such as inaccurate characterization of the bathymetry of the bay. Correlation of model to ADCP data has an r^2 of 0.36. Another measure of fit is root-mean square (RMS) differences (the square root of the mean squared difference between observations and predictions). This gives a value of 98 m^2/s for flow through the bridge opening. Both of these measures seem to suffer considerably from the inability of the model to simulate the high frequency changes in real currents that are smoothed out by the model. Overall, however, in terms of simulating the mass flows of water at the bridge, the model appears to be doing a good job, with net flows about 15% lower and total exchange flows about 19% higher than those calculated from the ADCP data.

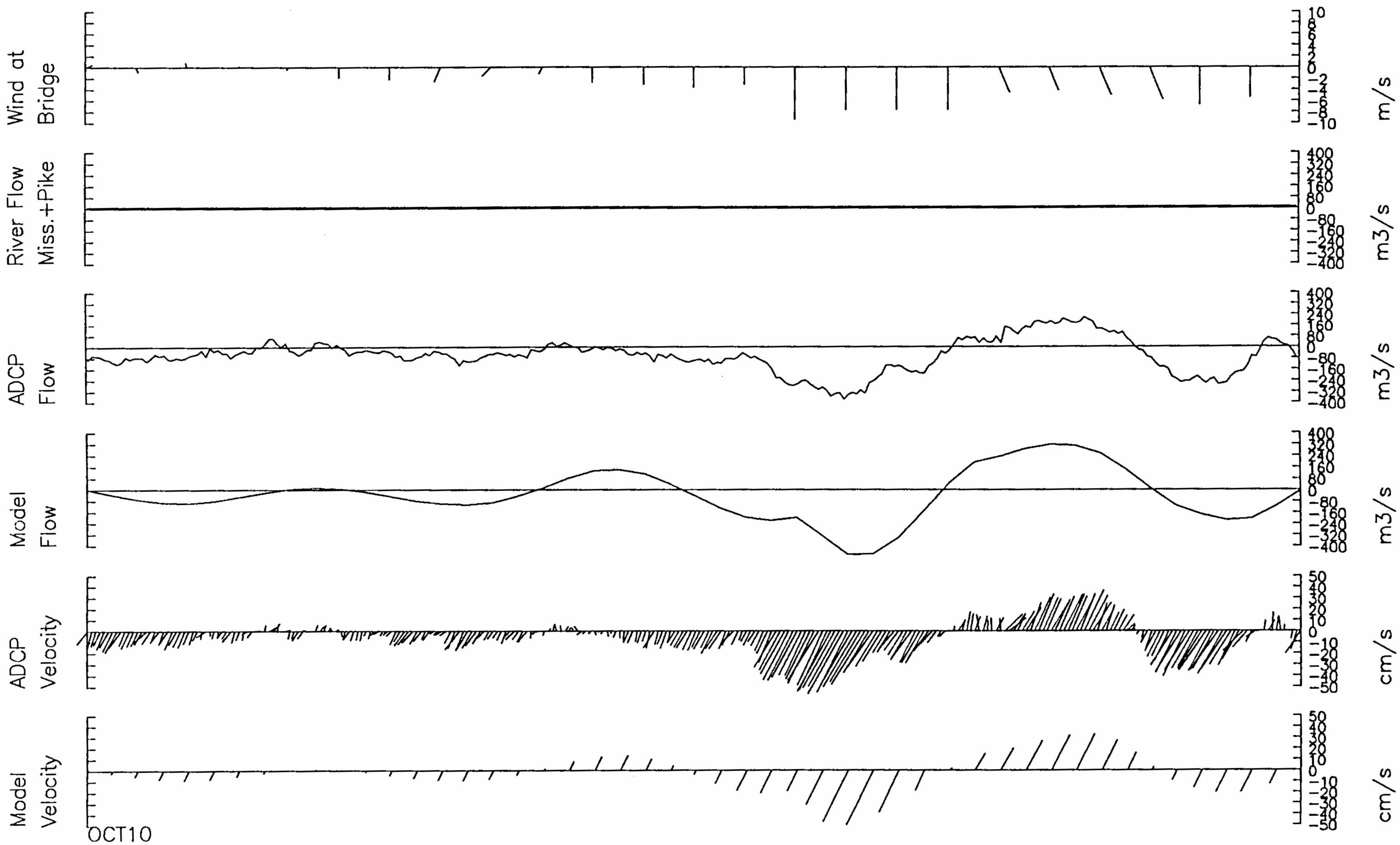

Figure 6.2 Results of the model calibration for October 10, 1996.

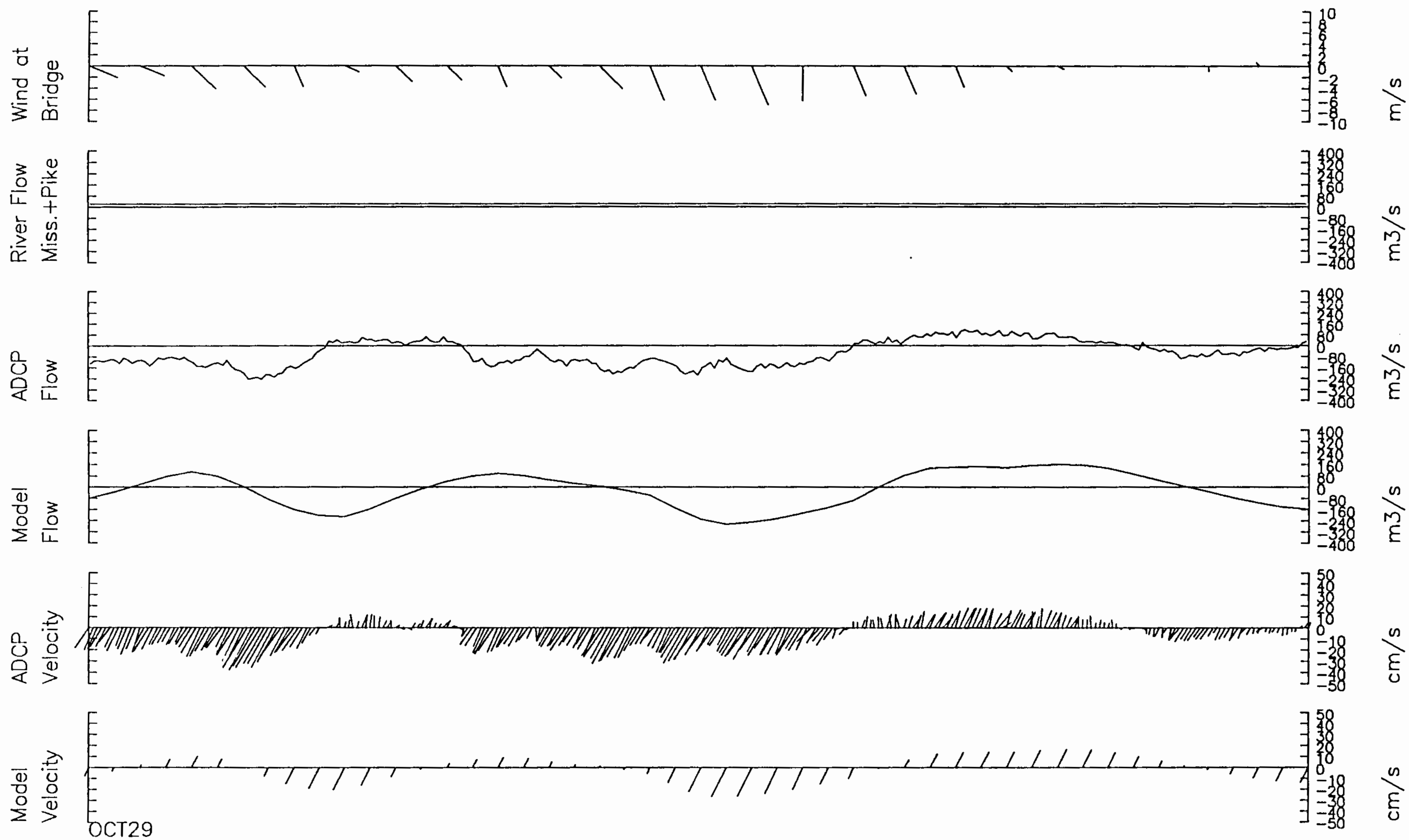

Figure 6.3 Results of the model calibration for October 29, 1996.

Data from the drogue studies were also compared to model predictions. The fit was generally poor, with certain areas doing better than others. Results are shown in Figure 6.3a. Heavy arrows show the drogue paths during the study, and light arrows show the model-predicted paths for the same time periods. If one allows for the lag in currents at the bridge that has been previously observed (the model predicts a strong reversal of the drogue path at the bridge immediately following the period of simulation), a condition that may be more prevalent at low wind speeds, then the area at the bridge and generally in the area west of the Missisquoi River delta is adequately simulated by the model. In other parts of the bay, the model generally predicts a more complex circulation than drogue tracks would suggest. Interestingly, it is difficult to account for conservation of water mass from the drogue studies, for which there appear to be large areas of nearly unidirectional flow with no measured return flow. Relatively small changes in the placement of the drogue to be simulated can result in significant effects on the predicted drogue track. The poor fit of the model to observations over large areas of the central and western parts of the bay may create some concern about the overall performance of the model. Over much of the bay, transport of pollutants of concern (phosphorus and suspended solids) may take place somewhat differently than shown in the simulations, but ultimately this will only result in small displacements of areas of relatively high or low concentrations from one part of the bay to another. Ultimately, the events that occur in the bay will be controlled by the exchanges that happen at the bridge, and these areas are well simulated.

In calibrating the model, emphasis was placed on matching volume flow at the bridge. This is because this flux is the primary factor controlling flushing in the bay and the consequent levels of constituents (phosphorus, suspended solids) that will be found within the bay. The detailed resolution of currents at fixed locations, while desirable, will have little effect on constituent concentrations in the bay as a whole, thought they may alter their local distributions.

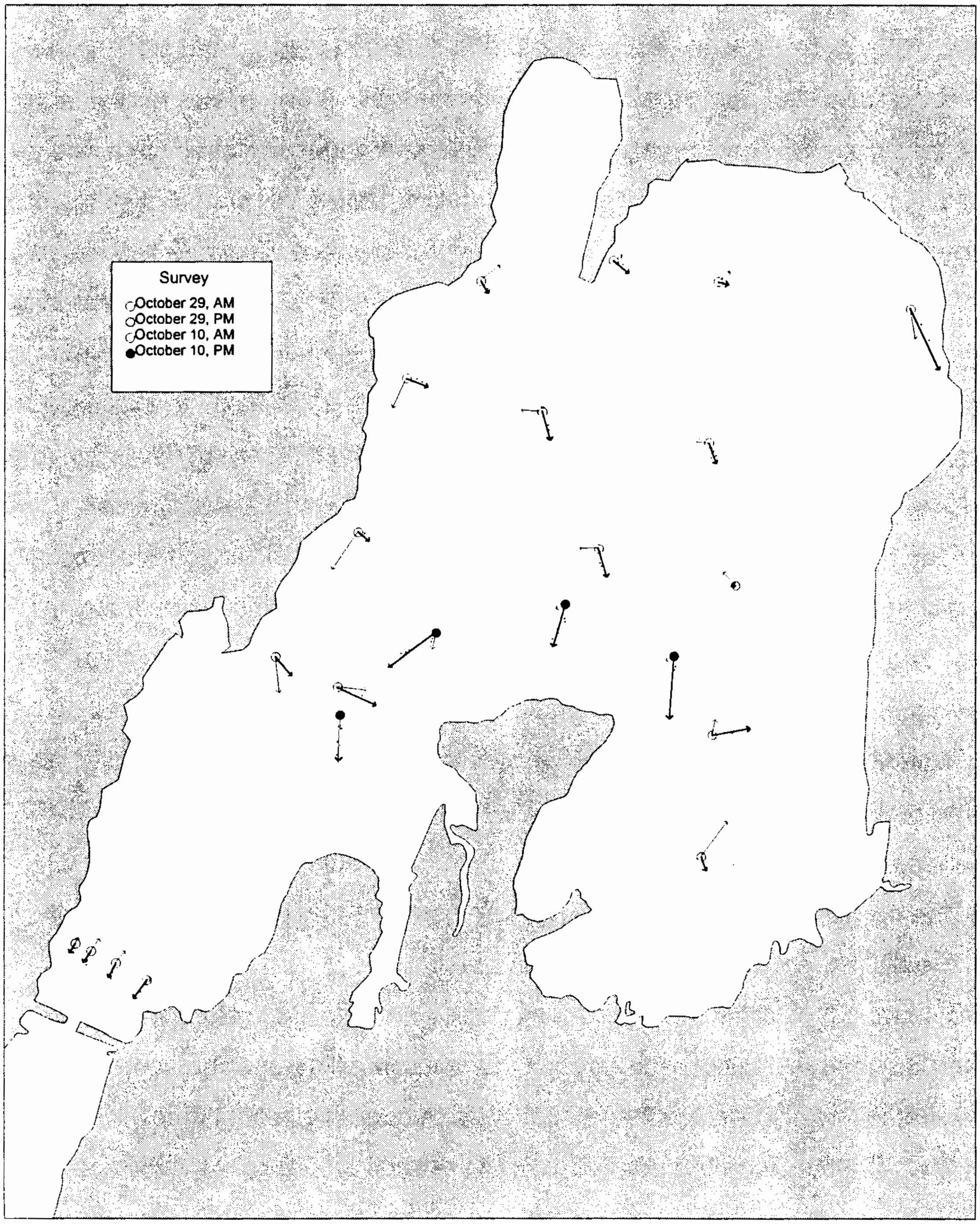

Figure 6.3a Drogue tracks during the four drogue studies (heavy arrows) and model predicted paths of drogues (light arrows).

Long Term Simulations - Hydrodynamics

Long term simulations were run for the conditions with and without the causeway using the calibrated model and river and wind data from May through October 1991. Figure 6.4 shows some of the results for the hydrodynamic model output. At the top of the figure is a stick plot of the wind record and a line plot of total river flows used to force the model runs. The next two plots down show the predicted volume flow of water under the bridge with the causeway (above) and without it (below). The bottom two plots compare current velocities at the bridge with and without the causeway. At this scale, we cannot detect any significant differences in volume flow with and without the causeway. As would be expected, however, with the removal of the causeway, and the consequent increase in area through which the water can flow, there would be a dramatic decrease in current speeds at the bridge compared to the present condition.

There is some impedance of flow in and out of the bay as a result of the causeway, and we may evaluate this using the model. Net flow through the bridge opening, equal to about 25.8 m^3/sec, is the result of river flow and long term lake level changes. There is considerable exchange that takes place on this net flow as we have already seen, and this may be quantified as the exchange flow. The absolute values of flows in and out of the bay through the bridge opening were summed over time. This is a measure of the exchange flow, and for the existing condition, with the causeway in place, the model predicts exchange flow of 241.8 m^3/s. With the causeway removed, the predicted exchange flow increases to 337.3 m^3/s.

How can this difference in exchange affect the flushing of the bay? Figure 6.5 is a diagram of flushing time in the bay, based on conditions during the long term simulation. In this figure, flushing time is calculated as follows:

$$F = \frac{V}{Q_r + Q_x * E_x}$$

In which F is flushing time (in days), V is the bay volume (290 x 10^6 m^3) Qr is the river flow rate or net flow (25.8 m^3/s), Q_x is the exchange flow (241.8 or 337.3 m^3/s, as noted above), and E_x is the effective mixing factor. If river flow alone accounted for flushing in the bay, then the average turnover time of the bay would be about 130 days. There are, however, significant additional water exchanges that take place between the bay and the rest of Lake Champlain, and these will contribute to flushing. The horizontal axis of the plot is the value of a mixing coefficient. If water that entered the bay with wind-driven exchange flow experienced no mixing with the surrounding water and left unchanged during the return flow, then the value of the effective mixing factor would be zero, at the left of the plot, with 130 days flushing time. At the other extreme, if exchange flow entering the bay were to mix completely with the entire volume of the bay before any of it returned back to the rest of the lake, then the mixing factor would be one (100%), and the flushing time under these conditions would be reduced to about 10 days. Because there is some impedance of water flow under the bridge resulting from the constriction by the causeway, this flushing time would actually be shorter without the causeway present (due to differences in the value of Qx, the exchange flow), and this effect will increase with increased values of effective mixing. It is important to note, however, that the mixing factor value never approaches a value of one and probably is less than a tenth of that. In estuarine systems, with continuous and regular tidal flushing, values typically are about 0.1 to 0.2. In Missisquoi Bay, where much of the exchange flow is rapid and short-lived, it seems likely that the effective mixing is significantly less. We can still expect that there is a small improvement in flushing time that may result from removal of the causeway, but it is likely to be less than 10%.

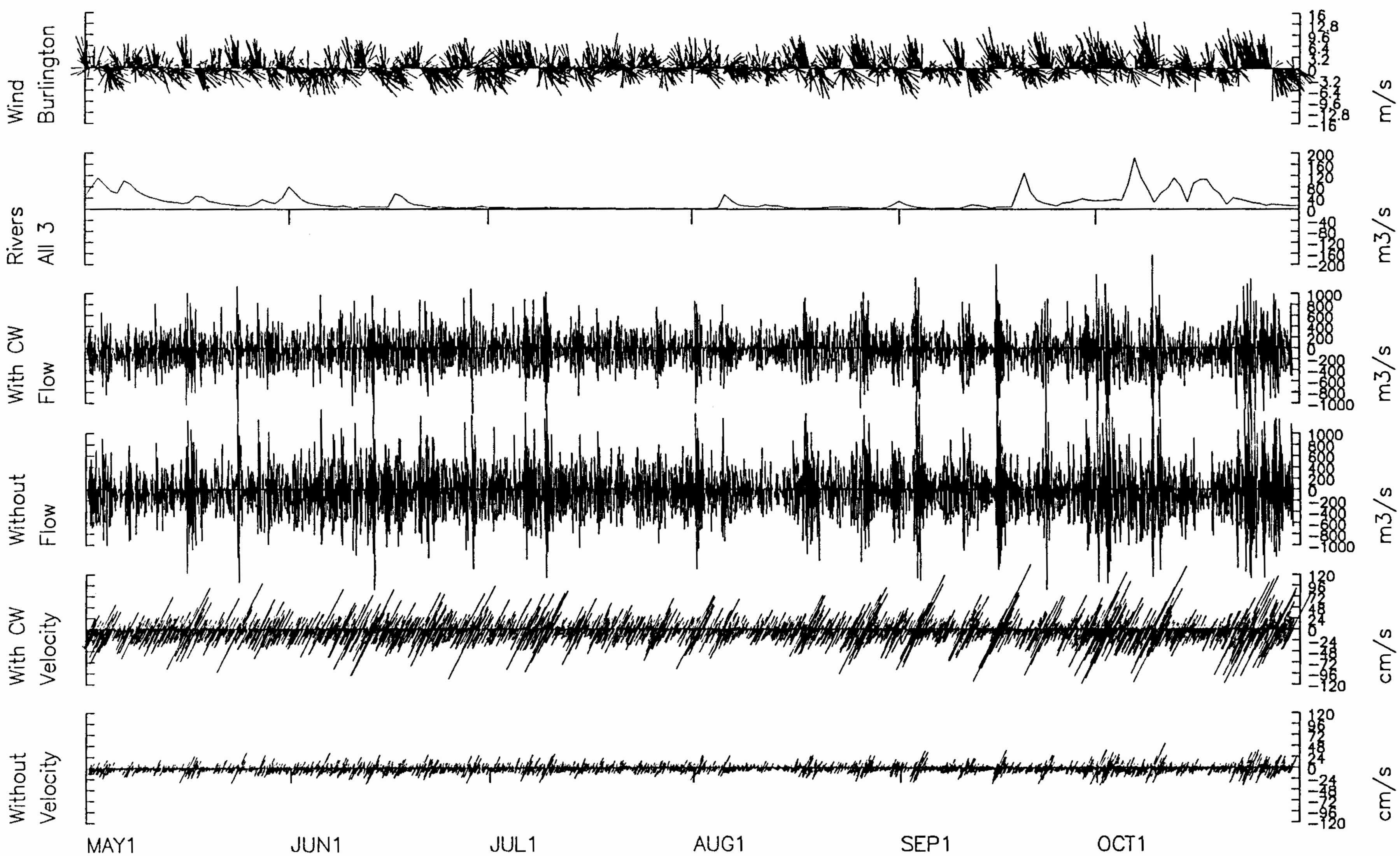

Figure 6.4 Wind and river flow records used to force the long term simulations of the model with hydrodynamic model predictions of current velocities and volume flows at the bridge with and without the causeway.

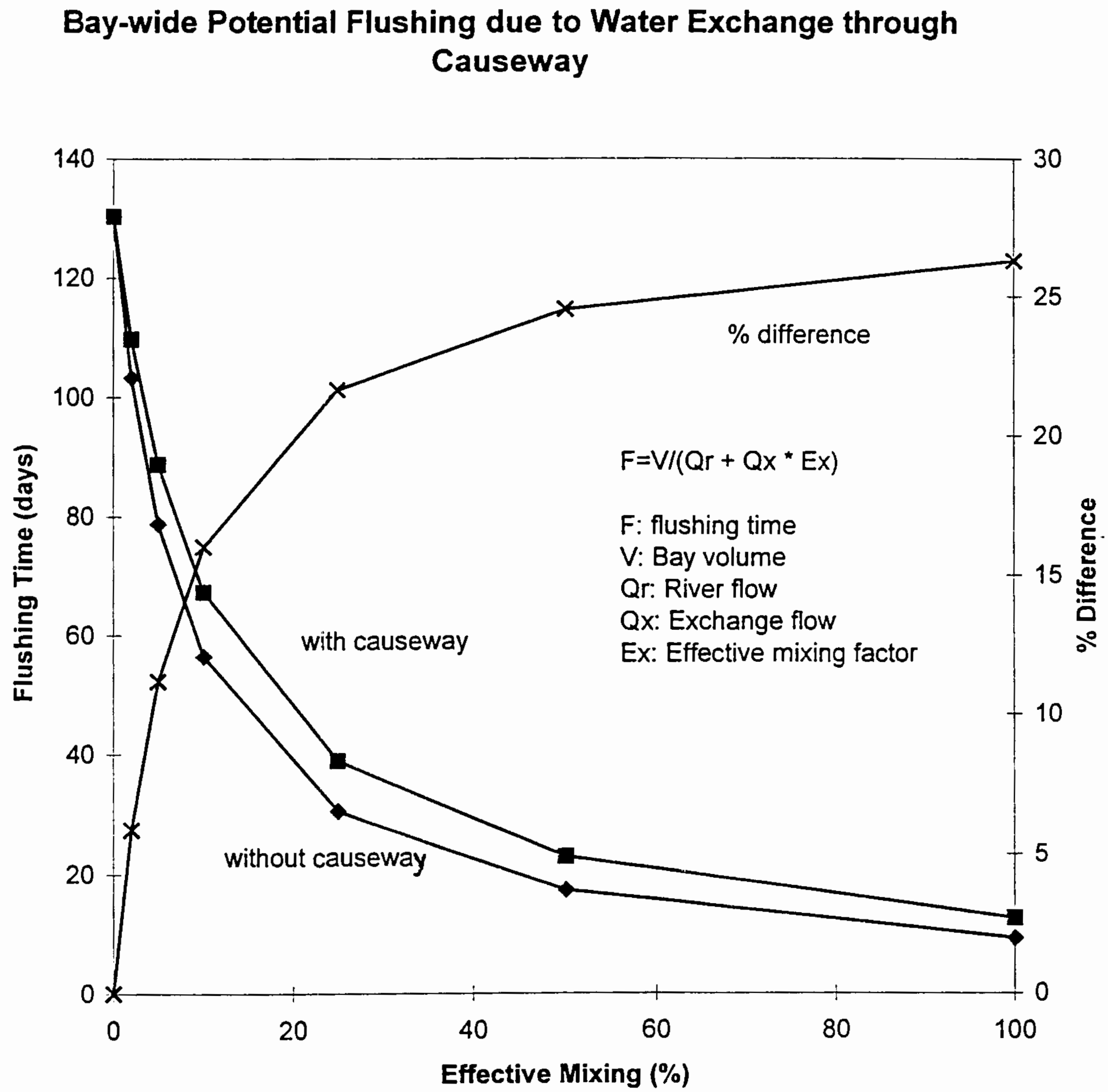

Figure 6.5 Potential flushing time of Missisquoi Bay due to exchange flow through the mouth of the bay as a function of the effective mixing factor for exchanged water.

Lower effective mixing here, compared to an estuary, is expected primarily because of reduced flow. Mixing characteristics are directly related to flow shear, and the magnitude of this shear depends primarily upon the speed of flow and how it is induced. In open water, flow shear is generated at the surface by wind and at depth by friction with the bottom. Though these conditions exist in both lakes and estuaries, flows in estuaries typically result in far more mixing due to the continuous, large-volume flux of the tidal currents.

Note that the foregoing discussion assumes that E_x remains constant with or without the causeway present. What actually would occur, should the causeway be removed, would depend on how shear flow changes. Since the model predicts a substantial reduction in current speeds near the bridge with the causeway removed, it is to be expected that these would actually be a resultant decrease in the value of E_x, at least in the vicinity of the bridge.

With reduced flow, and the consequent reduced mixing, that would occur with removal of the causeway, there is then the increased possibility of vertical stratification. In effect, the area near the bridge becomes nearly a uniform straight channel with slower, more uniform flows than exist there now, while there is no apparent change in the pattern of currents at greater distances from the bridge. The model cannot predict changes in vertical stratification that would result, however, Missisquoi Bay is such a shallow system that significant stratification would only be expected during short transitional periods, during the year.

The Lake Champlain Disagnostic – Feasibility Study (VT DEC and NYS DEC, 1997) calculated effective exchange rates for each lake segment based on chloride loads and concentrations. For Missisquoi Bay this value was calculated to be 297 x 10^6 m^3/yr, or 9.4 m^3/s. If this is assumed to be an independent measure of Q_x*E and compared to the model-predicted exchange flow of 242 m^3/s, then the value of E_x is estimated to be 9.4/242 or about 4%. This will give bay flushing times in the range of 80 to 100 days in Figure 6.5 with differences in flushing time with and without the causeway of 10% or less.

Long Term Phosphorus Simulations

Simulations of total phosphorus in the bay were run with and without the causeway. Figure 6.6 shows the model predictions of the time history of the mass of total phosphorus in the bay, as a fraction of the river load, over the time of the simulation. This plot does not take account of the background concentrations that existed in the bay prior to the start of the simulation. Because the bay is being constantly flushed, there is generally a trend of removal of phosphorus from the bay, however, near the end of the simulation there are large loads to the system that take place such that there are increases in the relative mass remaining in September and October. The figure shows total portion of load remaining both with and without the causeway as two very similar lines. At the bottom of the figure is a line representing the percent difference between the two cases (right vertical scale). Typically, the case without the causeway is found to be between zero and one percent lower than with the causeway. The increase in flushing is so small that its effect on phosphorus concentration in the bay would be too small to measure.

Separate areas within the bay have different flushing rates which will vary the response to phosphorus loading. Figure 6.7 shows four points within Missisquoi Bay at which the model was used to make separate evaluations of total phosphorus concentrations over time during the long term simulations. The results are shown in Figure 6.8. The top of Figure 6.8 shows the daily loads from each of the three rivers together with the sum. The lower four plots show the concentrations at each of the four points over the course of the simulations For the present causeway configuration, concentrations are shown by the bold lines.

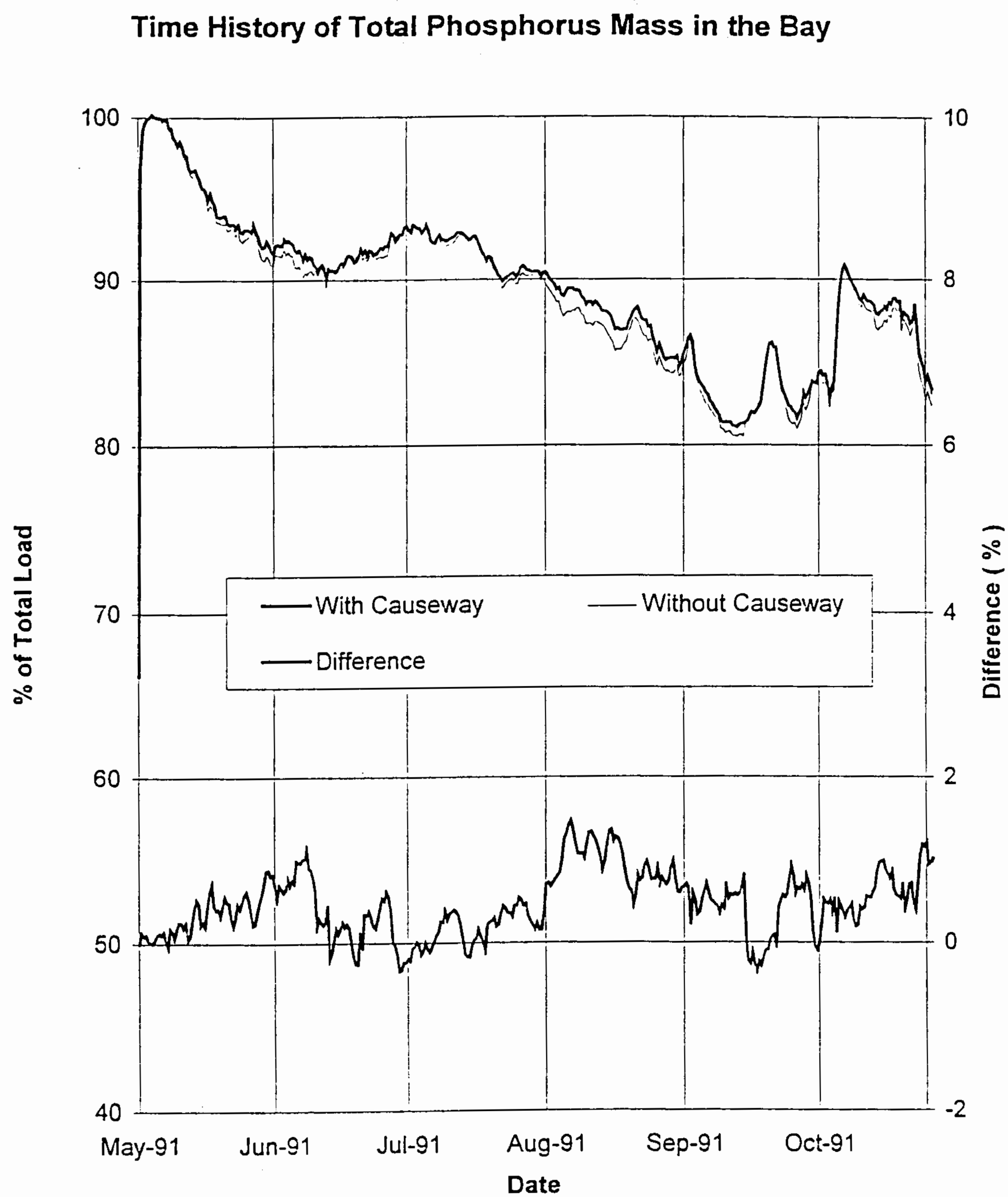

Figure 6.6 Predicted time history of total phosphorus mass in the bay, as a fraction of load, with and without the causeway, for the long term phosphorus model simulation. The bottom plot, which uses the right vertical scale, shows the relative difference between predictions for the two cases.

The lighter line represents the concentrations predicted when the causeway is removed. Stars on these plots indicate concentrations of total phosphorous measured at nearby stations during the same period in time as that being modeled (VT DEC and NYS DEC, 1997). Clearly, the upper and lower bay locations reflect the proximity of river sources, while the middle bay location shows a more delayed and smoother response to changes in load. Note that the lower bay station is at a different scale than the others reflecting the larger total load from the Missisquoi River. The concentrations at the causeway are generally lower, consistent with its proximity to the lower concentration areas outside the bay. In all cases, the differences between concentrations with and without the causeway are small, sometimes indetectable at these scales. Though generally concentrations without the causeway are a bit lower, there are periods of variable duration at each of the locations when higher concentrations are predicted.

It is clear from a comparison of data (star symbols) with model predictions of phosphorous concentrations in Figure 6.8 that the model under-predicts phosphorous concentration over much of the bay. The model was set up to drive phosphorous concentrations from river loads. As such, there is no input from other possible sources such as sediment, or the open boundary. It is not surprising then, that the fit of prediction of data is poorest at the causeway station, nearest the open boundary (which is zero in the model) and best at the lower bay station near the mouth of the Missisquoi River, where river loads overwhelm the background levels. This increased gradient in the model between the sources and the open boundary should serve to emphasize any differences in concentrations predicted by the model when the causeway is removed.

Phosphorus concentrations at the end of the simulations are shown in Figure 6.9 for the present causeway configuration, and in Figure 6.10 for the case with the causeway removed. The differences between cases for the most part are fine details. The overall patterns are the same. Perhaps the most obvious differences are the areas of increased concentration in the northernmost parts of the bay without the causeway, and the areas of reduce concentration in the region of the causeway itself.

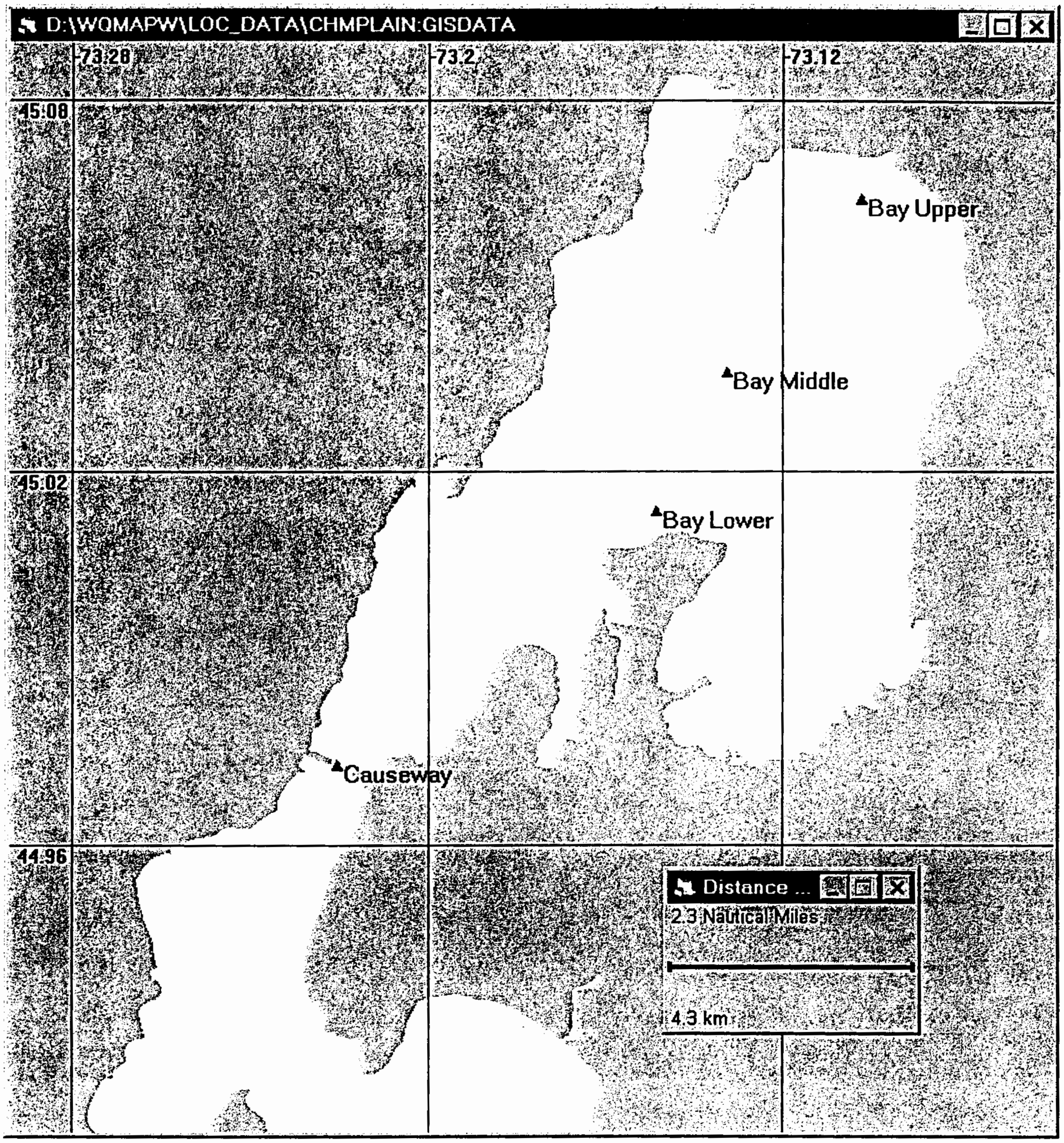

Figure 6.7. Missisquoi Bay area showing the selected sites at which model evaluations of local total phosphorous concentrations over time were made.

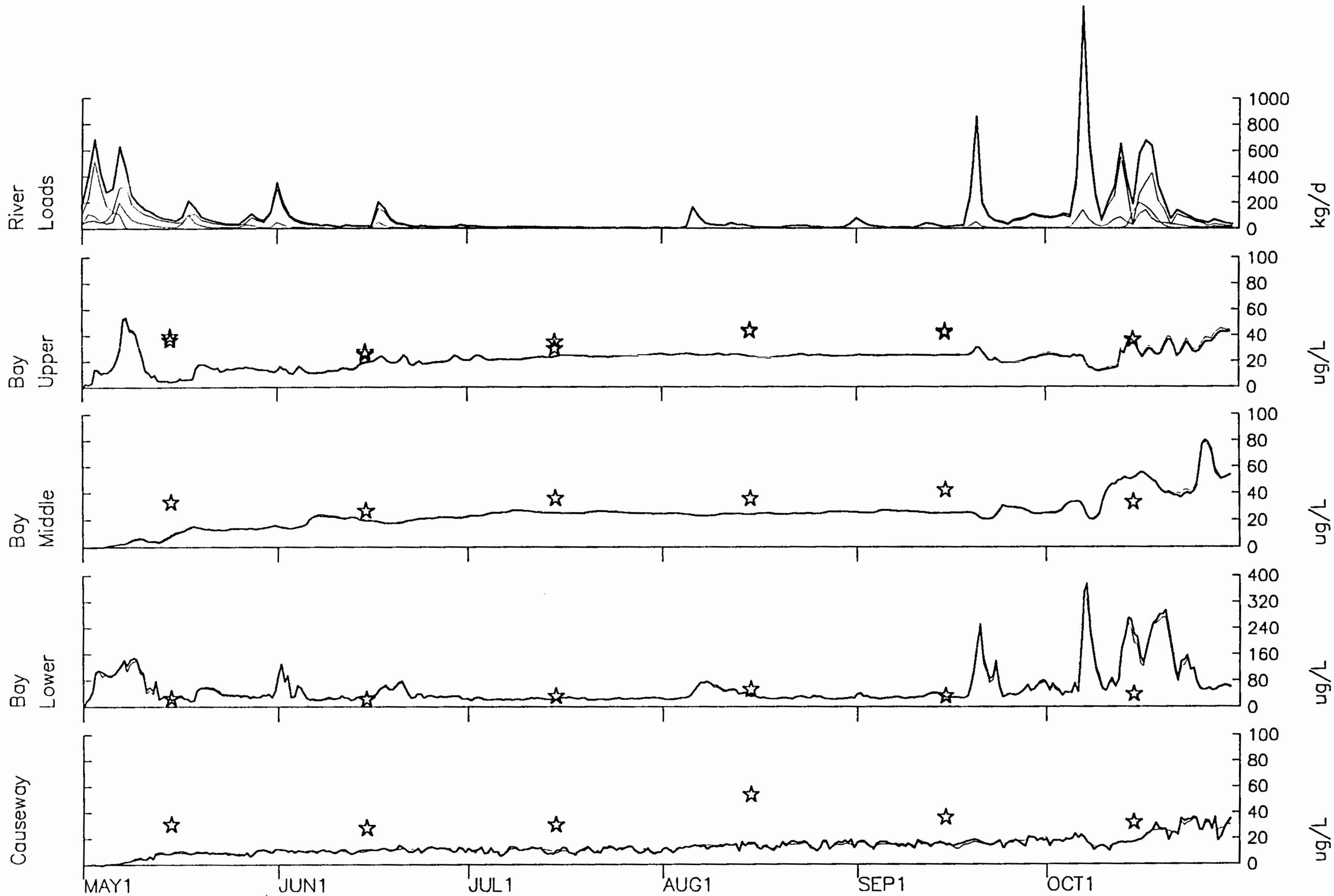

Figure 6.8. River loads of phosphorous over the period of the long term simulations together with the predicted localized concentrations of total phosphorous at the four locations shown in Figure 6.7. The top plot shows total phosphorous (daily load) for each of the three rivers together with the sum. In each of the four lower plots, the bolder line is concentration with the causeway present, and the lighter line is the concentration with the causeway removed. Stars indicate values measured at nearby stations during the same period, as reported in VTDEC, NY dEC, 1997.

Long Term Suspended Sediment Simulations

Simulations of the transport and sedimentation of riverine suspended sediment were run with and without the causeway for sediments with four different settling rates. In each case the simulations were run as if the total river load was of the one type, but it should be kept in mind that the actual condition will be a combination of sediments with a wide range of settling rates. Figures 6.11 to 6.14 show the model-predicted concentrations and settling of suspended sediments with settling rates of 0.4, 0.2, 0.1, and 0.01 meters per day respectively. Simulations both with and without the causeway are shown in each figure. As in Figure 6.6, the values are given as a proportion remaining in the water column (or settled to the sediment) of the total river load since the beginning of the simulation.

Looking at the four figures as a series, one can see a clear gradient of decreased settling in the bay and increased retention in the water column as the particle settling rate decreases. This gradient is also accompanied by increased export of the suspended sediment out of the bay. For all but the slowest settling particles, the effect of the removal of the causeway is almost indetectable on these plots. For particles settling at 0.01 m/day, there is a slightly lower overall concentration of suspended sediment in the water column without the causeway on the order of 1%. This appears to be due primarily to export, since no corresponding increase in settled material is evident. Figures 6.15 to 6.22 show the final distribution of sediments in the bay for each simulation. They are presented in order of decreasing particle settling rate with the case for the present causeway configuration immediately preceding the case without the causeway for each settling rate. These figures show settling mass as grams per square meter (g/m^2). To put this into the context of depth, a settled mass of 260 g/m^2 of sediment would add a depth, when compact, of about 100 μm. As we have already seen, there is a pattern of decreasing settling within the bay with decreasing particle settling rate. The riverine sources of these sediments is particularly evident in these figures.

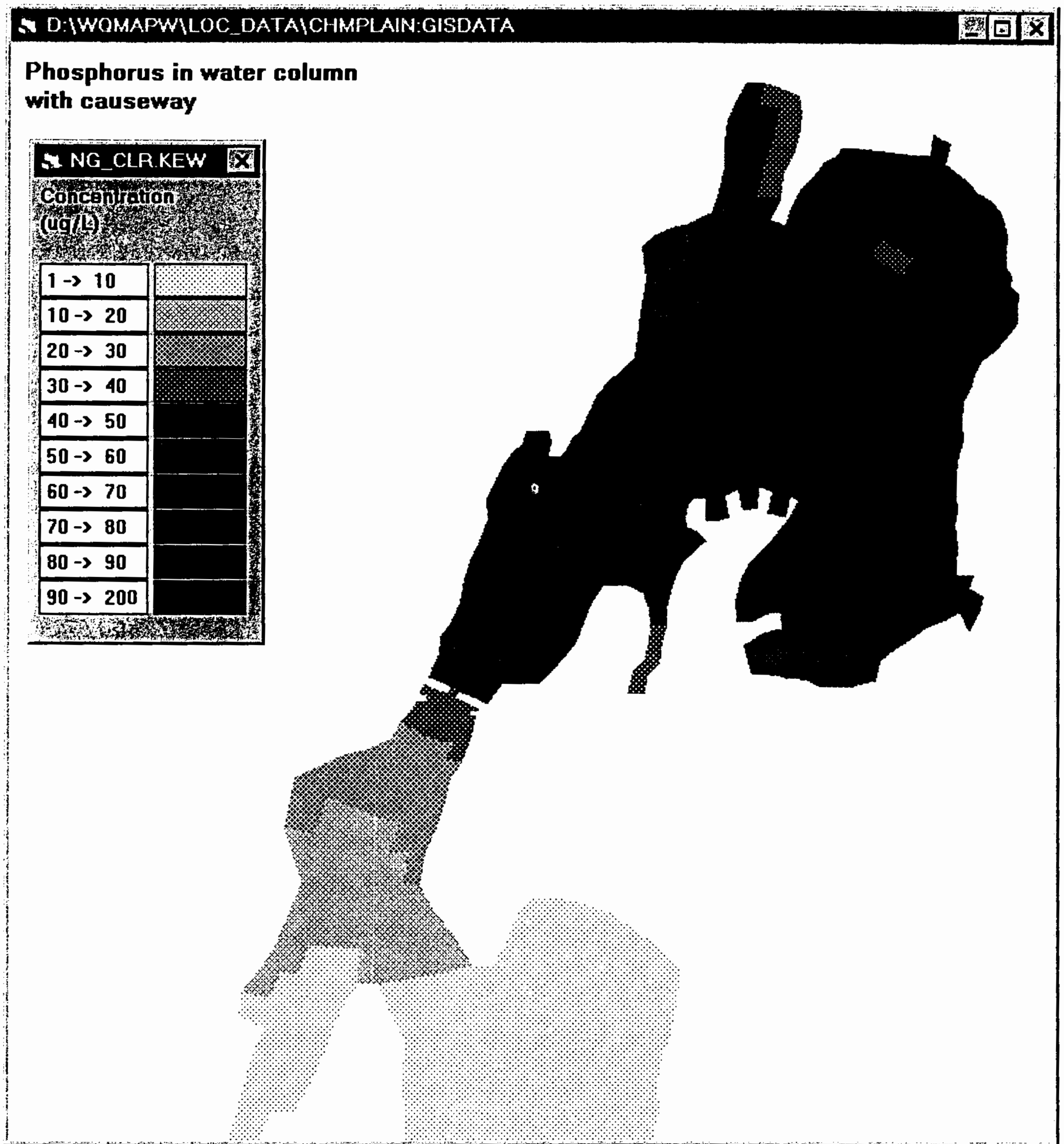

Figure 6.9. Total phosphorus concentrations in Missisquoi Bay and the Northeast Arm predicted for the last day of the long term simulation with the causeway in place.

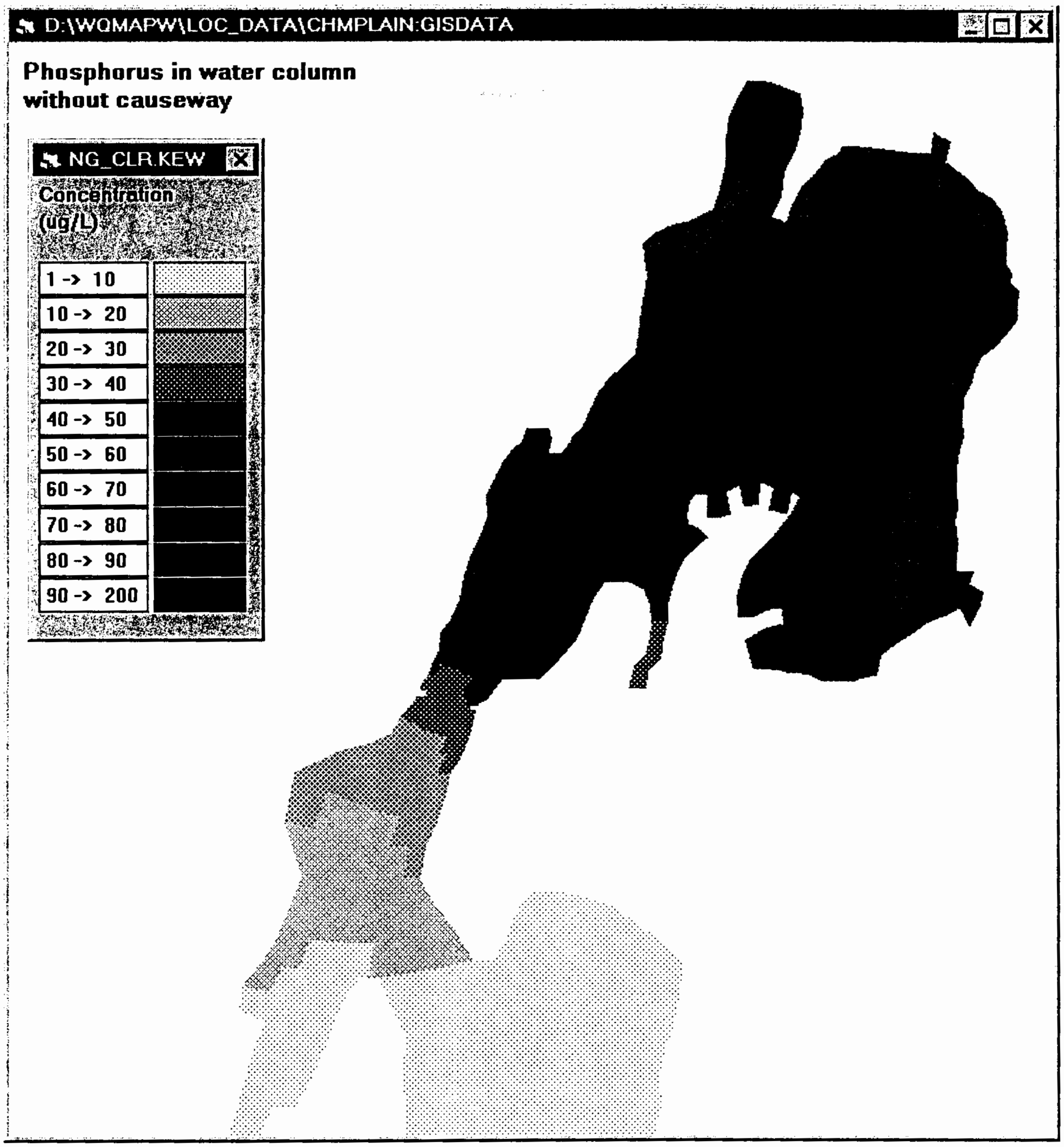

Figure 6.10. Total phosphorus concentrations in Missisquoi Bay and the Northeast Arm predicted for the last day of the long term simulation with the causeway removed.

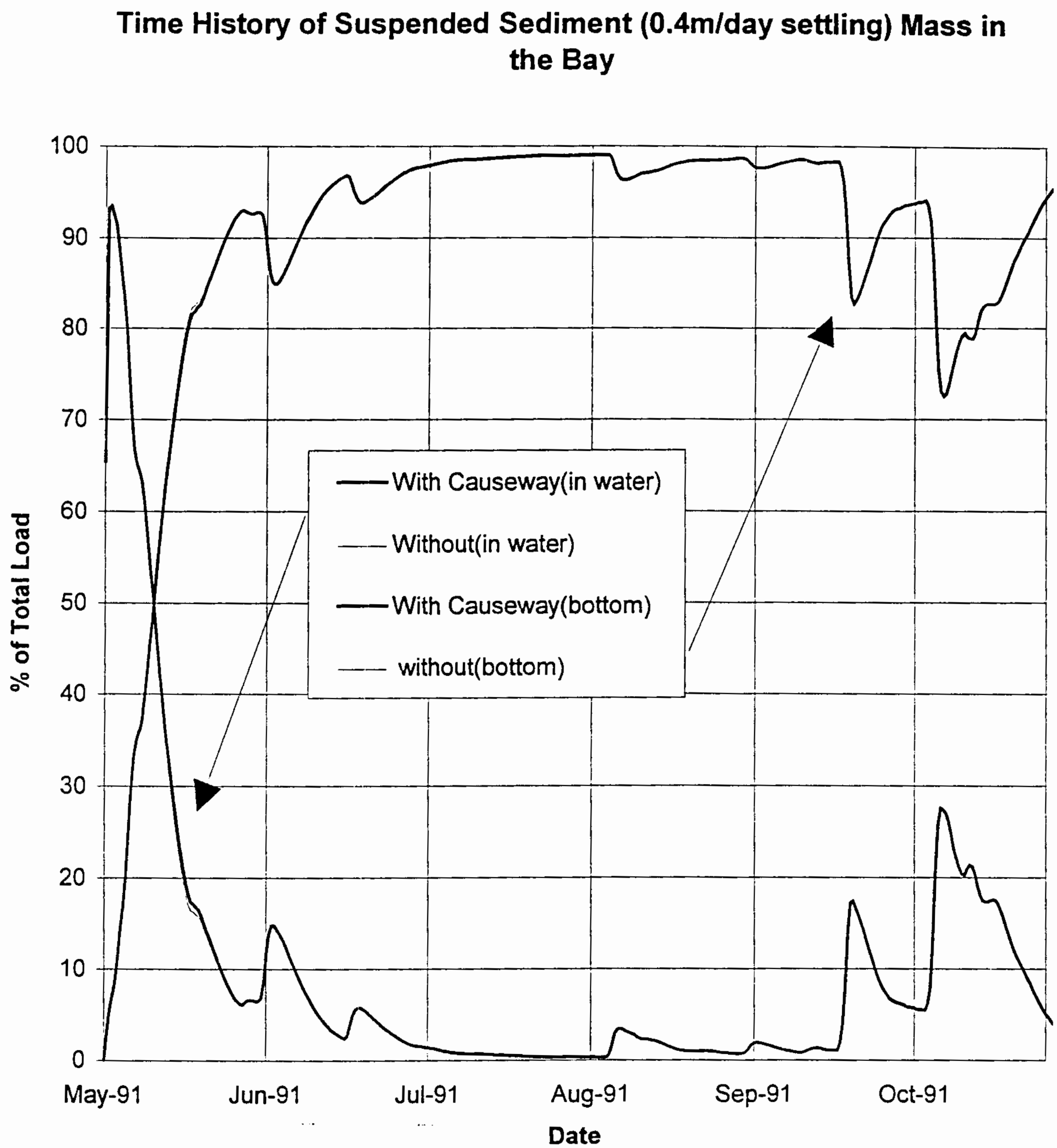

Figure 6.11 Predicted time history of suspended sediment mass in the bay, for the long term suspended sediment model simulations, for sediment with a settling rate of 0.4 meters per day. Both total mass remaining in the water column and mass settled to the bottom are shown as fractions of total load since the beginning of the simulation. The bold line is the simulation with the causeway, the finer line is for the case without the causeway.

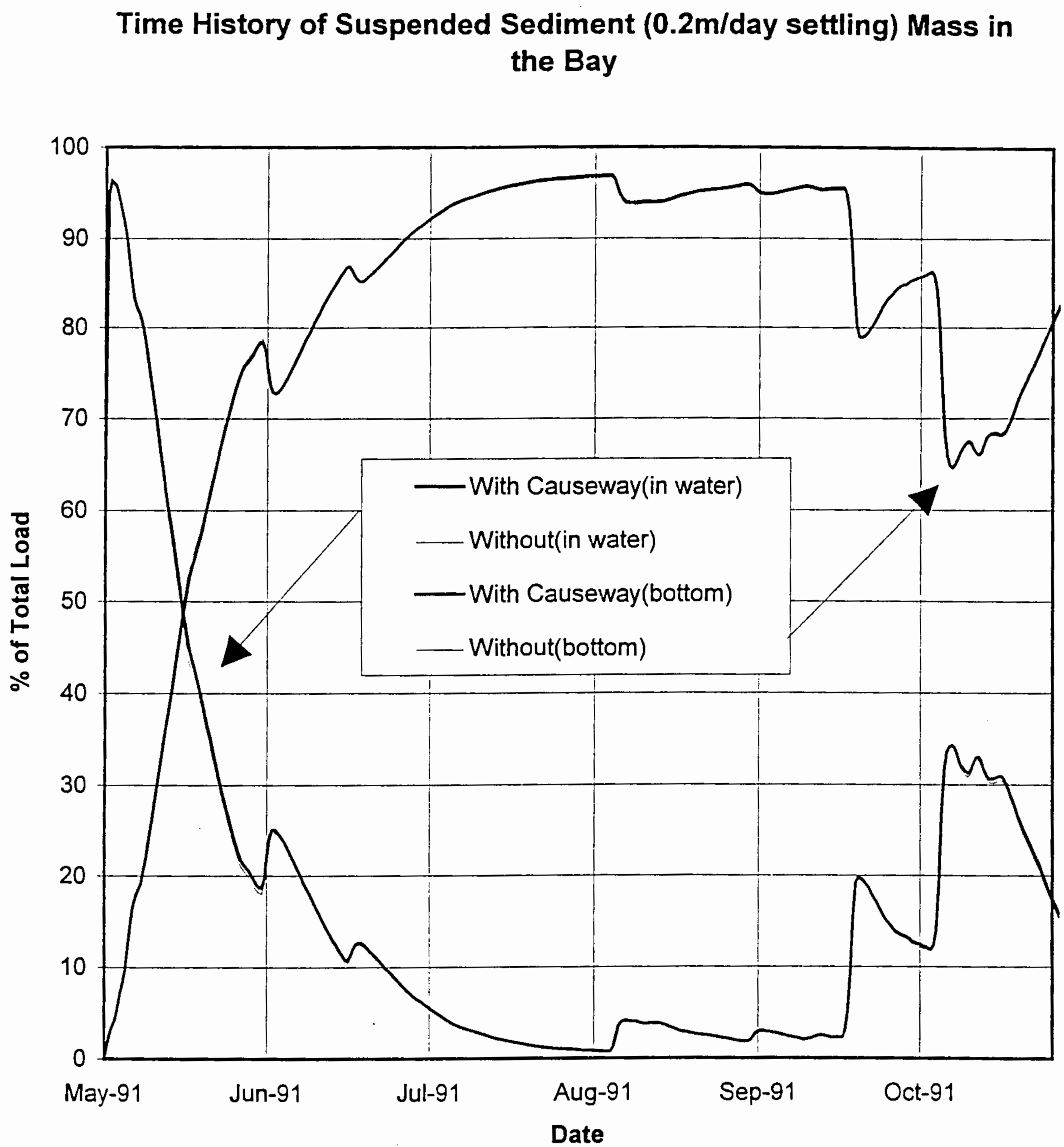

Figure 6.12 Predicted time history of suspended sediment mass in the bay, for the long term suspended sediment model simulations, for sediment with a settling rate of 0.2 meters per day. Both total mass remaining in the water column and mass settled to the bottom are shown as fractions of total load since the beginning of the simulation. The bold line is the simulation with the causeway, the finer line is for the case without the causeway.

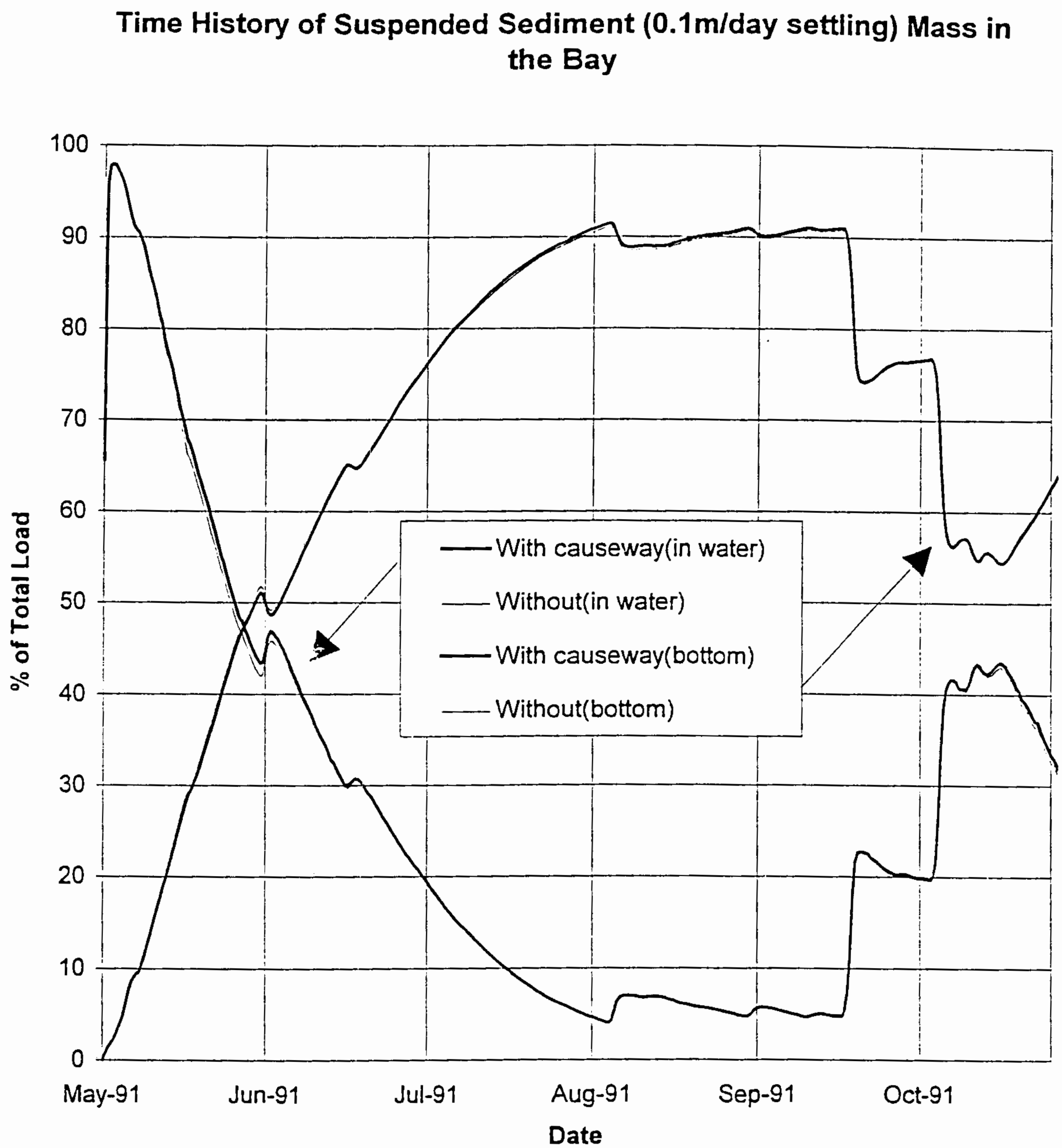

Figure 6.13 Predicted time history of suspended sediment mass in the bay, for the long term suspended sediment model simulations, for sediment with a settling rate of 0.1 meters per day. Both total mass remaining in the water column and mass settled to the bottom are shown as fractions of total load since the beginning of the simulation. The bold line is the simulation with the causeway, the finer line is for the case without the causeway.

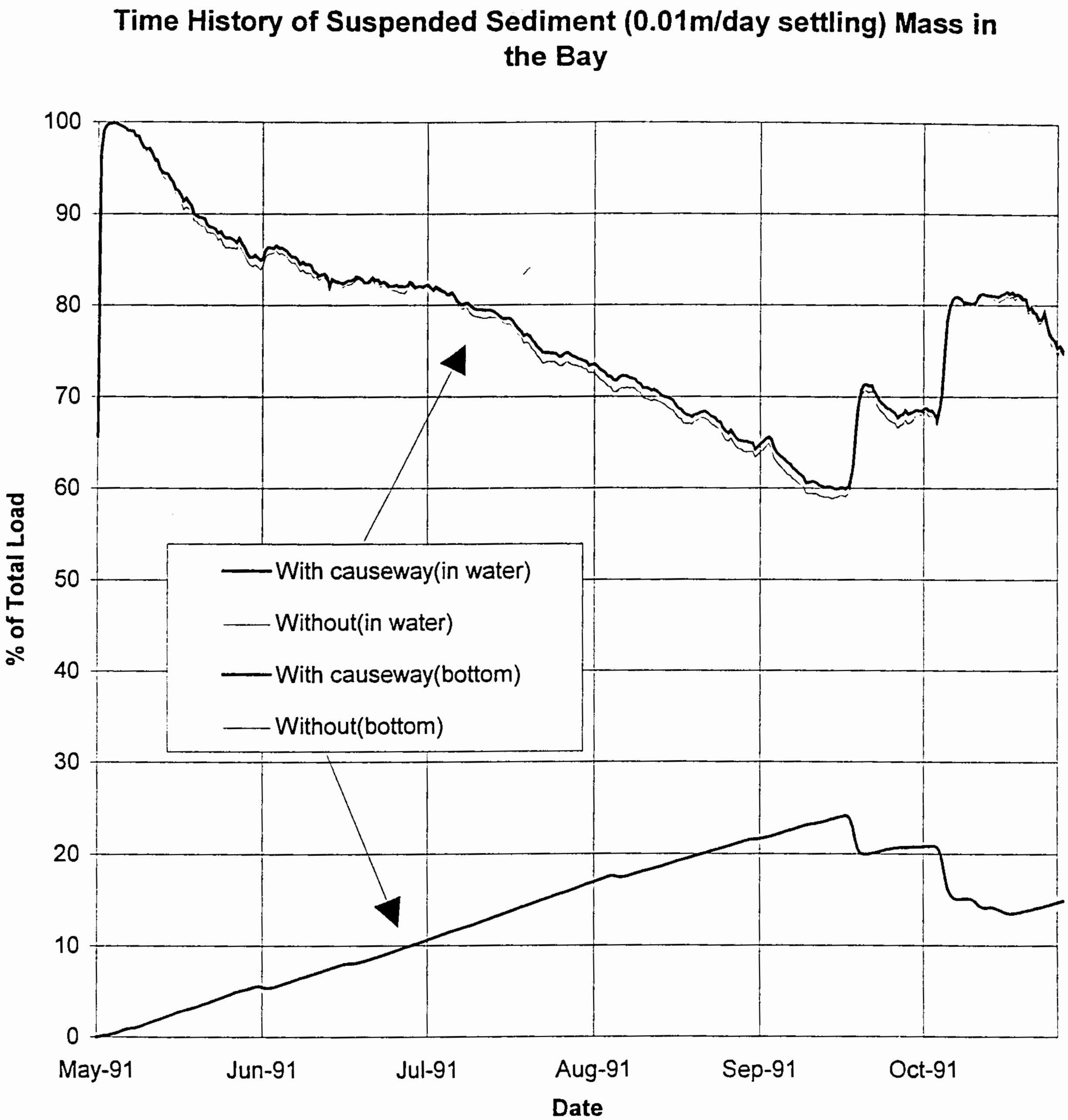

Figure 6.14 Predicted time history of suspended sediment mass in the bay, for the long term suspended sediment model simulations, for sediment with a settling rate of 0.01 meters per day. Both total mass remaining in the water column and mass settled to the bottom are shown as fractions of total load since the beginning of the simulation. The bold line is the simulation with the causeway, the finer line is for the case without the causeway.

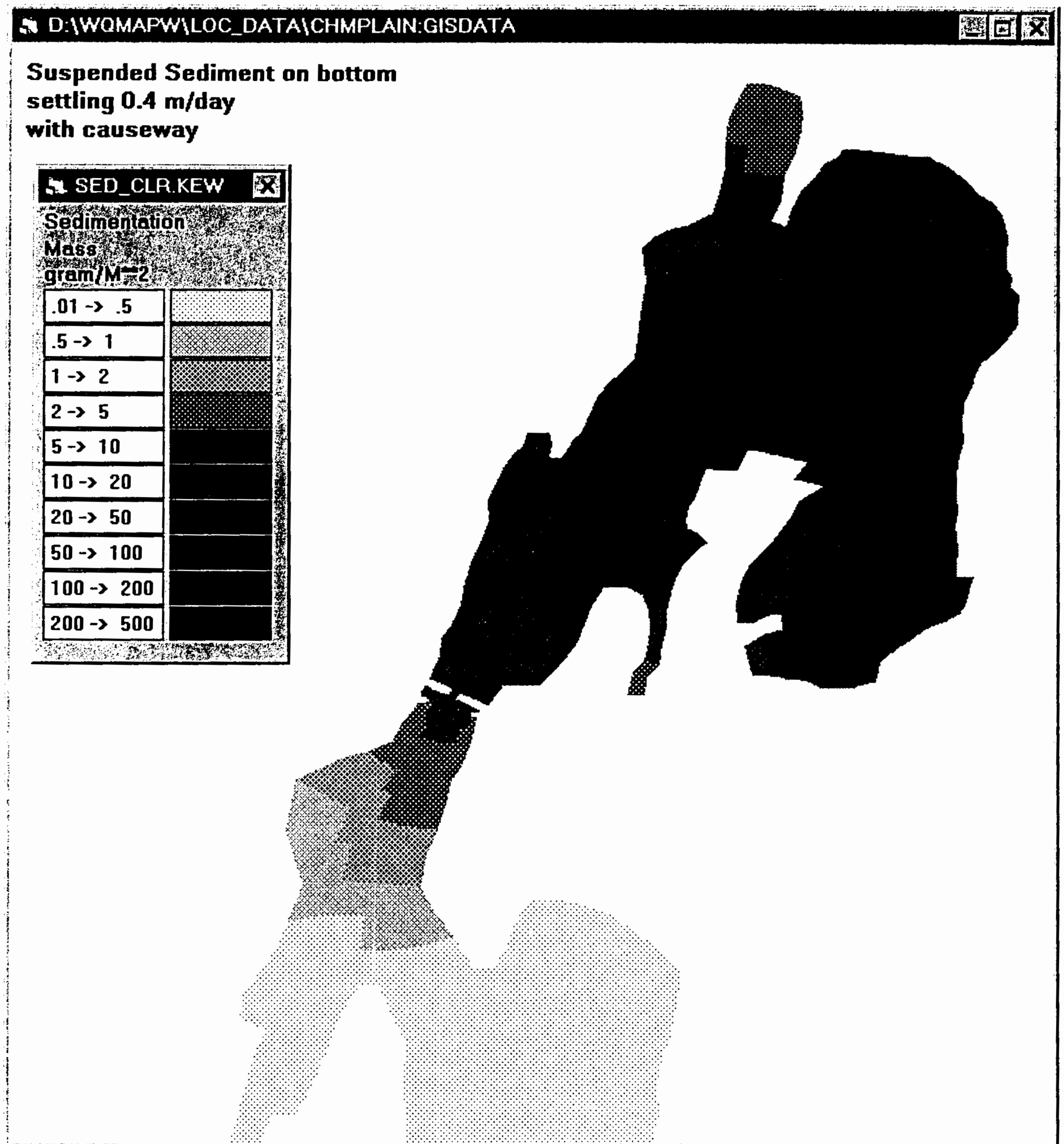

Figure 6.15. Distribution of sediments settled from riverine loads of suspended sediment over the course of the long term suspended sediment simulation for particles with a settling rate of 0.4 meters per day and for the present causeway configuration.

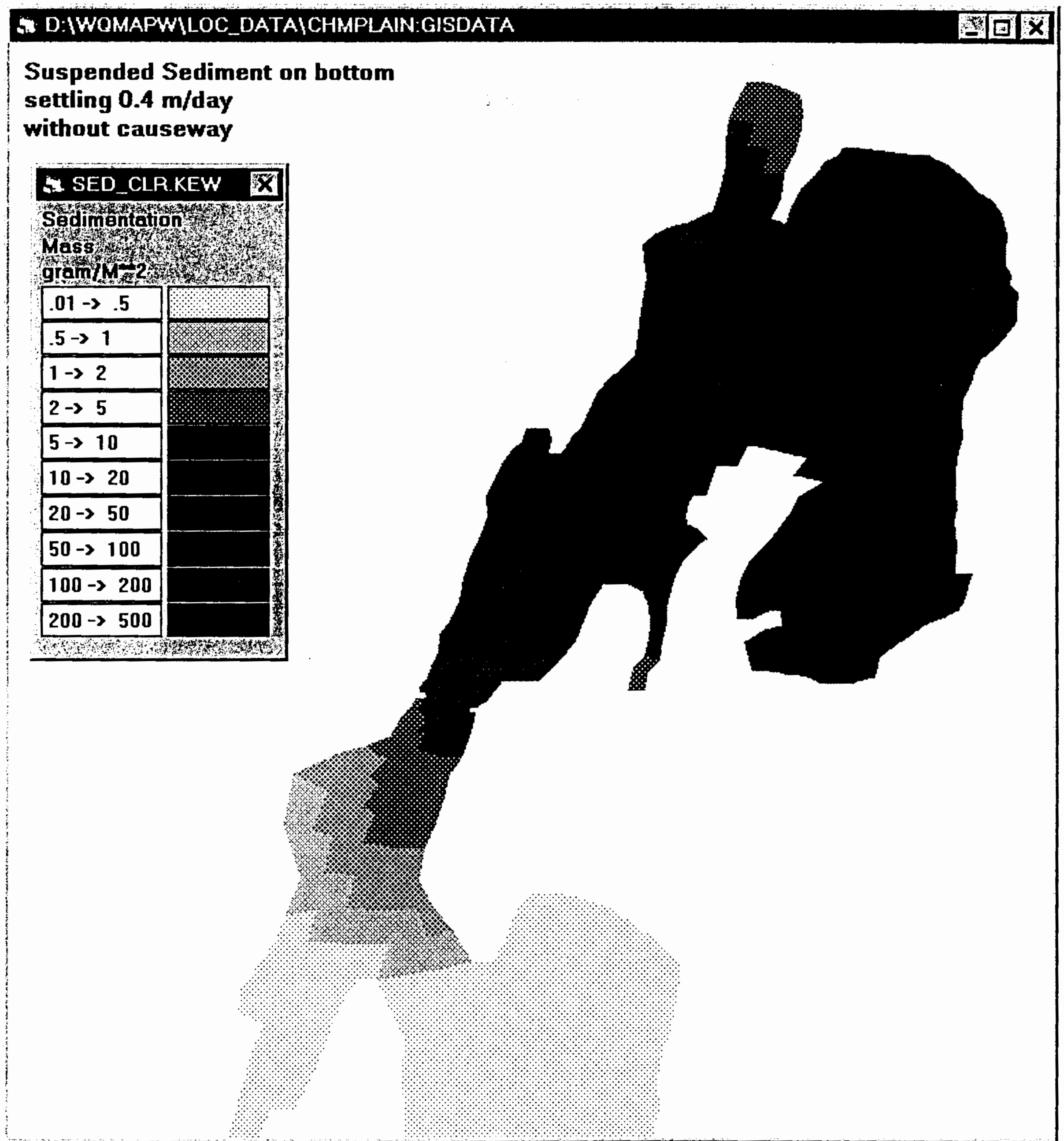

Figure 6.16. Distribution of sediments settled from riverine loads of suspended sediment over the course of the long term suspended sediment simulation for particles with a settling rate of 0.4 meters per day with the causeway removed.

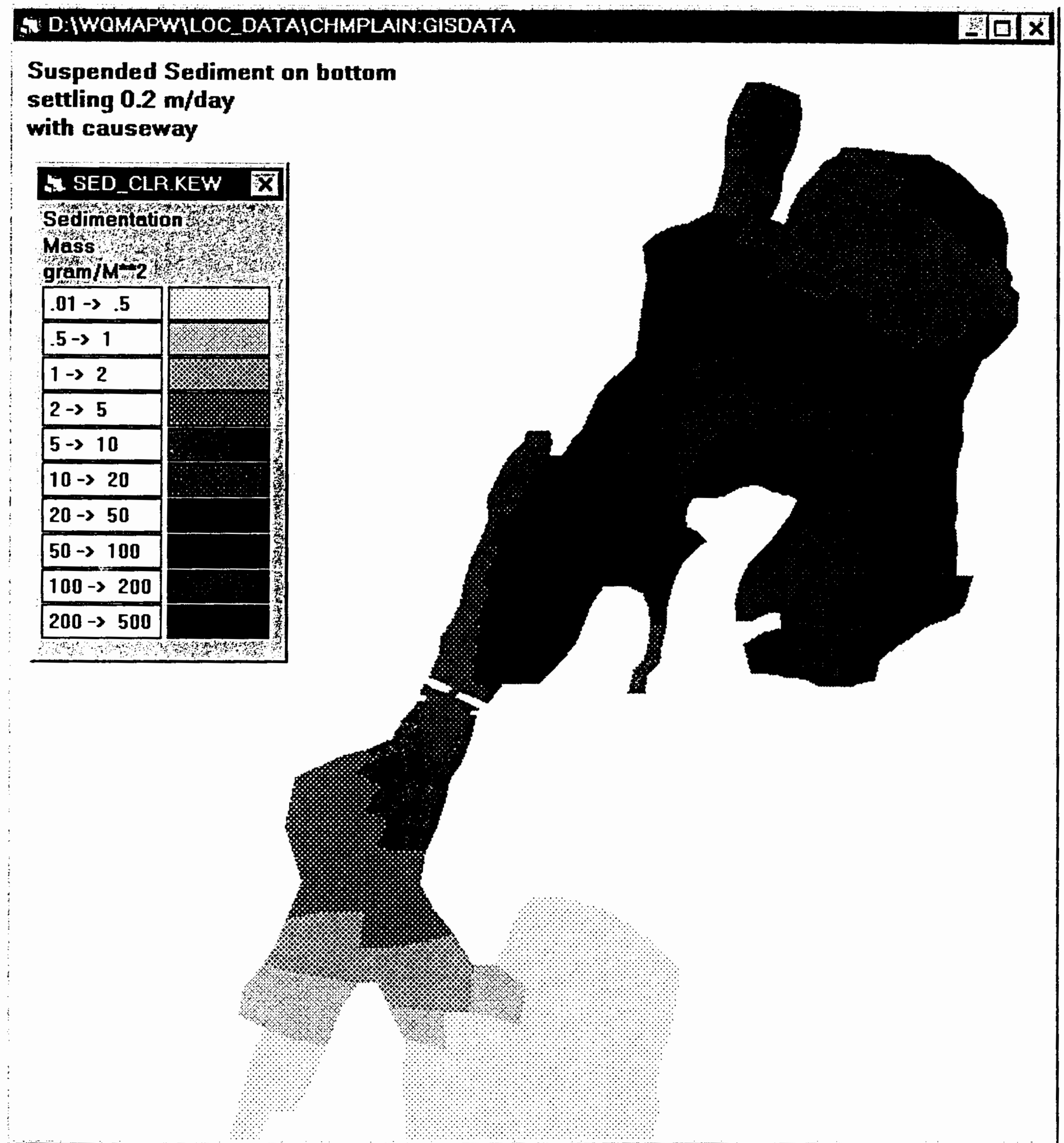

Figure 6.17. Distribution of sediments settled from riverine loads of suspended sediment over the course of the long term suspended sediment simulation for particles with a settling rate of 0.2 meters per day and for the present causeway configuration.

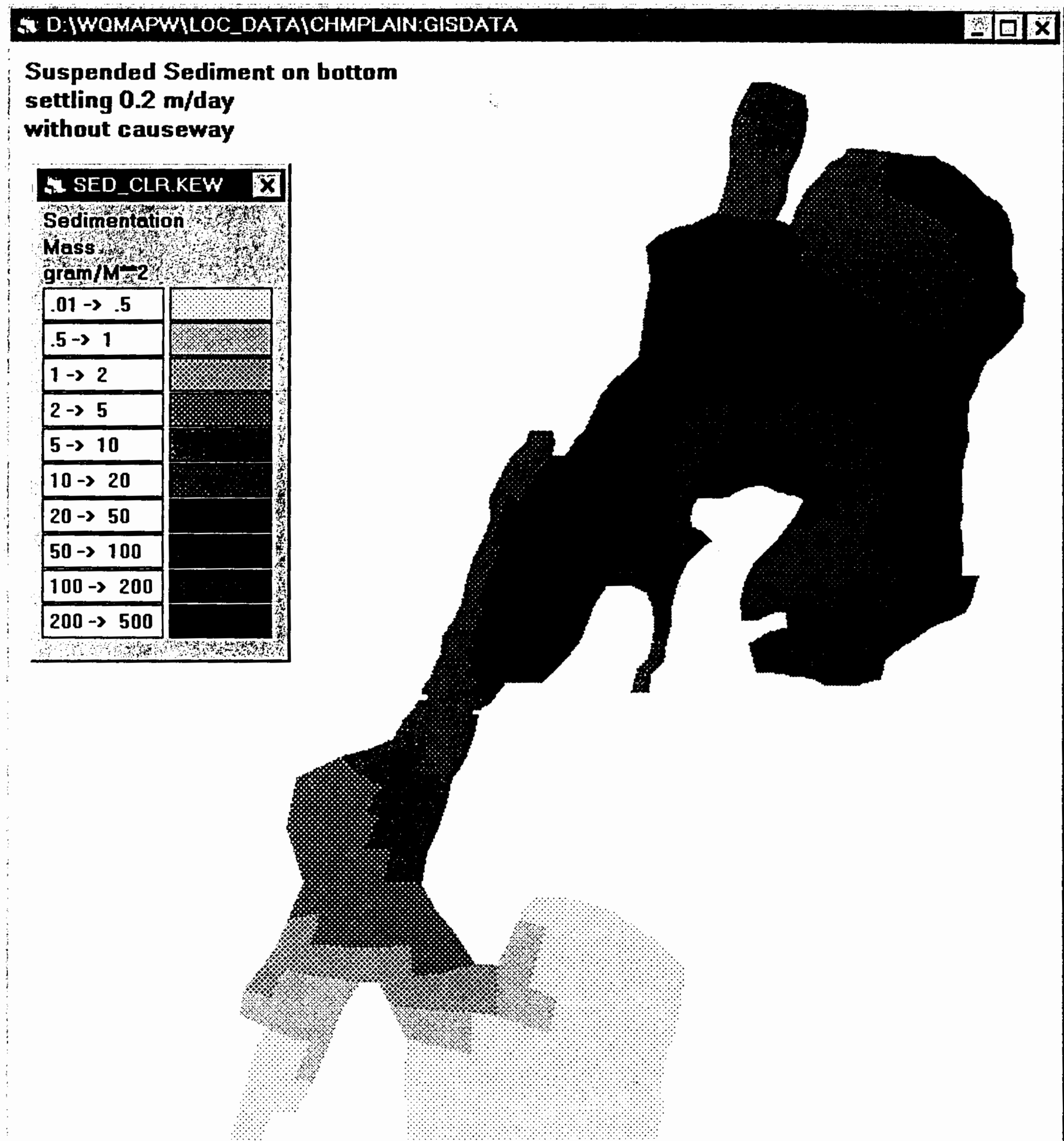

Figure 6.18. Distribution of sediments settled from riverine loads of suspended sediment over the course of the long term suspended sediment simulation for particles with a settling rate of 0.2 meters per day with the causeway removed.

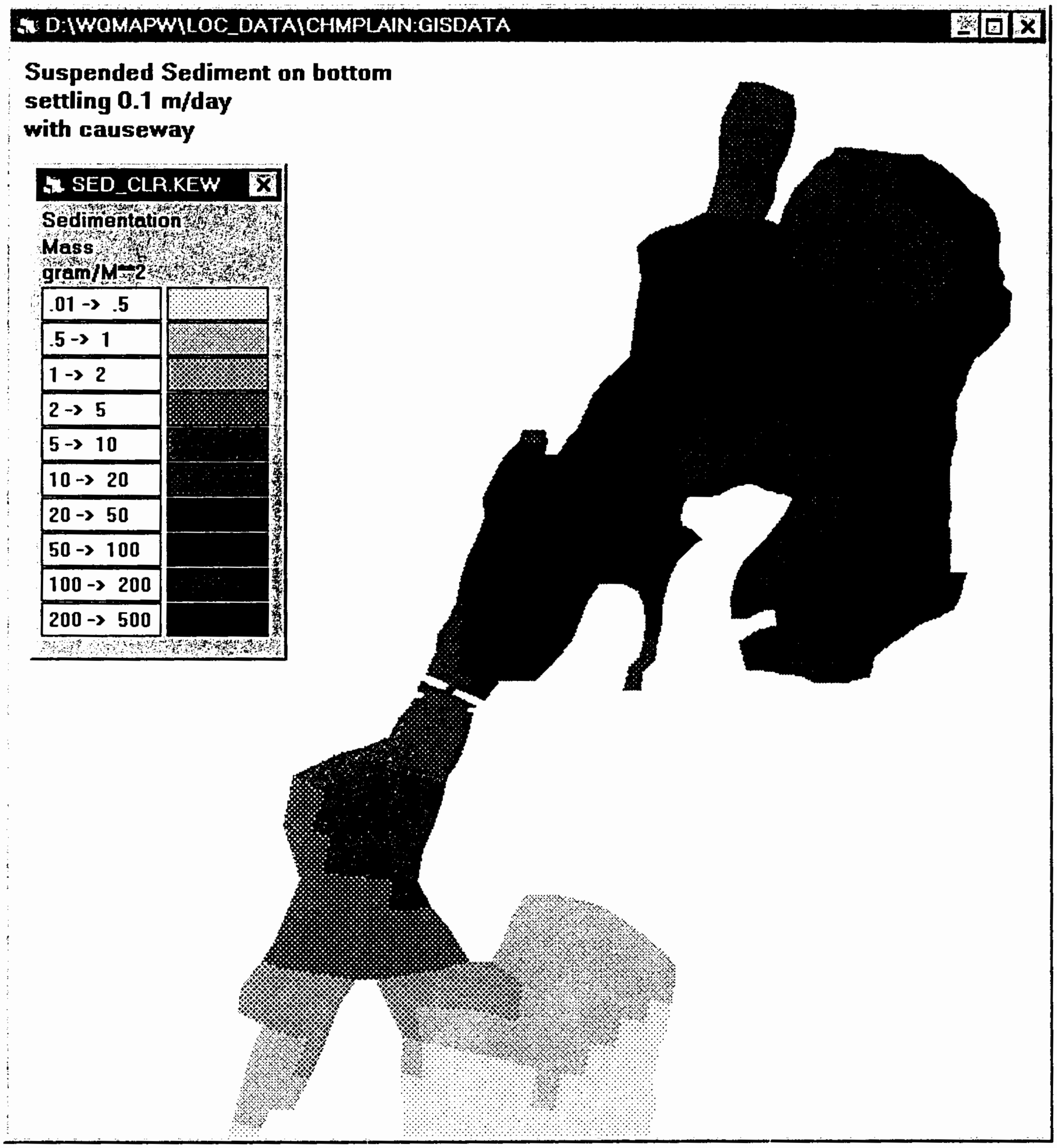

Figure 6.19. Distribution of sediments settled from riverine loads of suspended sediment over the course of the long term suspended sediment simulation for particles with a settling rate of 0.1 meters per day and for the present causeway configuration.

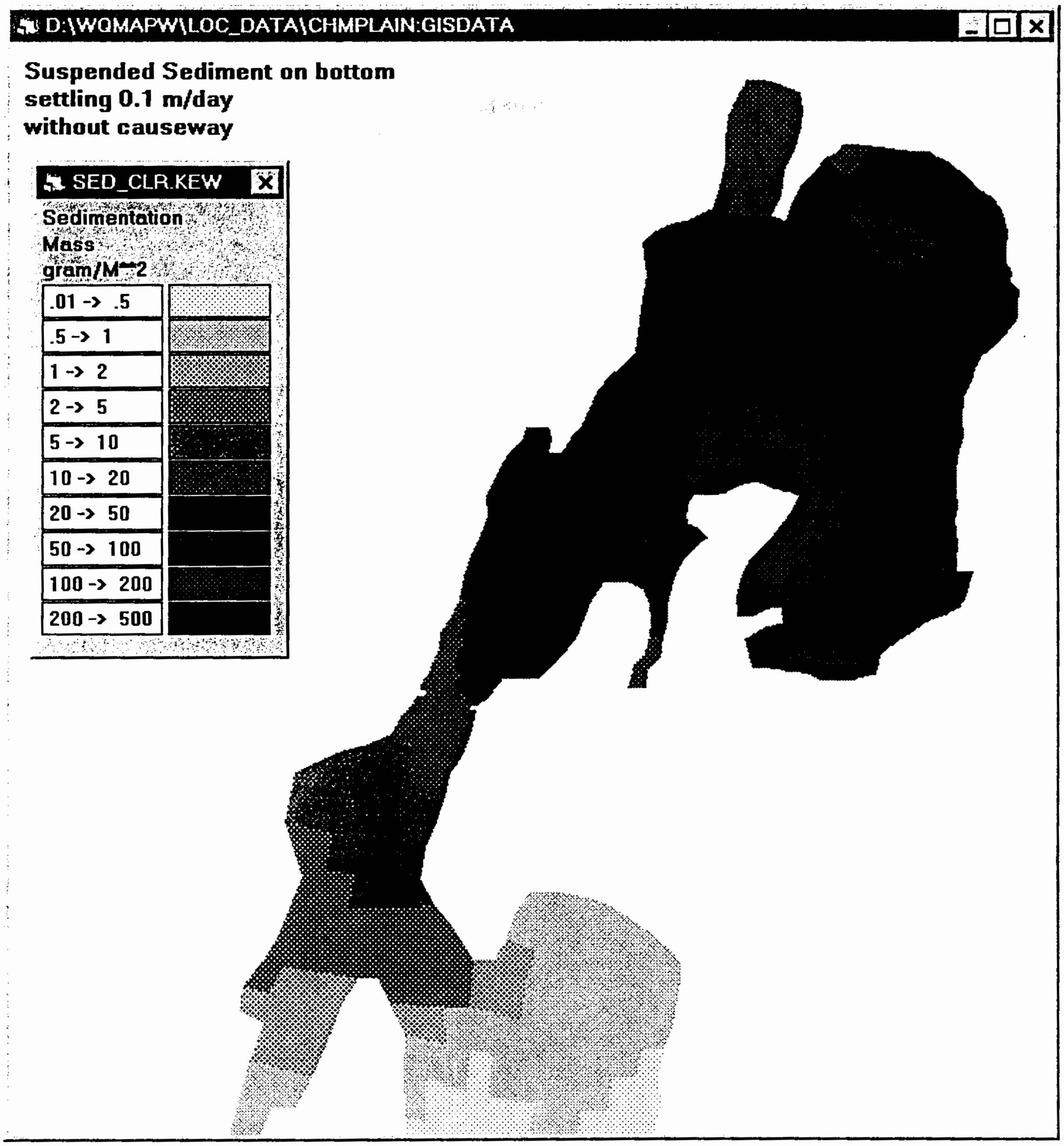

Figure 6.20. Distribution of sediments settled from riverine loads of suspended sediment over the course of the long term suspended sediment simulation for particles with a settling rate of 0.1 meters per day with the causeway removed.

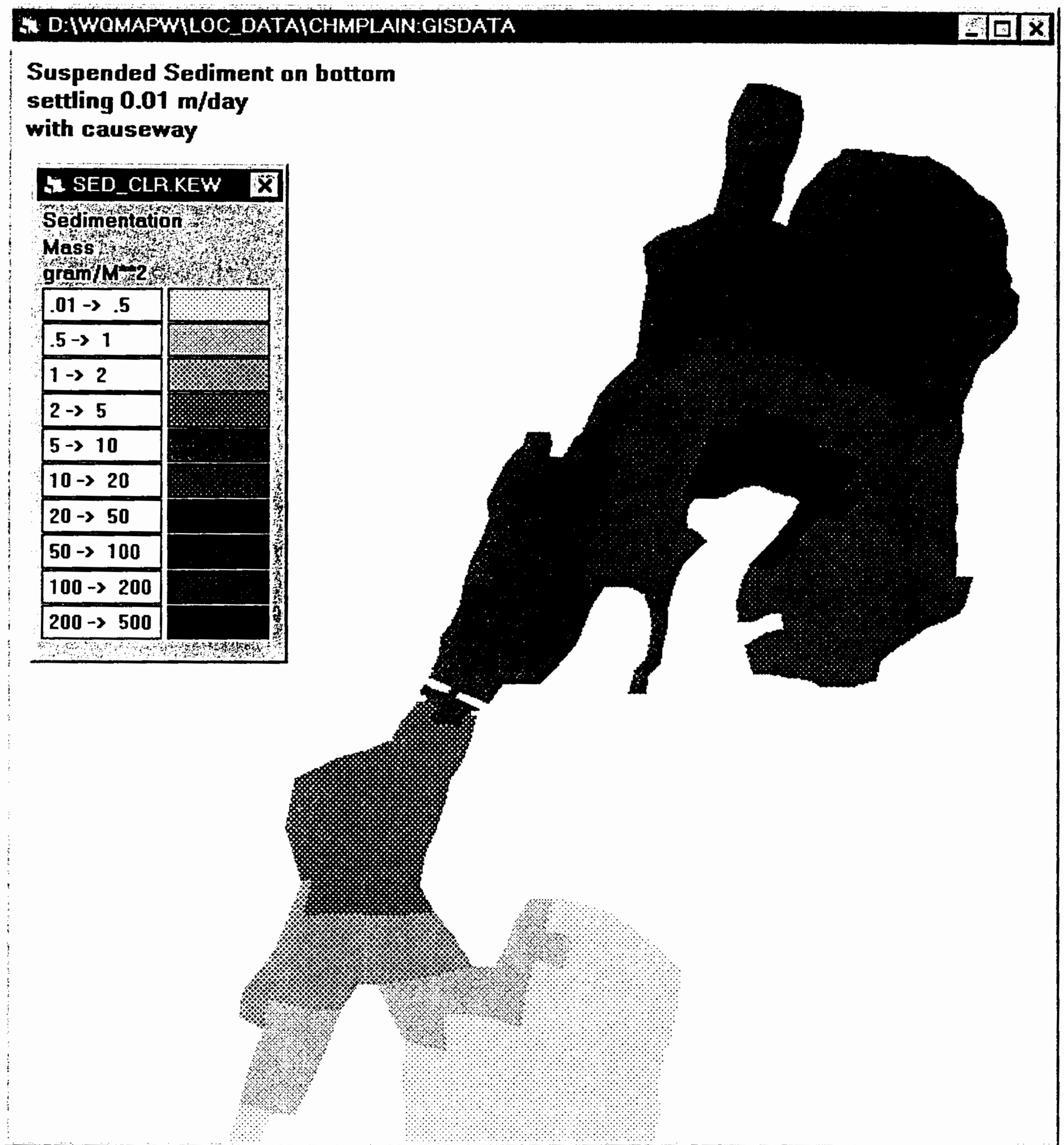

Figure 6.21. Distribution of sediments settled from riverine loads of suspended sediment over the course of the long term suspended sediment simulation or particles with a settling rate of 0.01 meters per day and for the present causeway configuration.

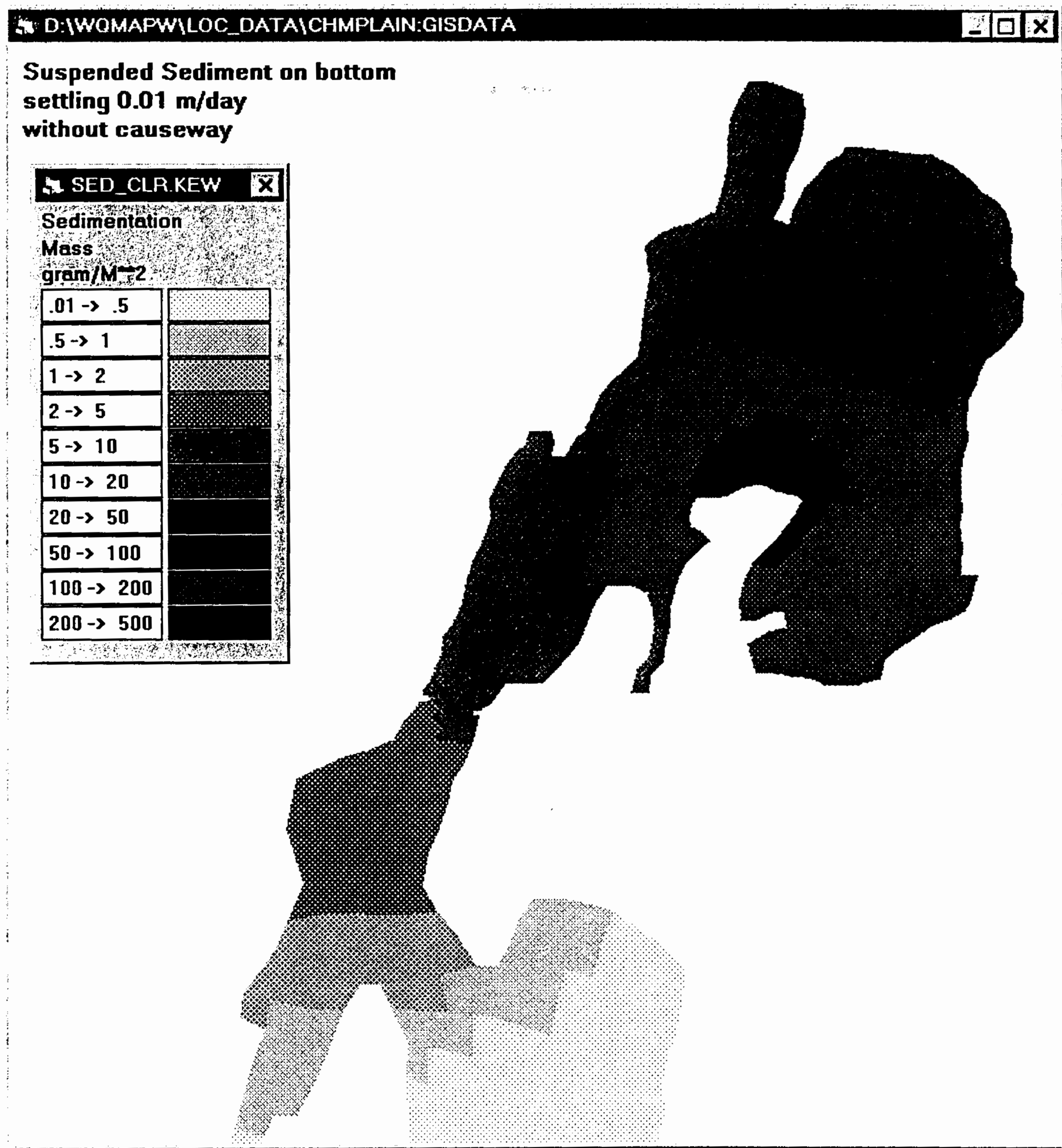

Figure 6.22. Distribution of sediments settled from riverine loads of suspended sediment over the course of the long term suspended sediment simulation for particles with a settling rate of 0.01 meters per day with the causeway removed.

Confidence Levels of the Findings

The modeled results predict differences in constituent concentrations in the bay with and without the causeway of about 1% or less. What alternative approaches to this analysis may be used to confirm these results? Smeltzer (1994) predicts a difference in phosphorus concentration of about 8% with the removal of the causeway. This analysis is based on a regression of exchange rates between basins (based on chloride data) on the interface area between these basins for 13 sub-areas of Lake Champlain. The isolation of Missisquoi Bay, however may constitute a special case. As it exists now, bay exchange rates fall on the low side of the regression, and the narrow channel separating it form the rest of the lake may additionally constrain exchanges that can occur, limiting any benefit to flushing that removal of the causeway might bring. The channel acts as an additional volume of water over which exchange must occur to effect flushing. It is thus considered likely that the 8% value calculated from the regression analysis overestimates the benefits to the bay that would result from removal of the causeway. While this difference cannot be quantified, note that while the regression analysis predicts a five-fold increase in exchange (294×10^6 to 1614×10^6 m^3/yr), calculations using the hydrodynamic model in the present study (the 1% values are based on the mass-transport model) predict an increase in exchange flow of only 242 to 337 m^3/s.

The exchange flow values from the present study predict a decrease in flushing time of up to 10% resulting from removal of the causeway. Given the present mean concentration differences between Missisquoi Bay and the Northeast Arm, this increased level of flushing could reduce present phosphorous concentrations by 6%, at the simplest level of analysis. This, however, is based on poorly-understood values and should not be considered an alternative hypothesis to the 1% value calculated by the mass transport model. It is more properly viewed as an upper bound to a possible range of values.

7. CONCLUSIONS

Water level in the bay rises in response to southerly winds and falls in response to northerly winds. This difference is generally greater at the north end of the bay than at the south end, but the north-south difference rarely reached a magnitude greater than 5 cm (2 inches).

Currents at the center of the bridge were uniform over the measured water column, with little detectable difference in speed or direction with depth. Measurements at the ends of the bridge were unsatisfactory, but calculations of water flux through the bridge opening suggest that flow through the bridge was uniform through the entire cross section.

The calibrated model predicts an overall smoother current record than was measured by the current meters at the bridge. This naturally results from the smoothing process inherent in modeling a complex system. The model did a good job of simulating the volume flux through the bridge opening, though, again, yielded a smoother record than was calculated from the current meter data. The model simulates what happens on a larger scale without the tiny variations that are seen at shorter time scales.

Drogue tracks measured in the field were not well simulated by the model except in some areas near the bay mouth.

The hydrodynamics simulations indicate that the causeways cause some impedance in the variance in flow through the bridge opening without affecting the net flow (due primarily to river inputs). This results in a small (less than10%) increase in flushing time of the bay. The long term phosphorus simulations indicated that differences in flushing in the bay from removal of the causeway would reduce phosphorus concentrations in the bay by about 1%. Likewise, the long term suspended sediment simulations show changes of 1% or less in suspended sediment concentrations or sedimentation in the bay with removal of the causeway.

8. REFERENCES

Davis, Richard A., 1983. Depositional Systems. Prentice-Hall, Inc., Englewood Cliffs, New Jersey. 07632.

Hunt, A.S., 1971. Bottom sediments of Lake Champlain, 1965-1971: A completion report to the Office of Water Resources and U.S. Department of Interior, University of Vermont, Burlington VT, 127 pp.

Madala, R.V. and S.A. Piascek, 1977. A semi implicit numerical model for Baroclinic Oceans. Journal of Computational Physics, 23, pp. 167-178.

Mendelsohn, D.L., T. Isaji, and H. Rines, 1994. Hydrodynamic and water quality modeling of Lake Champlain. Final report to Lake Champlain. US Environmental Protection Agency, Region I, Boston, MA and Region II, New York, NY.

Mendelsohn, D.L. and H.M. Rines, 1995. Development and application of a full phosphorous cycle water quality model to Lake Champlain. In Modern Methods for Modeling the Management of Stormwater Impacts. William James (ed.) Compiled and published by Computational Hydraulics International.

Mendelsohn, D.L. and J.C. Swanson, 1992. Application of a Boundary Fitted Coordinate Mass Transport Model, Estuarine and Coastal Modeling. Proceedings of the 2nd International Conference. ed. Malcolm Spaulding, ASCE.

Mendelsohn, D.L., C. Swanson, and T. Isaji, 1997. Hydrodynamic modeling of Missisquoi Bay in Lake Champlain. Final report to Vermont Geological Survey, Vermont Agency of Natural Resources, Applied Science Associates, Inc, Project 95-136.

Mendelsohn, D.L., E. Howlett and J. C. Swanson, 1995. WQMAP in a Windows environment. Presented at Estuarine and Modeling IV. Proceedings of the 4th International Conference, ASCE, San Diego, October 26-28, 1995.

Muin, M., and M.L. Spaulding, 1996(In review). A 3-D boundary fitted circulation model. Submitted to the ASCE J. of Hydraulic Engineering.

Muin, M. and M.L. Spaulding, 1993. Development and application of a three-dimensional boundary-fitted model in Providence River. Presented at the

Estuarine and Coastal Modeling III. Proceedings of the 3rd International Conference, Oak Brook, Illinois, September 8-10, 1993.

Muin, M., 1993. A three-dimensional boundary fitted circulation model in spherical coordinates. PhD Dissertation, University of Rhode Island.

Muin, M., 1993. A three-dimensional boundary fitted circulation model in spherical coordinates. Ph.D. Dissertation, Dept. of Ocean Engineering, University of Rhode Island, Narragansett, RI.

Myer, G.E. and G.K. Gruendling, 1979. Limnology of Lake Champlain. Prep for New England River Basins Commission. Burlington, VT.

New York State Department of Environmental Conservation, New York State Biological Survey, and Vermont Department of Environmental Conservation, 1992. Work/QA Project Plan. Long-term water quality and biological monitoring project for Lake Champlain. Prep. for U.S. Environmental Protection Agency. Regions I and II. Albany, NY and Waterbury, CT.

Smeltzer, E, 1994. Vermont Route 78 Swanton-Alburg bridge project water quality assessment update. Vermont Agency of Natural Resources, Department of Environmental Conservation, Water Quality Division, Waterbury, VT.

Spaulding, M.L., 1984. A vertically averaged circulation model using boundary-fitted coordinates. Journal of Physical Oceanography, 14, p. 973-982.

Swanson, J.C. and D.L. Mendelsohn, 1994. Application of a Water Quality Modeling, Mapping and Analysis System to Evaluate Effects of CSO Abatement Alternatives on Upper Narragansett Bay, Rhode Island. 1994 Water Environment Federation CSO Specialty Conference, Louisville, Kentucky, July 1994.

Swanson, J.C., 1986. A three dimensional numerical model system of coastal circulation and water quality. PhD Dissertation, University of Rhode Island.

Swanson, J.C., 1986. A three-dimensional numerical model system of coastal circulation and water quality. Ph.D. Dissertation, Department of Ocean Engineering, University of Rhode Island, Kingston, Rhode Island.

Swanson, J.C., M. Spaulding, J.P. Mathisen, O.O. Jenssen, 1989. A three dimensional boundary fitted coordinate hydrodynamic model: Part I, Development and testing. Deutsche Hydrographische Zeitschrift, 42, H.3-6, pp. 170-186.

Vermont Department of Conservation and New York State Department of Environmental Conservation, 1994. Lake Champlain diagnostic-feasibility study, Final Report, Part 1: A phosphorus budget, model and load allocation for Lake Champlain. US Environmental Protection Agency, Region I, Boston, MA and Region II, New York, NY.

Vermont Department of Conservation and New York State Department of Environmental Conservation, 1992. Lake Champlain diagnostic-feasibility study, Interim Progress Report. US Environmental Protection Agency, Region I, Boston, MA and Region II, New York, NY.

Vermont Department of Conservation and New York State Department of Environmental conservation, 1997. A phosphorous budget, model, and load reduction strategy for Lake Champlain. Lake Champlain Diagnostic – Feasibility Study Final Report. U.S. Environmental Protection Agency.

Appendix A

Table A-1. Drogue study data for the Missisquoi Bay field study. The speed and direction values are for the time period following each position reading, and the bold values are the mean values for the full deployment.

Morning survey, October 10

Drogue number	Depth (m)	Reading Number	Comments	Speed (cm/s)	Direction (deg, true)	Longitude	Latitude
1	**1**	1	each even, deep, drogue	0.65	106	-73.2200	44.9822
		2	released about 3 meters to	1.84	207	-73.2198	44.9821
		3	the north of the odd mate	1.68	186	-73.2202	44.9816
		4		**1.23**	**188**	-73.2203	44.9811
2	**2**	1		0.85	209	-73.2200	44.9822
		2		2.21	217	-73.2201	44.9820
		3		1.18	195	-73.2207	44.9815
		4		**1.45**	**209**	-73.2209	44.9811
3	**1**	1		1.32	190	-73.2175	44.9813
		2		2.61	208	-73.2176	44.9810
		3		1.88	188	-73.2181	44.9803
		4		**1.98**	**198**	-73.2183	44.9797
4	**3**	1		1.41	211	-73.2175	44.9813
		2		2.50	217	-73.2177	44.9811
		3		1.61	209	-73.2184	44.9805
		4		**1.89**	**213**	-73.2187	44.9800
5	**1**	1		1.79	191	-73.2135	44.9799
		2		2.49	205	-73.2136	44.9796
		3		2.43	193	-73.2141	44.9789
		4		**2.27**	**197**	-73.2143	44.9782
6	**3**	1		1.37	196	-73.2135	44.9799
		2		2.27	214	-73.2136	44.9797
		3		2.83	202	-73.2142	44.9791
		4		**2.25**	**206**	-73.2146	44.9783
7	**1**	1		2.83	210	-73.2085	44.9780
		2		3.66	216	-73.2088	44.9776
		3		3.11	222	-73.2098	44.9767
		4		**3.25**	**217**	-73.2106	44.9760
8	**2**	1		2.47	194	-73.2085	44.9780
		2		3.45	213	-73.2086	44.9776
		3		3.68	223	-73.2095	44.9767
		4		**3.28**	**214**	-73.2106	44.9759

Table A-1 continued. Drogue study data for the Missisquoi Bay field study.

Afternoon survey, October 10

Drogue number	Depth (m)	Reading Number	Comments	Speed (cm/s)	Direction (deg, true)	Longitude	Latitude
1	**1**	1	West end of Metcalf Is.	3.77	173	-73.1770	45.0085
		2	Wind started to blow	5.32	185	-73.1768	45.0070
		3	up about 13:20	6.14	182	-73.1771	45.0050
		4		**4.95**	**181**	-73.1773	45.0031
2	**3**	1		3.24	185	-73.1770	45.0085
		2		4.93	185	-73.1772	45.0072
		3		4.67	181	-73.1775	45.0054
		4		**4.24**	**184**	-73.1776	45.0039
3	**1**	1	N of west edge of Metcalf Is.	1.94	211	-73.1614	45.0179
		2		6.84	242	-73.1620	45.0172
		3		8.96	228	-73.1663	45.0157
		4		**5.59**	**233**	-73.1691	45.0140
4	**3**	1		2.88	207	-73.1614	45.0179
		2		5.45	249	-73.1622	45.0169
		3		3.33	242	-73.1658	45.0160
		4	Grounded	**3.89**	**238**	-73.1671	45.0155
5	**1**	1	North of Shad Is.	4.16	179	-73.1405	45.0212
		2		5.40	209	-73.1405	45.0192
		3		5.22	200	-73.1416	45.0179
		4		**4.68**	**195**	-73.1424	45.0163
6	**3**	1		3.46	181	-73.1405	45.0212
		2		4.84	213	-73.1405	45.0196
		3		4.35	206	-73.1417	45.0184
		4	Possibly grounded	**3.97**	**199**	-73.1425	45.0172
7	**1**	1	NE of Shad Is.	3.31	176	-73.1228	45.0152
		2		7.07	187	-73.1227	45.0136
		3		11.23	182	-73.1232	45.0115
		4		**6.59**	**182**	-73.1235	45.0081
8	**3**	1		2.49	171	-73.1228	45.0152
		2		3.72	199	-73.1226	45.0140
		3		3.24	184	-73.1231	45.0130
		4	Probably grounded	**2.98**	**184**	-73.1232	45.0120

Table A-1 continued. drogue study data for the Missisquoi Bay field study

Morning survey, October 29

Drogue number	Depth (m)	Reading Number	Comments	Speed (cm/s)	Direction (deg, true)	Longitude	Latitude
1	**1**	1	W. shore, S of Campbell Pt.	2.49	92	-73.1661	45.0472
		2		2.92	116	-73.1645	45.0471
		3		2.68	127	-73.1636	45.0468
		4		**2.55**	**109**	-73.1627	45.0463
2	**1**	1	Opening of Venise Bay	2.47	139	-73.1540	45.0584
		2		1.25	150	-73.1530	45.0575
		3		0.84	186	-73.1528	45.0572
		4		**1.60**	**148**	-73.1528	45.0570
3	**1**	1	Open bay, NW quadrant	3.87	153	-73.1443	45.0433
		2		2.48	171	-73.1432	45.0418
		3		3.41	172	-73.1431	45.0412
		4		**3.35**	**162**	-73.1429	45.0401
4	**3**	1	Pair to no. 3	3.00	163	-73.1441	45.0432
		2		3.11	168	-73.1436	45.0420
		3		2.75	177	-73.1434	45.0412
		4		**2.93**	**168**	-73.1434	45.0404
5	**1**	1	Open bay, NE quadrant	3.71	148	-73.1171	45.0397
		2		2.40	152	-73.1164	45.0388
		3		2.68	178	-73.1160	45.0383
		4		**2.87**	**159**	-73.1160	45.0375
6	**3**	1	Pair to no. 5	2.79	152	-73.1171	45.0397
		2		1.95	171	-73.1167	45.0390
		3		1.67	196	-73.1166	45.0386
		4		**2.02**	**170**	-73.1168	45.0381
7	**1**	1	W. side of La Grande Baie	2.05	110	-73.1326	45.0607
		2		2.52	112	-73.1319	45.0605
		3		3.84	143	-73.1312	45.0603
		4		**2.75**	**127**	-73.1302	45.0593
8	**1**	1	Middle of La Grande Baie	2.18	107	-73.1156	45.0583
		2		1.52	114	-73.1148	45.0581
		3		1.02	79	-73.1144	45.0579
		4		**1.51**	**102**	-73.1140	45.0580
9	**1**	1	East side of La Grande Baie	8.01	144	-73.0843	45.0551
		2		10.12	152	-73.0826	45.0534
		3		10.29	160	-73.0813	45.0515
		4		**9.42**	**153**	-73.0798	45.0484

Table A-1 continued. drogue study data for the Missisquoi Bay field study

Afternoon survey, October 29

Drogue number	Depth (m)	Reading Number	Comments	Speed (cm/s)	Direction (deg, true)	Longitude	Latitude
1	**1**	1	Middle of SE embayment	1.13	162	-73.1183	44.9922
		2		2.56	156	-73.1181	44.9916
		3		**1.75**	**158**	-73.1175	44.9906
2	**1**	1	Mouth of SE embayment	4.32	83	-73.1166	45.0062
		2		4.89	76	-73.1133	45.0064
		3		**4.56**	**80**	-73.1105	45.0068
3	**1**	1	Open bay, SE quadrant	0.72	-71	-73.1129	45.0233
		2		0.20	256	-73.1134	45.0234
		3		**0.47**	**-77**	-73.1135	45.0234
4	**3**	1	Pair to no. 3	0.38	269	-73.1129	45.0233
		2		0.14	120	-73.1132	45.0233
		3		**0.16**	**257**	-73.1131	45.0233
5	**1**	1	Open bay, SW quadrant	3.78	171	-73.1350	45.0276
		2		3.47	151	-73.1346	45.0256
		3		**3.60**	**163**	-73.1337	45.0244
6	**3**	1	Pair to no. 5	3.11	174	-73.1350	45.0276
		2		3.01	153	-73.1348	45.0259
		3		**3.02**	**165**	-73.1341	45.0248
7	**1**	1	South of McFee Pt.	1.35	97	-73.1741	45.0295
		2		2.58	147	-73.1731	45.0294
		3		**1.71**	**126**	-73.1723	45.0285
8	**1**	1	East of Province Pt.	3.18	140	-73.1876	45.0152
		2		2.65	136	-73.1861	45.0139
		3		**2.95**	**138**	-73.1850	45.0131
9	**1**	1	Mid-channel between	5.46	108	-73.1774	45.0117
		2	Prov.Pt. and Metcalf Is.	4.62	126	-73.1735	45.0107
		3		**5.04**	**115**	-73.1714	45.0096